Doctoral Dissertation (Shinshu University)

Study for removal of toxic *Microcystis* cells and nutrients by electrochemical treatment

Professor: Ho-Dong PARK

March, 2015

BONG-SEOK JEON

Contents

I. General introduction ……..……..……..1

I.1 Problems of eutrophication lake …….……..1

I.2 Electrooxidation treatment ..……..6

I.3 Purpose of this study …….…….…….12

References ……...……..14

II. The removal of *Microcystis ichthyoblabe* cells and its hepatotoxin microcystin-LR during electrooxidation process using Pt/Ti electrodes ……...……....……18

II.1 Introduction ……..…….18

II.2 Materials and methods …….…..……20

II.2.1 Strain and culture conditions ……..……..20

II.2.2 Conditions of electrooxidation process …….……20

II.2.3 Analysis of cell density, cell size and cell morphology ……...…….21

II.2.4 Analysis of microcystin ……...…….21

II.3 Results and discussion …….…….25

II.3.1 Cell density and morphology changes ……...……...…25

II.3.2 Variations in MC-LR concentration ….....……...32

II.3.3 Effect of algal suspension volume ……....……35

II.3.4 Variation in current density …….....……..38

References ……..……..40

III. The variation in concentration of cations (Na^+, K^+ and Ca^{2+} ions) and nutrient species (N and P) during electrochemical treatment …….42

III.1 Introduction …….42

III.2 Materials and methods …….43

III.2.1 Algal culture ……..……...43

III.2.2 Apparatus ……..……44

III.2.3 Concentraion of cations (Na^+, K^+ and Ca^{2+} ions) ……..……..43

III.2.4 Nitrogen analysis ……...……..44

III.2.5 Phosphorus analysis ……..……...44

III.2.6 Analysis of the deposits on the cathode ……...…….45

III.3 Results and discussion ……..46

III.3.1 Variations in the concentration of cations (Na^+, K^+ and Ca^{2+} ions) ……..……..46

III.3.2 Variations in nitrogen species ……..……49

III.3.3 Variations in phosphorus species ……..……51

III.3.4 Analysis of the deposits on the cathode surface ……..…….53

References ……...58

IV. The effect of electrode material for removal of *Microcystis* sp. by electrochemical oxidation .....……...…….....59

IV.1 Introduction ……..59

IV.2 Materials and methods ……...……..…….60

IV.2.1 *Microcystis* cells 60

IV.2.2 Apparatus 60

IV.2.3 Cell and colony counting 60

IV.3 Results and discussion 61

References 67

V. Application of electrochemical treatment in a pond 68

V.1 Introduction 68

V.2 Materials and methods 69

V.2.1 Chikato pond 69

V.2.2 Electrochemical treatment equipment 69

V.2.3 Dissolved oxygen, OD_{405nm}, temperature, pH, conductivity of water and concentration of N and P species 69

V.3 Results and discussion 77

References 88

VI. General discussion and conclusions 89

VI.1 The removal of *Microcystis ichthyoblabe* cells and its hepatotoxin microcystin-LR during electrooxidation process using Pt/Ti electrodes 89

VI.2 The variation in concentration of cations (Na^+, K^+ and Ca^{2+} ions) and nutrient species (N and P) during electrochemical treatment 89

VI.3 The effect of electrode material for removal of *Microcystis* sp. by electrochemical

oxidation 90

VI.4 Application of electrochemical treatment in a pond 91

VI.5 Conclusions 91

References 95

Appendix. Microcystin extraction from *Microcystis* cells using boiling treatment.....97

1. Introduction.....98

2. Materials and methods.....98

2.1. Algal culture.....98

2.2. Heat stability of MC-LR.....99

2.3. MC-LR extraction methods.....99

2.3.1. Treatment 1.....99

2.3.2. Treatment 2.....100

2.3.3. Treatment 3.....100

2.4. Recovery for methods.....101

2.5. Analysis of MC-LR and MC-RR.....101

2.6. Statistical analysis.....102

3. Results and discussion.....102

3.1. Heat stability of MC-LR.....102

3.2. Effect of extraction efficiency of MC-LR for treatments.....102

3.3. Effect of recovery for methods.....103

4. Conclusions.....104

References.....110

List of Tables

Table I-1. Oxidation potentials and rate constants for MC-LR of chemical oxidants 10

Table II-1. Composition of MA medium for culturing *Microcystis ichthyoblabe* strain TAC 95 23

Table II-2. Conditions of all experiments carried out in this study 27

Table III-1. The contents of components for the spectra 1-5 of Fig. III-4 55

Table V-1. Components of electrodes set 1 and 2 74

List of Figures

Fig. I-1. The vicious circle caused by eutrophication of lake ….....……3

Fig. I-2. Schematic diagram of the release of inorganic phosphorus in anaerobic sediment (modified Wetzel, 2001). SRB and FeRB indicate sulfate-reducing bacteria and ferric-reducing bacteria …….....……4

Fig. I-3. General structure of microcystin where X and Y represent variable amino acids …….....……...5

Fig. I-4. Evolution potential of oxygen and hydrogen according to pH variation (equation I-3 and I-4) ……..…….11

Fig. II-1. Schematic of the electrochemical method reactor: (1) DC power supply; (2) Electrolysis chamber made of acrylic resins; (3) *M. ichthyoblabe* suspension (4 L or 34 L); (4) Anode electrode composed of Pt-coated Ti substrate (surface area (200 mm ×50 mm) = 100 cm^2); (5) Cathode electrode (same composition and size as the anode electrode). The anode and cathode are separated by 5 mm; (6) Magnetic stirring bar. All experiments were performed in an isothermal room at (23 ± 1) °C …….....……24

Fig. II-2. Cell densities in Trials 1–4 of Table II-2 as functions of (a) time; (b) applied charge ….....…...28

Fig. II-3. SEM images of untreated cells (a) and cells at an applied charge of 1.2×10^4 C in Trial 1 of Table II-2 (b, c and d). The arrows point to broken cells. The white bar indicates 1 μm.…….....……29

Fig. II-4. Particle concentration distributions with respect to diameter: (a) untreated cells; (b) Trial 1 of Table II-2 …….....……..31

Fig.II- 5. Effect of applied charge on (a) intracellular MC–LR; (b) extracellular MC–LR; and (c) total MC–LR concentration in Trials 1–6 of Table II-2. The total MC–LR concentration is the sum of the intracellular and extracellular MC–LR concentrations …….....…….33

Fig. II-6. Effect of applied charge on (a) cell density and intracellular MC–LR concentration; (b) extracellular MC–LR concentration; and (c) total MC–LR concentration. Results are plotted for Trials 4 and 7 of Table II-2 .....…..36

Fig. II-7. Analysis of the electrooxidation process: (a) temporal changes in current density, and (b) relationship between current density and conductivity ……....…….39

Fig III-1. Variation in concentration of cations. (a) Na^+, (b) K^+ and (c) Ca^{2+}. The results are from a single experiment.....…….48

Fig. III-2. Variation in nitrogen species. (a); PON, DON, NO_3-N, NO_2-N and NH_4-N, TN is the sum of PON, DON, NO_3-N, NO_2-N and NH_4-N. (b); DON, NO_3-N, NO_2-N and NH_4-N. The results are from a single experiment…….....……50

Fig. III-3. Variation in POP, DOP and DIP. TP is the sum of POP, DOP and DIP. The results shown are mean data from triplicate experiments, and error bars indicate standard deviations.....…..……..52

Fig. III-4. SEM image of the deposits from the cathode surface. Spectra 1 to 5 were analyzed by EDS, and the results are shown in Table III-1 ……..…….56

Fig. III-5. XRD patterns of the deposits from the cathode with and without annealing at 550 °C for 2 h …….57

Fig. IV-1. Variations in electric potential (a) and current (b) using the Pt/Ti electrodes and DSE electrodes during the electrochemical oxidation. The experiments were performed in duplicate …….....……...63

Fig. IV-2. Variations in conductivity of algal solution using the Pt/Ti electrodes and DSE

electrodes during the electrochemical oxidation. The experiments were performed in duplicate 64

Fig. IV-3. Variations in cell density (a) and colony density (b) using the Pt/Ti electrodes and DSE electrodes during the electrochemical oxidation. The results are the sum of MC-LR and MC-RR. The results are from a single experiment .....……..…….65

Fig. IV-4. SEM images of untreated cells (a) and treated cells (b and c). The arrows point to broken cells …….....……66

Fig. V-1. Image of Chikato pond (Matsumoto, Japan) and sampling station. The electrochemical treatment equipment was installed at St. b ……..71

Fig. V-2. Photograph of the electrochemical treatment equipment. (a) electrodes set 1 and 2; (b) W-motion; and (c) electrochemical treatment equipment ….....……..72

Fig. V-3. Schematic diagram of the water flow by rotating W-motion .....……75

Fig. V-4. Photograph of the electrochemical treatment equipment installation ……..……79

Fig. V-5. Variations in electric potential and current of the electrodes set in 0.9 m depth 79

Fig. V-6. Variations in temperature in St. a, b, c and equipment in 0.73, 1.35 and 2.21 m depth. The lack of data from October 7 to October 9 was caused by the stop operation of the electrochemical equipment because of typhoon …….....……..80

Fig. V-7. Variations in pH in St. a, b, c and equipment in 0.46 m depth. The lack of data from October 7 to October 9 was caused by the stop operation of the electrochemical equipment because of typhoon ….....……..…81

Fig. V-8. Variations in conductivity in St. a, b and c …….…….……82

Fig. V-9. Variations in dissolved oxygen in St. a, b, c and equipment in 0.73, 1.35 and 2.21 m depth. The lack of data from October 7 to October 9 was caused by the stop operation of the electrochemical equipment because of typhoon 83

Fig. V-10. Variations in total nitrogen (a), dissolved total nitrogen (b) and particulate organic nitrogen (c) in St. a, b and c 84

Fig. V-11. Variations in total phosphorus (a), dissolved total phosphorus (b) and particulate organic phosphorus (c) in St. a, b and c 86

Fig. VI-1. Purification of eutrophic lake by electrochemical treatment 93

Fig. VI-2. Schematic diagram of purification of eutrophic lake by electrochemical treatment; (a) before treatment (modified Wetzel, 2001) and (b) after treatment. SRB and FeRB indicate sulfate-reducing bacteria and ferric-reducing bacteria 94

Fig. 1. The MC-LR concentration heated during 10 min (a) and 1 h (b). Asterisk (*) represent significant differences with 25ºC treated sample (Tukey's multiple-comparison test, $p < 0.05$).....106

Fig. 2. The extracted MC-LR concentration by treatment 1, 2 and 3 (1, 2 and 3). Different letters represent significant differences between treatment concentrations (Tukey's multiple-comparison test, $p < 0.05$).....107

Fig. 3. The recovery of MC-RR concentration by not treated (0) and treatment 1, 2 and 3 (1, 2 and 3). Different letters represent significant differences between treatment concentrations (Tukey's multiple-comparison test, $p < 0.05$).....108

Fig. 4. The MC-LR concentration without the loss during process by treatment 1, 2 and 3 (1, 2 and 3). These results were calculated by eq. 1. Different letters represent significant differences between treatment concentrations (Tukey's multiple-comparison test, $p < 0.05$).....109

I. General introduction

I.1 Problems of eutrophication lake

Eutrophication of lake is commonly caused by human activities and it produces a lot of negative effects. Fig. I-1 shows the vicious circle caused by eutrophication of lake. Cyanobacteria dominate the freshwater phytoplankton community under certain conditions (usually a combination of high nutrient load and warm temperature), and they can form blooms. When algae die they sink to the bottom where they are decomposed and the nutrients contained in cells are converted into inorganic form by bacteria. The range of anaerobic sediment and deeper water extend because the decomposition process uses oxygen. Inorganic nutrients (such as phosphorus) are released into the water bodies (Fig. I-2, modified from Wetzel, 2001).

Cyanotoxins produced by freshwater cyanobacteria have been reported to cause negative effects in both wild and domestic animals and humans (Carmichael, 2001; Dawson, 1998; Pouria et al., 1998; Ueno et al., 1996). Many types of cyanotoxins (microcystins, nodularin and cylindrospermopsin as hepatotoxin; anatoxin-a, anatoxin-a(s) and saxitoxins as neurotoxin) are produced by a variety of cyanobacteria including *Microcystis*, *Oscillatoria,*

Nostoc, Anabaenopsis, Nodularia, Cylindrospermopsis, Aphanizomenon, Lyngbya, Planktothrix, Anabaena and *Oscillatoria* (Carmichael, 1992; Huisman et al., 2005).

Microcystins are produced by *Microcystis, Anabaena, Oscillatoria* and *Nostoc* (Lawton and Edwards 2001). Microcystins are cyclic heptapeptides contained γ-linked $_{D}$-glutamic acid ($_{D}$-Glu), $_{D}$-alanine ($_{D}$-Ala), β-linked $_{D}$-*erythro*-β-methylaspartic acid ($_{D}$-MeAsp), *N*-methyldehydroalanine (Mdha) and C_{20}β-amino acid, (2*S*,3*S*,8*S*,9*S*)-3-amino-9-methoxy-2,6,8-trimethyl-10-phenyl-4(*E*),6(*E*)-dienoic acid (Adda) (Fig. I-3) (Lawton and Edwards 2001). The other two $_{L}$-amino acids are variable (X and Y of Fig. I-3). For example, Microcystin-LR (MC-LR) contains leucine and arginine in X and Y, respectively. Microcystins have toxicity because they inhibit the regulatory enzymes protein phosphatase 1 and 2A (PP1 and 2A) (Lawton and Edwards 2001). MC-LR is one of the most toxic cyanotoxins. A guideline value for MC-LR of 1.0 μg L^{-1} has been suggested by the WHO (Chorus and Bartam, 1999). Sivonen and Jones (1999) reported that the LD_{50} of MC-LR is approximately 50 μg per kg body weight.

Moreover, cyanobacteria cells and cyanotoxins can affect drinking water. Current drinking water treatment systems cannot remove all contaminants from freshwater supplies containing toxic cyanobacteria blooms. Therefore, if algal cells and their toxins enter drinking water supplies, they pose a serious threat to human health (Hoeger et al. 2005).

Therefore, to minimize the threat, the removal of cyanobacteria and cyanotoxin, the removal of nutrients and the supply of oxygen into deeper water and sediment are necessary.

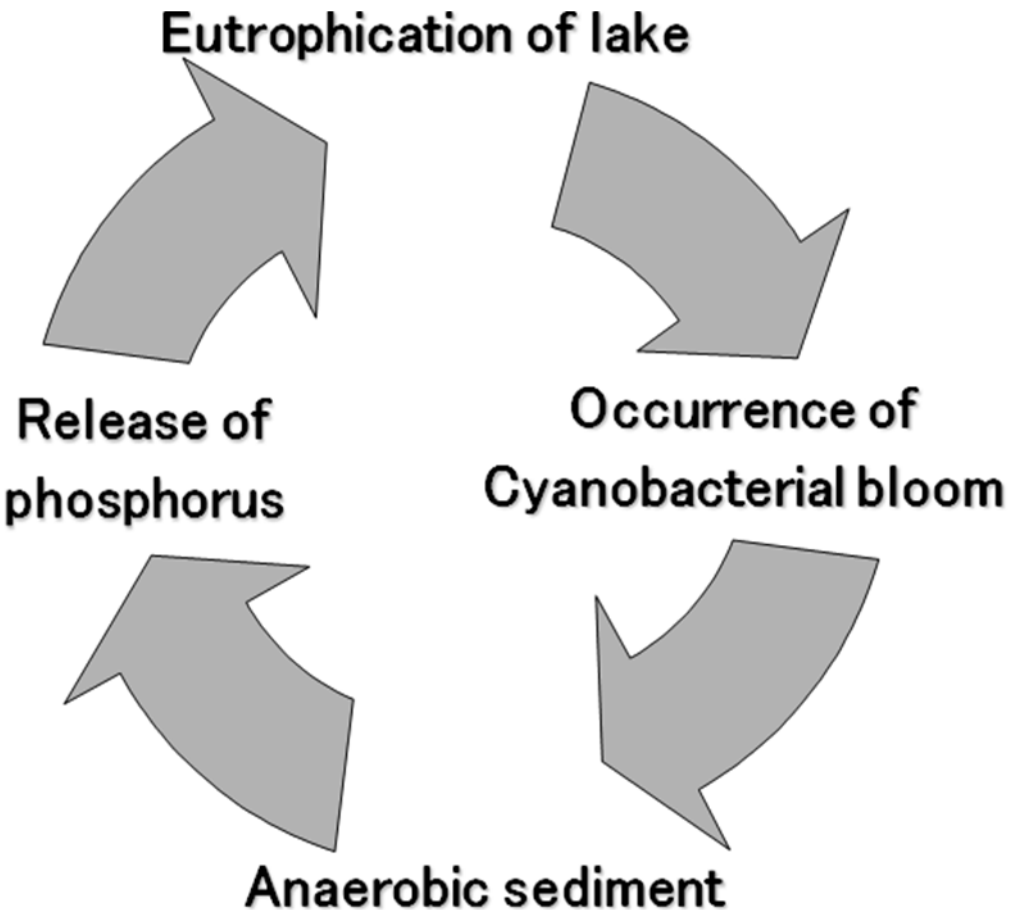

Fig. I-1. The vicious circle caused by eutrophication of lake

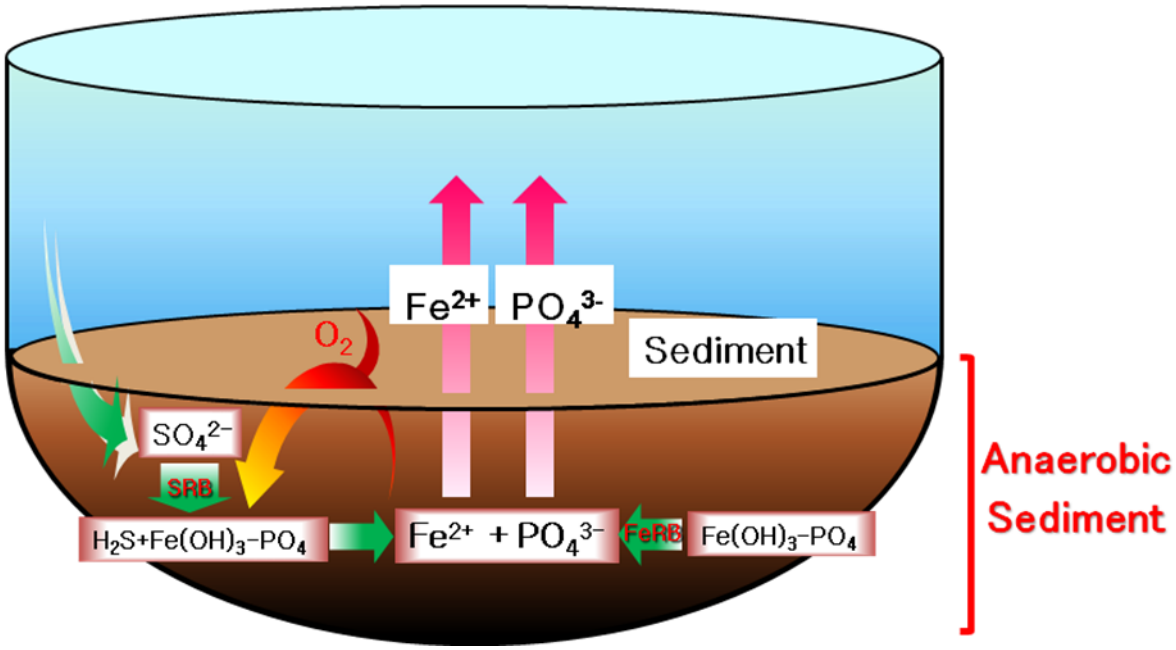

Fig. I-2. Schematic diagram of the release of inorganic phosphorus in anaerobic sediment (modified Wetzel, 2001). SRB and FeRB indicate sulfate-reducing bacteria and ferric-reducing bacteria.

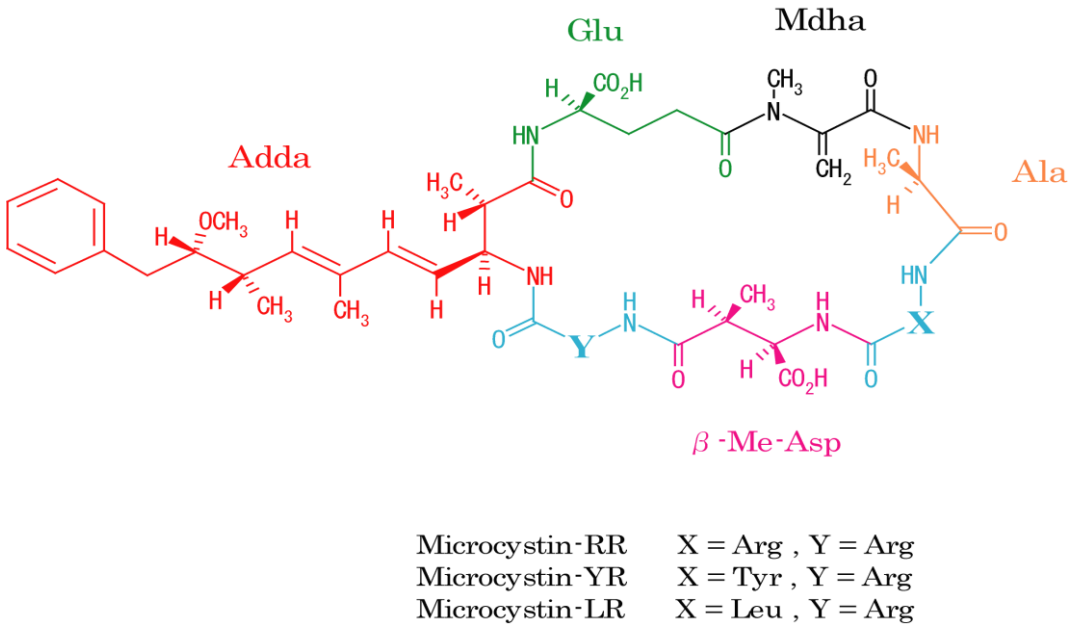

Fig. I-3. General structure of microcystin where X and Y represent variable amino acids.

I.2 Electrooxidation treatment

A DC power supply is connected to two electrodes (anode and cathode) which are placed in the water. Oxygen and hydrogen are generated on the anode and cathode surface, respectively. Oxygen and hydrogen are generated according to the reaction below.

$$2H_2O(l^*) \rightarrow O_2(g^{**}) + 4H^+(aq^{***}) + 4e^- \qquad \text{(I-1)}$$

$$2H_2O(l^*) + 2e^- \rightarrow H_2(g^{**}) + 2OH^-(aq^{***}) \qquad \text{(I-2)}$$

l^*: liquid state, g^{**} : gas state, aq^{***} : aqueous state

The evolution of oxygen and hydrogen reaction equilibria can be determined by the following equations.

$$E_{0(O2)} = 1.23 - 0.06pH \qquad \text{(I-3)}$$

$$E_{0(H2)} = -0.06pH \qquad \text{(I-4)}$$

Fig. I-4 shows the generation potential and pH of oxygen and hydrogen according to equation I-3 and I-4. Oxygen is easily generated under higher pH conditions (Reyter et al., 2010), while hydrogen is easily generated under lower pH conditions. However, oxygen and

hydrogen are generated regardless of the pH value when the potential between the anode and cathode is 1.23V, and the pH value only affects the concentration of gases.

Oxidants (such as hypochlorite, chlorine dioxide, chlorine, hypochlorous acid, hydrogen peroxide, ozone, hydroxyl radical, etc.) can be generated by electrochemical treatment. Oxidants are generated when the actual potential exceeds the oxygen generating potential at the anodic side. Electrochemically generated oxidants are decomposed to other oxidants or oxidize organics (Xu et al., 2007).

Ozone can be generated at the high anodic potentials according to the reaction below (Amadelli et al., 2000):

$$H_2O \rightarrow H^+ + (OH)_{ads} + e^- \qquad \text{(I-5)}$$

$$(OH)_{ads} \rightarrow (O)_{ads} + H^+ + e^- \qquad \text{(I-6)}$$

$$2(O)_{ads} \rightarrow O_2 \qquad \text{(I-7)}$$

$$(O)_{ads} + O_2 \rightarrow O_3 \qquad \text{(I-8)}$$

Ozone can be decomposed by OH^- ions, and hydroxyl radicals are formed according to the reaction below (Kerwick et al., 2005; Szpyrkowicz et al., 2001):

$$O_3 + OH^- \rightarrow HO_2^- + O_2 \qquad \text{(I-9)}$$

$$O_3 + HO_2^- \rightarrow OH^\bullet + O_2^{\bullet -} + O_2 \qquad \text{(I-10)}$$

In the presence of chloride ions, chlorine, hypochlorous acid and hypochlorite ions can thus be produced electrochemically (Szpyrkowicz et al., 2001):

$$Cl^- \rightarrow Cl_{ads}^{\bullet} + e^- \qquad \text{(I-11)}$$

$$2Cl_{ads}^{\bullet} \rightarrow Cl_2 \qquad \text{(I-12)}$$

$$Cl_2 + H_2O \leftrightarrow HClO + H^+ + Cl^- \qquad \text{(I-13)}$$

$$HClO \leftrightarrow H^+ + ClO^- \qquad \text{(I-14)}$$

Hypochlorous Acid (HOCl), ozone (O_3) and hydroxyl radical ($OH^{\bullet}$) are highly reactive and efficiently remove MC-LR (Acero et al., 2005; Onstad et al., 2007). These oxidants can oxidize also *Microcystis* cells.

In the presence of sulphate and bromide ions, $H_2S_2O_8$ and HBrO which are powerful oxidants capable of oxidaising organic molecules can be formed (Tran and Drogui, 2013).

$$2SO_4^{2-} + 2H^+ \rightarrow H_2S_2O_8 + 2e^- \qquad \text{(I-15)}$$

$$Br^- + 2H_2O \rightarrow HBrO + H_3O+ + 2e^- \qquad \text{(I-16)}$$

The oxidation potentials of various chemical oxidants are listed in Table I-1. Oxidation rate for organic materials are generally followed with the oxidation potential. However, discrepancies in the MC-LR removal among different compounds have been

reported (Sharma et al. 2012). Electrochemically generated oxidants are decomposed to other oxidants or to oxidized organics (Xu et al., 2007).

Table I-1. Oxidation potentials and rate constants for MC-LR of chemical oxidants.

Reagent	Oxidation potential (Volts vs. NHE)	Rate constant for MC-LR ($M^{-1}s^{-1}$)	Reference
Hypochlorite (OCl^-)	0.89	6.78	Acero et al. (2005)
Chlorine Dioxide (ClO_2)	1.28	1.20 to 0.80	Kull et al. (2004)
Chlorine (Cl_2)	1.36	-	
Hypochlorous Acid (HOCl)	1.49	1.16×10^2	Acero et al. (2005)
Hydrogen Peroxide (H_2O_2)	1.78	0	Welker and Steinberg (2000)
Ozone (O_3)	2.07	4.1×10^5	Onstad et al. (2007)
Hydroxyl Radical ($^{\bullet}OH$)	2.80	1.1×10^{10}	Onstad et al. (2007)
		2.3×10^{10}	Song et al. (2009)

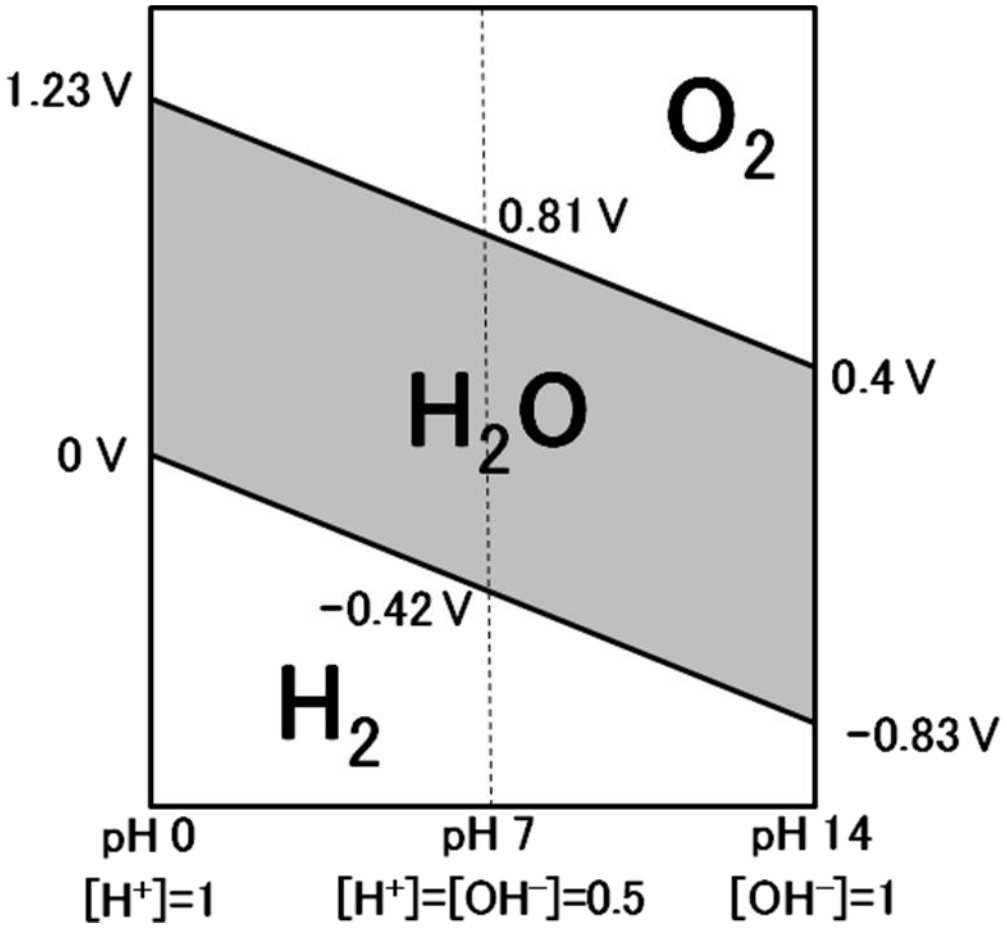

Fig. I-4. Evolution potential of oxygen and hydrogen according to pH variation (equation I-3 and I-4).

I.3 Purpose of this study

Few studies have been conducted to investigate the removal of cyanobacteria and cyanotoxins by electrochemical oxidation. Liang et al. (2005) investigated the removal of *Microcystis aeruginosa* cells by continuous electrochemical treatment using Ti/RuO_2 electrodes and then evaluated the removal efficiency under different current densities. Xu et al. (2007) evaluated the effects of operating conditions such as different electrode materials, current density and agitation on the growth inhibition of *Microcystis aeruginosa*. Shi et al. (2005) investigated the removal efficiency of microcystin-LR and microcystin-RR (MC-LR and MC-RR) under different chlorine concentrations, pH, current densities and initial microcystin (MC) concentrations. Previous studies have focused on improving the removal efficiency by determining the optimum conditions.

However, to the best of our knowledge, no studies have been conducted to investigate the simultaneous removal of *Microcystis* cells and their microcystins by electrochemical oxidation, despite the fact that microcystins present in *Microcystis* cells can be released when the cells are damaged. No studies have been conducted to investigate using constant voltage system.

Nitrogen and phosphorus are nutrients that strongly influence the occurrence of a cyanobacteria bloom. Reyter et al. (2010) showed nitrate can be removed using copper and Ti/IrO_2 coupled electrodes by changing the anode/cathode surface area ratio. Kerwick et al. (2005) reported phosphate adsorption on the cathode. However, the mechanism was not determined.

Therefore, this study was conducted to evaluate the dynamics of simultaneous *Microcystis* and its microcystin removal by electrochemical oxidation. Especially, MC-LR

was divided into intracellular MC-LR and extracellular MC-LR and the cell morphology was observed by scanning electron microscopy (SEM) analysis. The effects of different current densities and algal suspension volume on *Microcystis* cells and MC-LR removal and variations of cells size by electrochemical oxidation were evaluated. The change of cations, nitrogen species and phosphorus species during electrochemical oxidation were evaluated. In addition, I provide a possible mechanism for the removal of phosphorus.

The results of laboratory studies using unicellular strain could not explain natural environmental phenomenon. In addition, the electrode material has a significant impact on the electrochemical kinetics and the reactions occurring. Therefore, this study was conducted to evaluate the possibility of removal for colonial *Microcystis* cells using electrochemical oxidation and removal efficiency of *Microcystis* sp. (colonial cells) by electrode material (Pt/Ti electrode and oxide electrode) of electrochemical oxidation.

Moreover, an electrochemical treatment equipment was established in a pond (Chikato pond, Matsumoto, Japan) and evaluated the change of biomass, nutrient (N and P) and concentration of dissolved oxygen.

References

Acero, J.L., Rodriguez, E., Meriluoto, J. (2005) Kinetics of reactions between chlorine and the cyanobacterial toxins microcystins. Water Research 39, 1628-1638.

Amadelli, R., De Battisti, A., Girenko, D.V., Kovalyob, S.V., Velichenko, A.B. (2000). Electrochemical oxidation of *trans*-3,4-dihydroxycinnamic acid at PbO_2 electrodes: direct electrolysis and ozone mediated reactions compared. Electrochimica Acta 46, 341-347.

Carmichael, W. (1992) Cyanobacteria secondary metabolites—the cyanotoxins. Journal of Applied Microbiology 72(6), 445-459.

Carmichael, W. (2001) Health effects of toxin-producing cyanobacteria:" The CyanoHABs". Human and Ecological Risk Assessment: An International Journal 7, 1393-1407.

Chorus, I., Bartam, J. (1999) Toxic cyanobacteria in water. A guide to their public health consequences, monitoring and managements. WHO.

Comninellis, C., Pulgarin, C. (1993) Electrochemical oxidation of phenol for wastewater treatment using SnO_2 anodes. Journal of Applied Electrochemistry 23, 108-112.

Comninellis, Ch. (1994) Electrocatalysis in the electrochemical conversion/combustion of organic pollutants for waste water treatment. Electrochimica Acta 39, 1857-1862.

Dawson, R. M. (1998) The toxicology of microcystins. Toxicon 36(7), 953-962.

Hoeger, S.J., Hitzfeld, B.C., Dietrich, D.R. (2005) Occurrence and elimination of cyanobacterial toxins in drinking water treatment plants. Toxicology and Applied Phamacology 203, 231–242.

Holst, T., Jørgensen, N. O. G., Jørgensen, C., Johansen, A. (2003) Degradation of microcystin in sediments at oxic and anoxic, denitrifying conditions. Water Research 37, 4748-4760.

Huisman, J., Matthijs, H.C. and Visser, P.P.M. (2005) Harmful cyanobacteria, Springer, Dordrecht, Netherlands.

Kerwick, M.I., Reddy, S.M., Chamberlain, A.H.L., Holt, D.M. (2005) Electrochemical disinfection, an environmentally acceptable method of drinking water disinfection?. Electrochimica Acta 50, 5270-5277.

Kraft, A., Stadelmann, M., Blaschke, M., Kreysig, D., Sandt, B., Schröder, F., Rennau, J. (1999) Electrochemical water disinfection Part I: Hypochlorite production from very dilute chloride solutions. Journal of Applied Electrochemistry 29, 861-868.

Kull, T.P.J., Backlund, P.H., Karlsson, K.M., Meriluoto, J.A.O. (2004) Oxidation of the cyanobacterial hepatotoxin microcystin-LR by chlorine dioxide: reaction kinetics, characterization, and toxicity of reaction products. Environmental Science & Technology 38, 6025-6031.

Lawton, L.A., Edwards, C. (2001) Purification of microcystins (Review). Journal of Chromatography A 912, 191-209.

Liang, W.Y., Qu, J.H., Chen, L.B., Liu, H.J., Lei, P.G. (2005) Inactivation of *Microcystis aeruginosa* by continuous electrochemical cycling process in tube using Ti/RuO_2 electrodes. Environmental Science & Technology 39, 4633-4639.

Onstad, G.D., Strauch, S., Meriluoto, J., Codd, G.A., Gunten, U.V. (2007) Selective oxidation of key functional groups in cyanotoxins during drinking water ozonation.

Environmental Science & Technology 41, 4397-4404.

Pouria, S., de Andrade, A., Barbosa, J., Cavalcanti, R. L., Barreto, V. T. S., Ward, C. J., Preiser, W., Poon, G. K., Neild, G. H., Codd, G. A. (1998) Fatal microcystin intoxication in haemodialysis unit in Caruaru, Brazil. The Lancet 352, 21-26.

Reyter, D., Bélanger, D., Roué, L. (2010) Nitrate removal by a paired electrolysis on copper and Ti/IrO_2 coupled electrodes – Influence of the anode/cathode surface area ratio. Water Research 44, 1918-1926.

Sharma, V.K., Triantis, T.M., Anoniou, M.G., He, X.X., Pelaez, M., Han, C.S., Song, W.H., O'Shea, K.E., De La Cruz, A.A., Kaloudis, T., Hiskia, A., Dionysiou, D.D. (2012) Destruction of microcystins by conventional and advanced oxidation processes: A review. Separation and Purification Technology 91, 3-17.

Shi, H.X., Qu, J.H., Wang, A.M., Ge, J.T. (2005) Degradation of microcystins in aqueous solution with in situ electrogenerated active chlorine. Chemosphere 60(3), 326-333.

Sivonen, K. and Jones, G. (1999) Cyanobacterial toxins, in I. Chorus and J. Bartram (eds.). Toxic Cyanobacteria in Water: a guide to their public health consequences, monitoring, and management, 41-111.

Song, W.H., Xu, T.L., Cooper, W.J., Dionysiou, D.D., De La Cruz, A.A., O'Shea, K.E. (2009) Radiolysis studies on the destruction of microcystin-LR in aqueous solution by hydroxyl radicals. Environmental Science & Technology 43, 1487-1492.

Stucki, S., Kötz, R., Carcer, B., Suter, W. (1991) Electrochemical waste water treatment using high overvoltage anodes Part II: Anode performance and applications. Journal of Applied Electrochemistry 21, 99-104.

Szpyrkowicz, L., Juzzolino, C., Kaul, S.N. (2001) A comparative study on oxidation of disperse dyes by electrochemical process, ozone, hypochlorite and fenton reagent. Water Research 35, 2129-2136.

Tanaka, S., Nakata, Y., Kimura, T., Yustiawati, Kawasaki, M. Kuramitz, H. (2002) Electrochemical decomposition of bisphenol A using Pt/Ti and SnO_2/Ti anodes. Journal of Applied Electrochemistry 32, 197-201.

Tran, N., Drogui, P. (2013) Electrochemical remocal of microcystin-LR from aqueous solution in the presence of natural organic pollutants. Journal of Environmental Management 114, 253-260.

Ueno, Y., Nagata, S., Tsutsumi, T., Hasegawa, A., Watanabe, M., Park, H.D., Chen, G., Chen, G., Yu, S. (1996) Detection of microcystins, a blue-green algal hepatotoxin, in drinking water sampled in Haimen and Fusui, endemic areas of primary liver cancer in China, by highly sensitive immunoassay. Carcinogenesis 17, 1317-1321.

Welker, M., Steinberg, C. (2000) Rates of humic substance photosensitized degradation of microcystin-LR in natural waters. Environmental Science & Technology 34, 3415-3419.

Wetzel, R. (2001) Limnology, 3 E. Lake and River Ecosystems. Academic Press, 525 B Street, Ste. 1900, San Diego, CA 92101, USA.

Xu, Y.F., Yang, J., Ou, M.M., Wang, Y.L., Jia, J.P. (2007) Study of *Microcystis aeruginosa* inhibition by electrochemical method. Biochemical Engineering Journal 36, 215-220.

II. The removal of *Microcystis ichthyoblabe* cells and its hepatotoxin microcystin-LR during electrooxidation process using Pt/Ti electrodes

II.1 Introduction

Current drinking water treatment systems cannot remove all contaminants from freshwater supplies containing toxic cyanobacteria blooms. Therefore, if algal cells and their toxins enter drinking water supplies, they pose a serious threat to human health (Hoeger et al., 2005).

Harmful organic materials can be effectively removed by a process called electrooxidation. In numerous recent studies, electrooxidation has been investigated in water disinfection, bisphenol A removal, and organic pollutant decontamination (Kerwick et al., 2005; Kraft et al., 1999; Tanaka et al., 2002; Comniellis and Pulgarin, 1993; Comninellis, 1994; Stucki et al., 1991).

However, few studies have investigated the removal of cyanobacteria and cyanotoxins by electrooxidation. Liang et al. (2005) investigated the removal of *Microcystis aeruginosa* cells by continuous electrochemical treatment using Ti/RuO_2 electrodes, and evaluated the removal efficiency at different current densities. Xu et al. (2007) varied the electrode materials, current density and agitation of electrooxidation, and evaluated the consequent effects on the growth inhibition of *M. aeruginosa*. Shi et al. (2005) investigated the removal efficiency of MC–LR and microcystin–RR (MC–RR) at different chlorine concentrations, pH, current densities and initial microcystin (MC) concentrations. Tran and Drogui (2013) investigated MC–LR removal in the presence of natural organic pollutants. These studies focused on determining the optimal conditions for efficient removal.

However, the simultaneous removal of *Microcystis* cells and their microcystins by electrooxidation has yet to be investigated, and forms the topic of the present paper. Such study is important, because microcystins present in *Microcystis* cells can be released when the cells are damaged.

In addition, the applied charge for removal of *Microcystis* cells and their microcystins was measured. The effect of algal suspension volume was also evaluated. The cell morphology and cell size distribution was observed by scanning electron microscopy (SEM) analysis and particle analyzer, respectively.

II.2 Materials and methods

II.2.1 Strain and culture conditions

A unialgal culture of *Microcystis ichthyoblabe* strain, TAC95 (Tsukuba Algae Collection, National Science Museum) was used in this study. TAC95 was cultured in the late exponential growth phase or early stationary growth phase, which was entered after 14 days' incubation in batch mode containing 10 L sterilized MA medium (Table II-1). Cultures were incubated at (23 ± 1) °C under continuous (24 h light cycle) illumination of approximately 16 μmol m^{-2} s^{-1}. TAC95 is known to produce MC–LR alone (Yokoyama and Park, 2003).

To investigate the effects of electrooxidation on free MC–LR, algal cells were removed from the solution (4 L) by autoclaving for 30 min at 121°C.

II.2.2 Conditions of electrooxidation process

Fig. II-1 is a schematic of the electrooxidation reactor. The cultured cells were directly introduced into the sterilized electrochemical reactor. The volume of the algal solutions (*Microcystis* cells + MA medium) to be treated was 4 L and 34 L. The anode and cathode materials for both volumes were Pt coated onto Ti substrate, and the electrode dimensions were 50 mm × 200 mm × 1 mm. The surface area immersed in the algal solution was 100 cm^2, and the anode–cathode separation was 5 mm. During the electrooxidation, the solution was agitated by a magnetic stirrer (150–250 rpm) and 10 V was maintained throughout the experiments by a DC power supply. All electrochemical oxidation treatments were carried out under ca. 16 μmol m^{-2} s^{-1} illumination with a 24 h light cycle at (23 ± 1) °C.

The conductivity of the algal solution was measured by an electrical conductivity meter (HEC-110, DKK-TOA Co., Tokyo, Japan).

II.2.3 Analysis of cell density, cell size and cell morphology

At certain points in the treatment, a 60 mL sample was harvested and divided into 10 mL and 50 mL aliquots. The 10 mL aliquots were fixed with formaldehyde (final concentration = 2%) (Han et al., 2012). Next, a small amount of each fixed sample was pipetted into a Fuchs–Rosenthal hemocytometer, and the cells were counted under the microscope at 400× magnification (BK51, Olympus, Tokyo, Japan). From the same 10 mL sample, a second small amount was withdrawn for particle concentration and diameter measurements, performed by a Multisizer 4 Particle Analyzer (Beckman Coulter, Fullerton, Canada). The remainder of the 10 mL sample was retained for cell morphology analysis. For this purpose, samples were dehydrated in ethanol at graded concentrations (50–100%), after which the 100% ethanol content was substituted by *t*–butyl alcohol. The samples were then freeze-dried (JFD–310, JEOL, Tokyo, Japan), and finally deposited with osmium (Osmium coater Neo–AN, Meiwafosis Co., Ltd., Tokyo, Japan). The cell morphology was measured under a scanning electron microscope (SEM) (JSM–7600F, JEOL, Tokyo, Japan).

II.2.4 Analysis of microcystin

The MC–LR concentrations were measured as described by Xie et al. (2007). Briefly, the 50 mL sample aliquots were filtered through a glass–fiber filter (GF/C, Whatman, Maidstone, UK) and immediately freeze-dried at −80°C (FDU–2100, EYELA, Tokyo, Japan).

The freeze-dried filters were then weighed. For intracellular MC–LR analysis, the freeze-dried filters were homogenized and extracted by 5% aqueous acetic acid. The supernatant was applied to an HLB cartridge (0.5 g, Oasis, Waters, Milford, MA, USA) preconditioned with MeOH (10 mL) and distilled water (10 mL). For extracellular MC–LR analysis, the filtered water (the 50 mL sample) was directly applied to the HLB cartridge. The intracellular and extracellular MC–LR was eluted from the HLB cartridge by MeOH. The MeOH solution containing MC–LR was injected into a high–performance liquid chromatography (HPLC) machine for analysis.

The HPLC system consisted of a Shimadzu (Kyoto, Japan) LC–9A pump coupled to a SPD–10A set to 238 nm, an SPD–M10A photodiode array detector, and a C–R6A integrator and ODS column (Cosmosil 5C18–MS–II; 4.6 mm × 150 mm, Nacalai Tesque, Kyoto, Japan). The sample was separated using a mobile phase of methanol:0.05 M phosphate buffer (pH 3.0, 58:42) applied at a flow rate of 1 mL/min. The MC–LR concentration was quantified against MC–LR standards (Kanto Ltd., Tokyo, Japan).

Table II-1. Composition of MA medium for culturing *Microcystis ichthyoblabe* strain TAC 95.

Components	**Concentration (mg/L)**
$Ca(NO_3)_2 \cdot 4H_2O$	50
KNO_3	100
$NaNO_3$	50
Na_2SO_4	40
$MgCl_2 \cdot 6H_2O$	50
β-Na_2 glycerophosphate	100
Na_2EDTA	5
$FeCl_3 \cdot 6H_2O$	0.5
$MnCl_2 \cdot 4H_2O$	5
$ZnCl_2$	0.5
$CoCl_2 \cdot 6H_2O$	5
$NaMoO_4 \cdot 2H_2O$	0.8
H_3BO_3	20
Bicine	500
pH	8.6

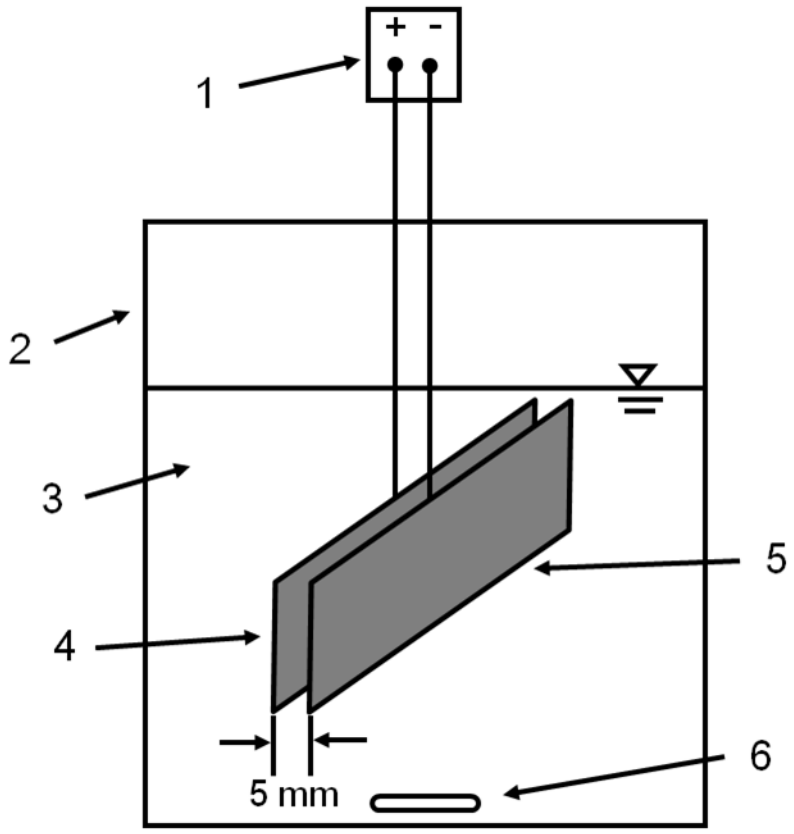

Fig. II-1. Schematic of the electrochemical method reactor: (1) DC power supply; (2) Electrolysis chamber made of acrylic resins; (3) *M. ichthyoblabe* suspension (4 L or 34 L); (4) Anode electrode composed of Pt-coated Ti substrate (surface area (200 mm ×50 mm) = 100 cm^2); (5) Cathode electrode (same composition and size as the anode electrode). The anode and cathode are separated by 5 mm; (6) Magnetic stirring bar. All experiments were performed in an isothermal room at (23 ± 1) °C.

II.3 Results and discussion

II.3.1 Cell density and morphology changes

Table II-2 lists the conditions of all experiments undertaken in this study. In trials 1–4 and trial 7, the initial extracellular MC–LR concentration was non-zero, probably because MC–LR was released from the naturally dead cells. Trials 5 and 6 were autoclaved at 121°C for 30 min to remove algal cells, and contained only MC–LR.

Fig. II-2 plots the cell density as a function of time in trials 1–4. The cell density was reduced by 97% after 12 h in trials 1 and 4, and after 23 h in trials 2 and 3 (Fig. II-2a). However, as shown in Fig. II-2b, a charge of 3×10^4 C reduced the cell density by 97% in all four trials, irrespective of initial cell density and initial algal solution conductivity.

Changes in cell morphology resulting from the electrooxidation process were investigated by SEM analysis. As shown in Fig. II-3a, the surfaces of *M. ichthyoblabe* cells in the control group were undamaged, and both single cells and dividing cells (DCs) were visible. However, the treated cells were broken, and in some cases only the cell membranes remained (indicated by arrows in Fig. II-3 b, c and d).

Fig. II-4 (a) and (b) plots the size–concentration distribution of the untreated and treated cells, respectively. The reported size of *M. ichthyoblabe* cells is 2.0–3.2 μm (Komárek, 1991). However, in this study, the *M. ichthyoblabe* diameters ranged from 2.5 to 3.5 μm (Fig. II-4), possibly because the particle analyzer measured both single and dividing cells. The frequency of dividing cells in the control was constant (21.3 ± 1.6%), whereas the concentration of 2.5–3.5 μm particles increased over time (Fig. II-4a).

Under an applied charge of 3.2×10^4 C (see Fig. II-4b), the concentration of 2.5–3.5 μm *M. ichthyoblabe* cells decreased, while that of 2.0–2.5 μm particles first increased (arrow 1), and then declined (arrow 2). These results indicate damage and size reduction in *M. ichthyoblabe* cells subjected to the electrooxidation process.

Table II-2. Conditions of all experiments carried out in this study.

Experiments	Initial cell density ($\times 10^6$ Cells mL^{-1})	Initial intracellular MC–LR conc. ($\mu g\ L^{-1}$)	Initial extracellular MC–LR conc. ($\mu g\ L^{-1}$)	Current density at 0 h ($mA\ cm^{-2}$)	Initial conductivity of solution ($\mu S\ cm^{-1}$)	Algal solution volume (L)
Trial 1	1.41	47.40	28.33	4.2	247	4
Trial 2	2.08	59.67	83.13	6.5	368	4
Trial 3	2.08	59.11	83.13	6.8	385	4
Trial 4	2.97	118.54	27.03	3.6	209	4
Trial 5	0	0	146.21	10.4	-	4
Trial 6	0	0	133.81	10.4	-	4
Trial 7	3.01	112.66	25.12	3.8	212	34

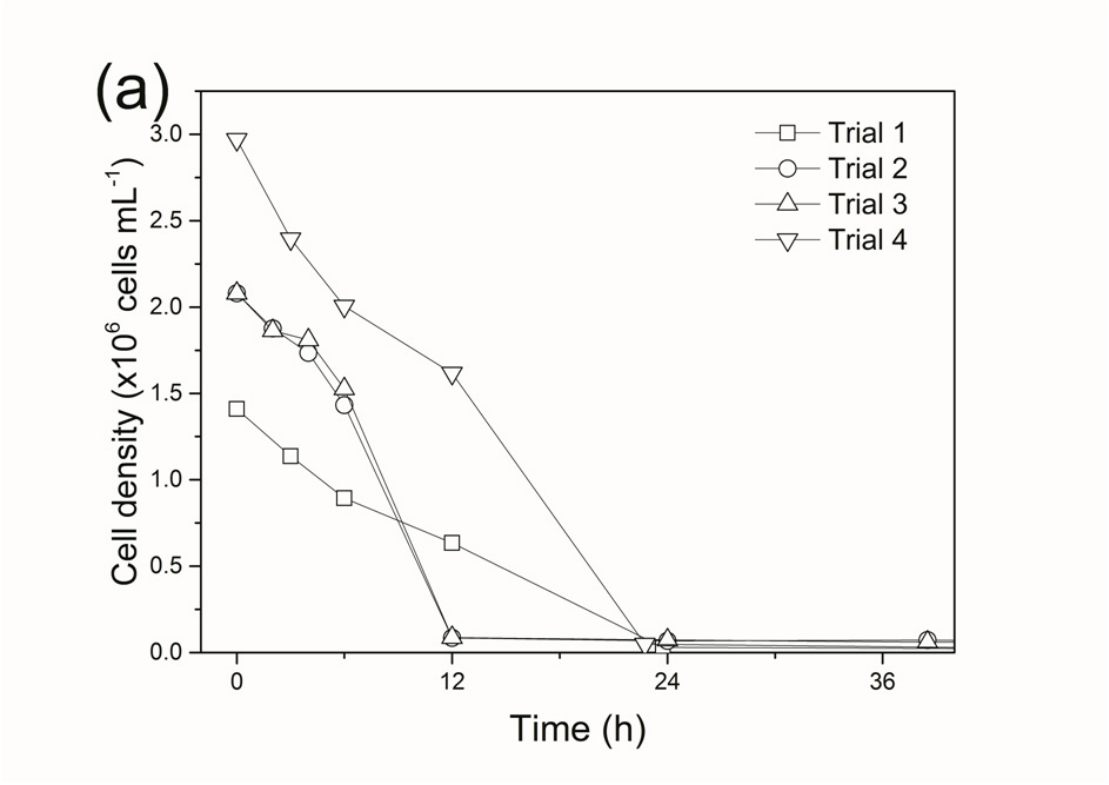

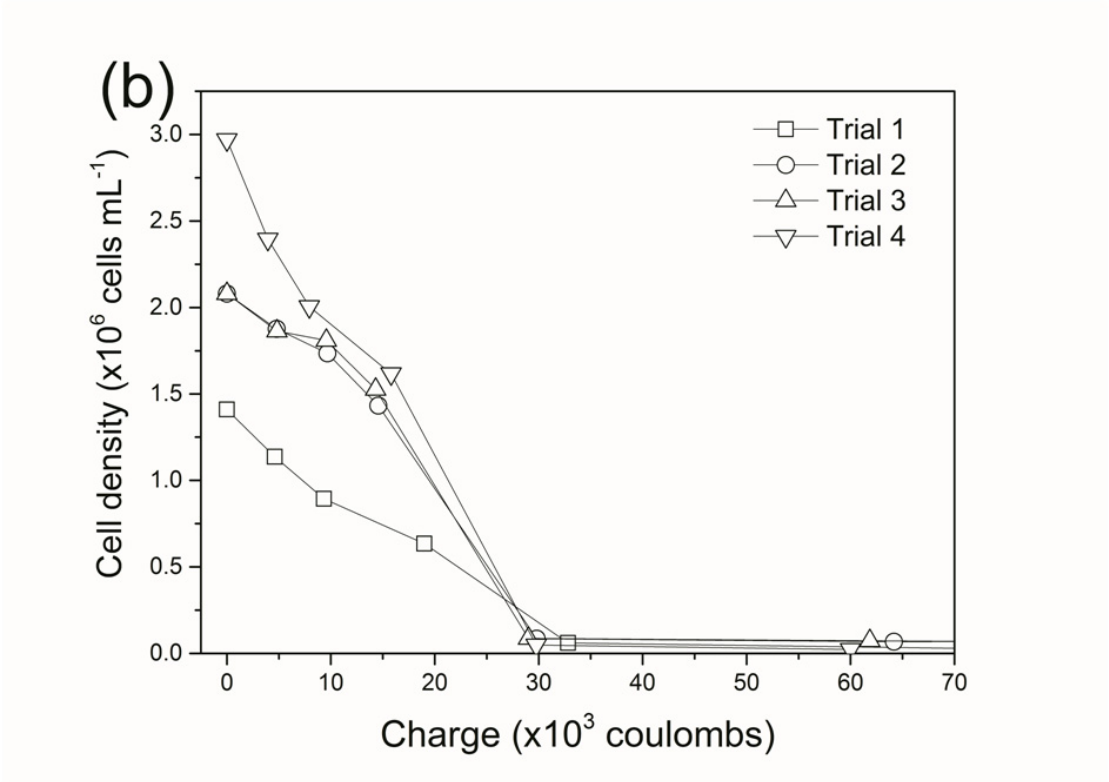

Fig. II-2. Cell densities in Trials 1–4 of Table II-2 as functions of (a) time; (b) applied charge.

(a)

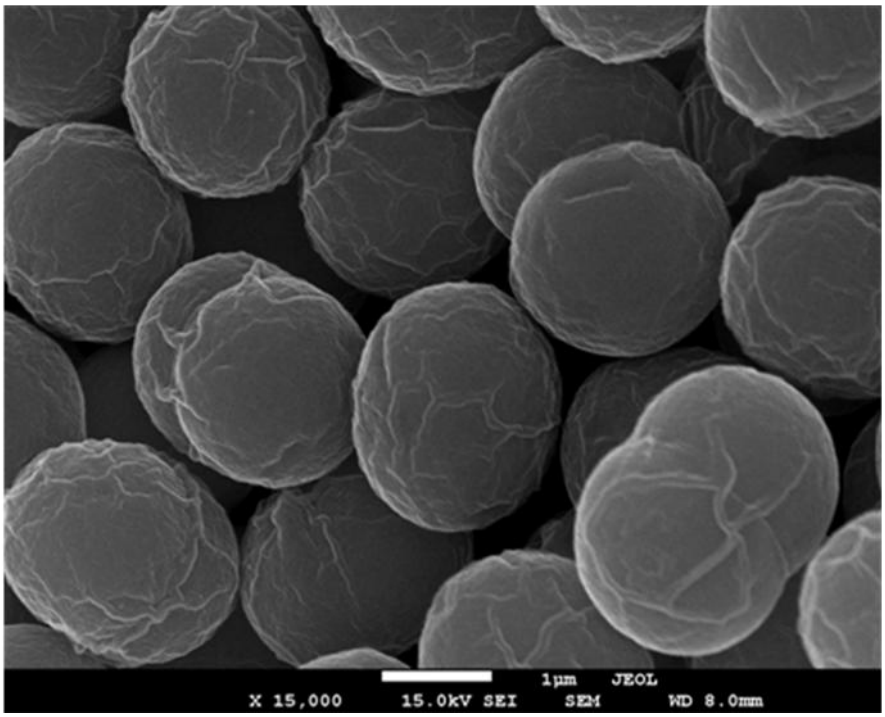

(b)

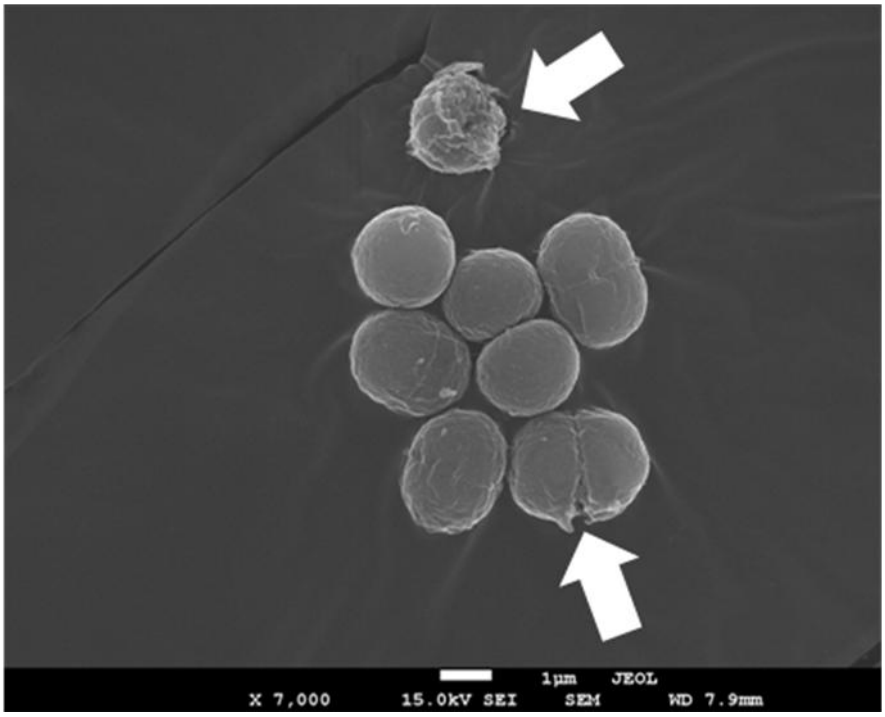

(Continued)

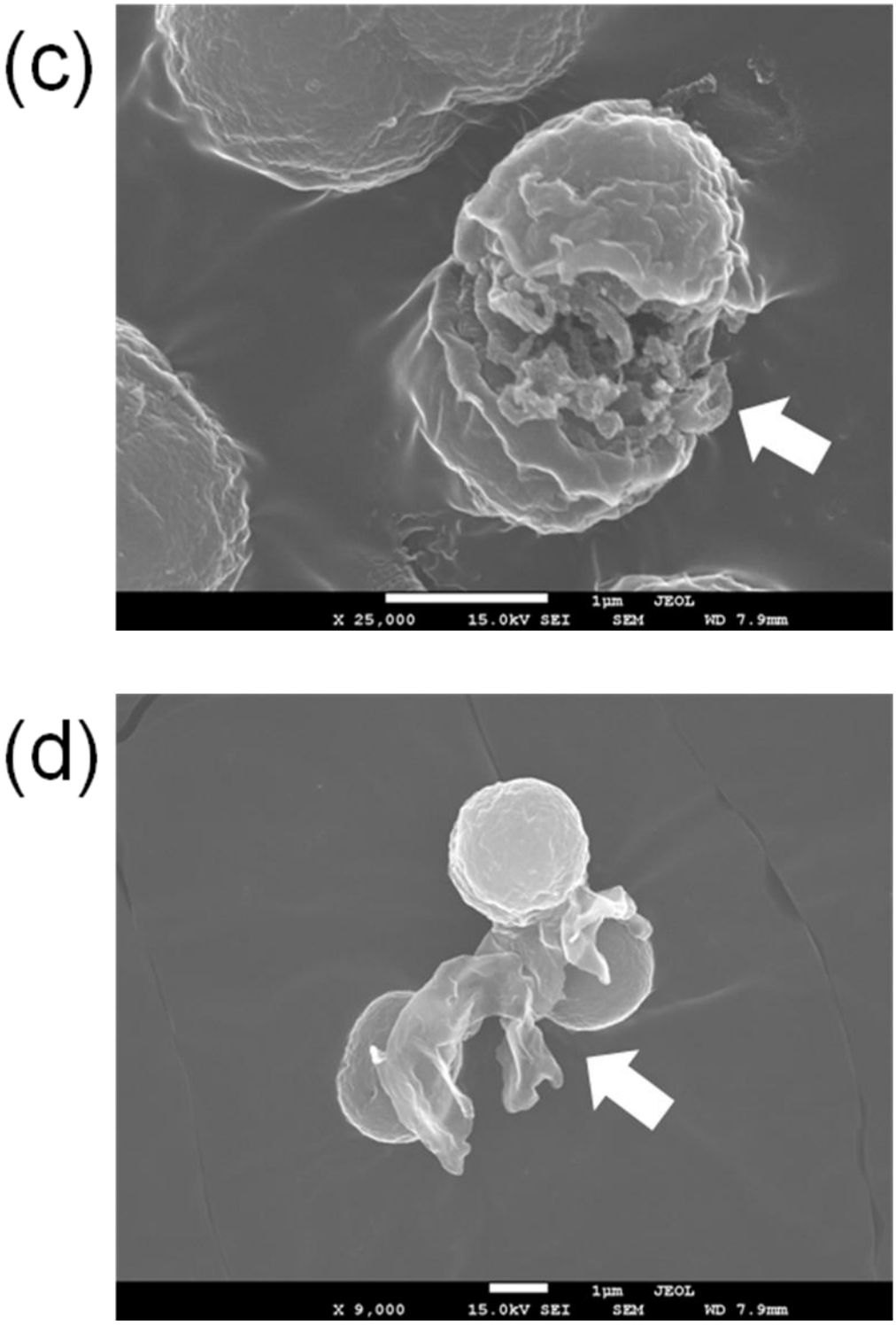

Fig. II-3. SEM images of untreated cells (a) and cells at an applied charge of 1.2×10^4 C in Trial 1 of Table II-2 (b, c and d). The arrows point to broken cells. The white bar indicates 1 μm.

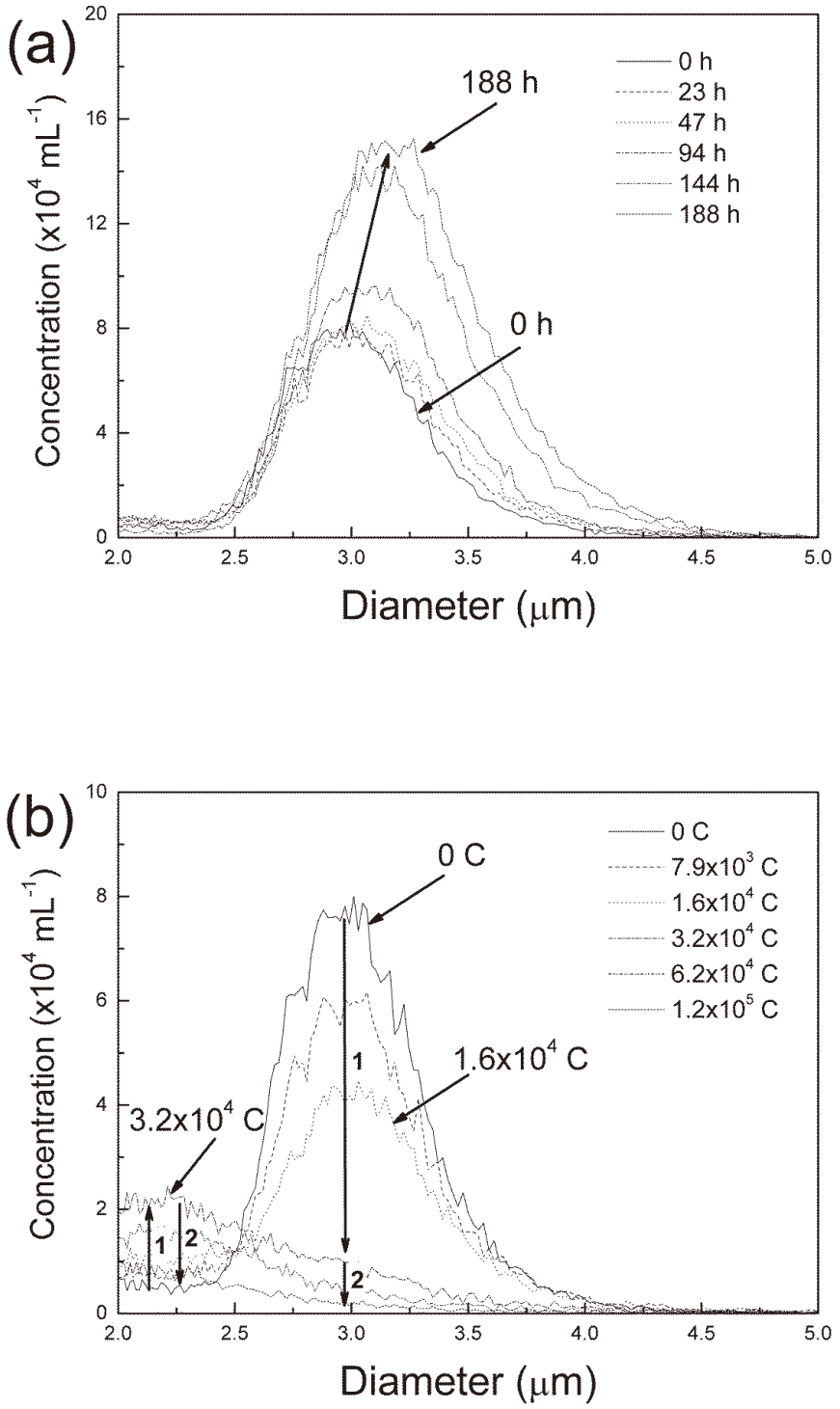

Fig. II-4. Particle concentration distributions with respect to diameter: (a) untreated cells; (b) Trial 1 of Table II-2.

II.3.2 Variations in MC–LR concentration

The total MC–LR concentration is the sum of the intracellular and extracellular MC–LR concentrations (Fig. II-5a and b, respectively), and is plotted as a function of applied charge in Fig. II-5c. The effects of charge on the free MC–LR concentration (without algal cells; Trials 5 and 6) are also plotted in Fig. II-5c.

The intracellular MC–LR rapidly decreased with increasing applied charge. The trends are similar to the cell degradation trends (Fig. II-2a), reflecting the release of intracellular MC–LR from damaged cells. Both cell density and intracellular MC–LR were reduced by 97% at an applied charge of approximately 3×10^4 C.

The extracellular MC–LR concentration was raised by the intracellular MC–LR release during the initial treatment, but decreased thereafter (Fig. II-5b). The total MC–LR fell to below detectable levels under an approximate charge of 6×10^4 C. Cell-free MC-LR displayed similar trends, and was similarly undetectable at around 6×10^4 C. Although the algal cells were removed by autoclave treatment in trials 5 and 6, cellular-derived organic materials might remain in the solution. These organic materials might influence the efficiency of MC–LR removal.

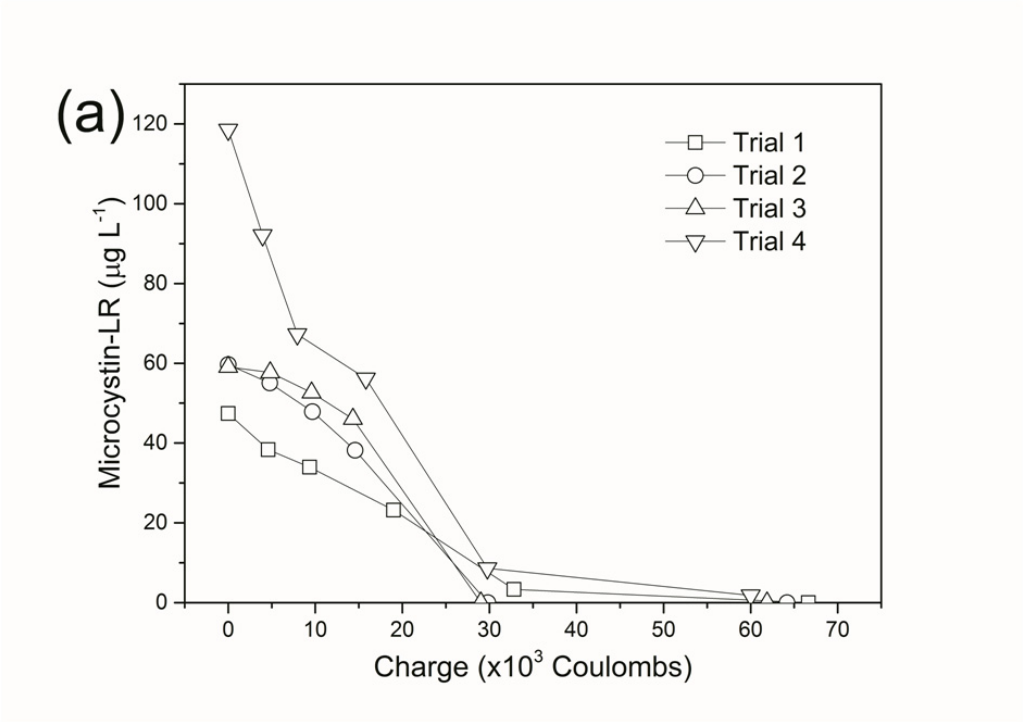
(a)
Trial 1
Trial 2
Trial 3
Trial 4
Microcystin-LR (μg L-1)
Charge (x10^3 Coulombs)
0
20
40
60
80
100
120
0
10
20
30
40
50
60
70

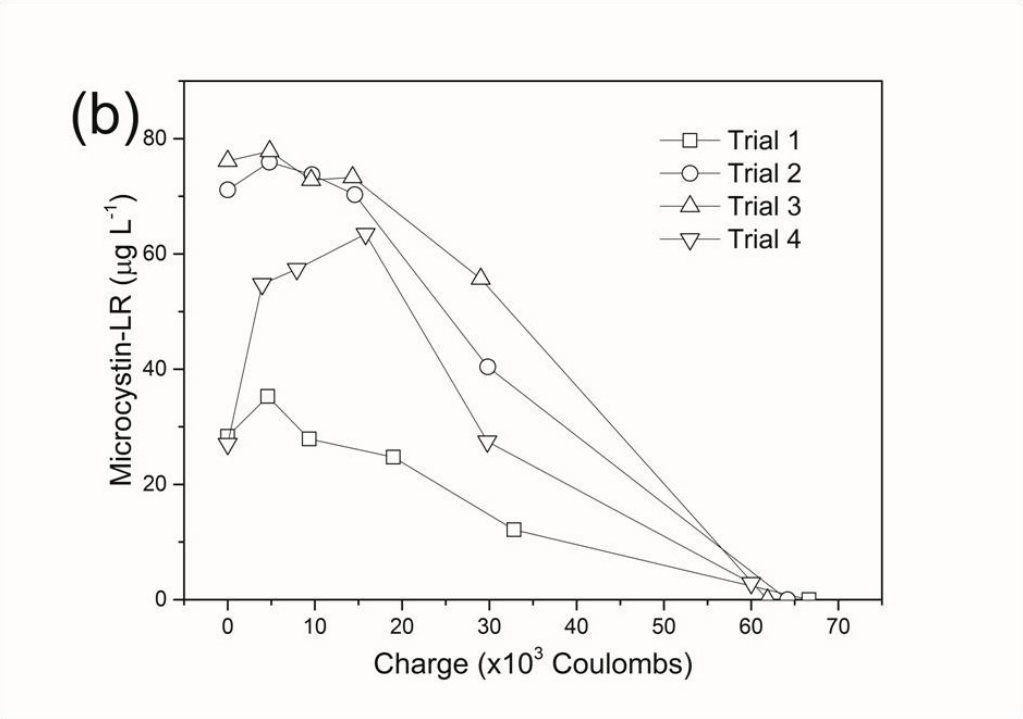
(b)
Trial 1
Trial 2
Trial 3
Trial 4
Microcystin-LR (μg L-1)
Charge (x10^3 Coulombs)
0
20
40
60
80
0
10
20
30
40
50
60
70

(Continued)

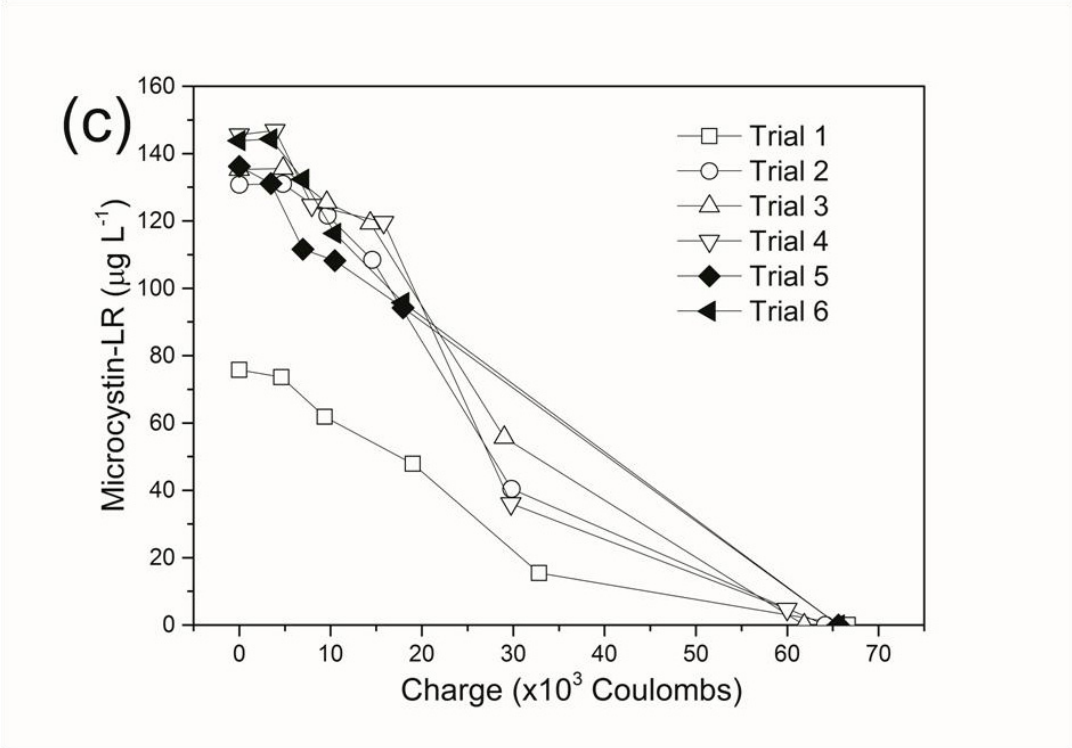

Fig.II- 5. Effect of applied charge on (a) intracellular MC–LR; (b) extracellular MC–LR; and (c) total MC–LR concentration in Trials 1–6 of Table II-2. The total MC–LR concentration is the sum of the intracellular and extracellular MC–LR concentrations.

II.3.3 Effect of algal suspension volume

Two volumes of algal solutions (4 L (Trial 4) and 34 L (Trial 7)) were prepared and subjected to electrooxidation. Plotted as a function of applied charge (Fig. II-6a), the intracellular MC–LR concentration trended similarly to the cell degradation. The intracellular MC–LR was reduced to negligible levels under an applied charge of 3×10^4 C in Trial 4, but more than 15% of the MC–LR remained under 20×10^4 C in Trial 7. Similar results appear in the plots of extracellular MC–LR (Fig. II-6b) and total MC–LR (Fig. II-6c).

In the constant-voltage electrooxidation treatment, the charge applied to the *M. ichthyoblabe* cells and MC–LR was fixed and the removal efficiency was independent of initial cell density, initial MC–LR concentration and solution conductivity. However, the removal efficiency was greatly reduced at the higher algal suspension volume. These findings indicate that *M. ichthyoblabe* cells and their MC–LR can be effectively removed by reducing the treatment volume.

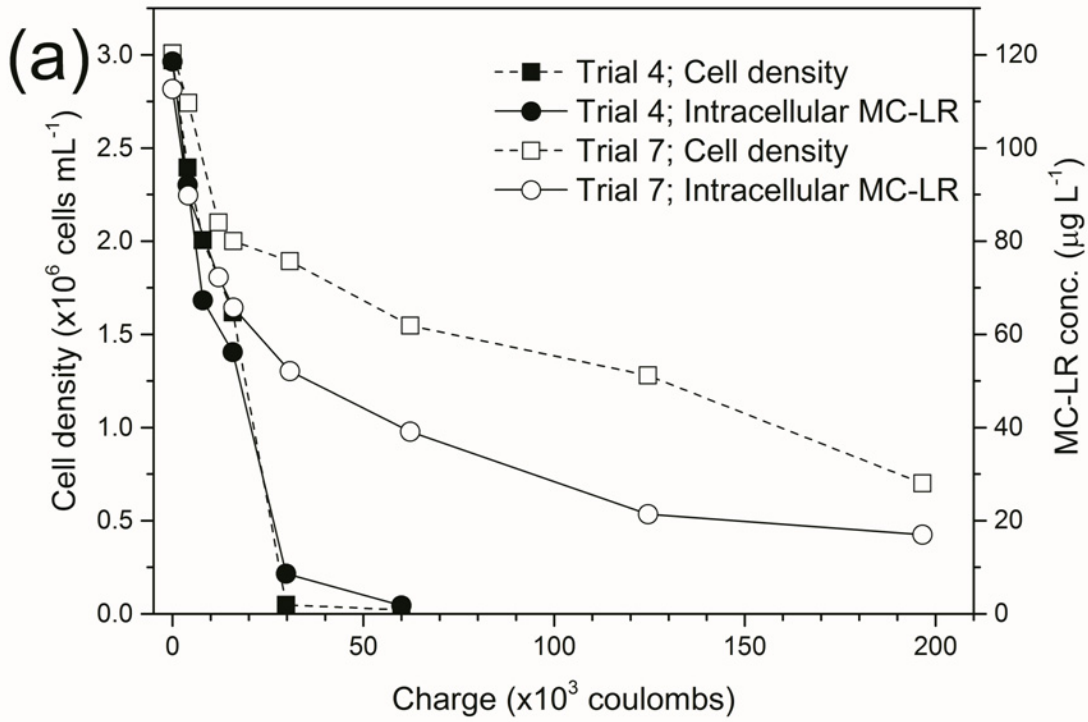
(a)
Trial 4; Cell density
Trial 4; Intracellular MC-LR
Trial 7; Cell density
Trial 7; Intracellular MC-LR
Cell density (x10^6 cells mL^-1)
MC-LR conc. (µg L^-1)
Charge (x10^3 coulombs)
0.0
0.5
1.0
1.5
2.0
2.5
3.0
0
20
40
60
80
100
120
0
50
100
150
200

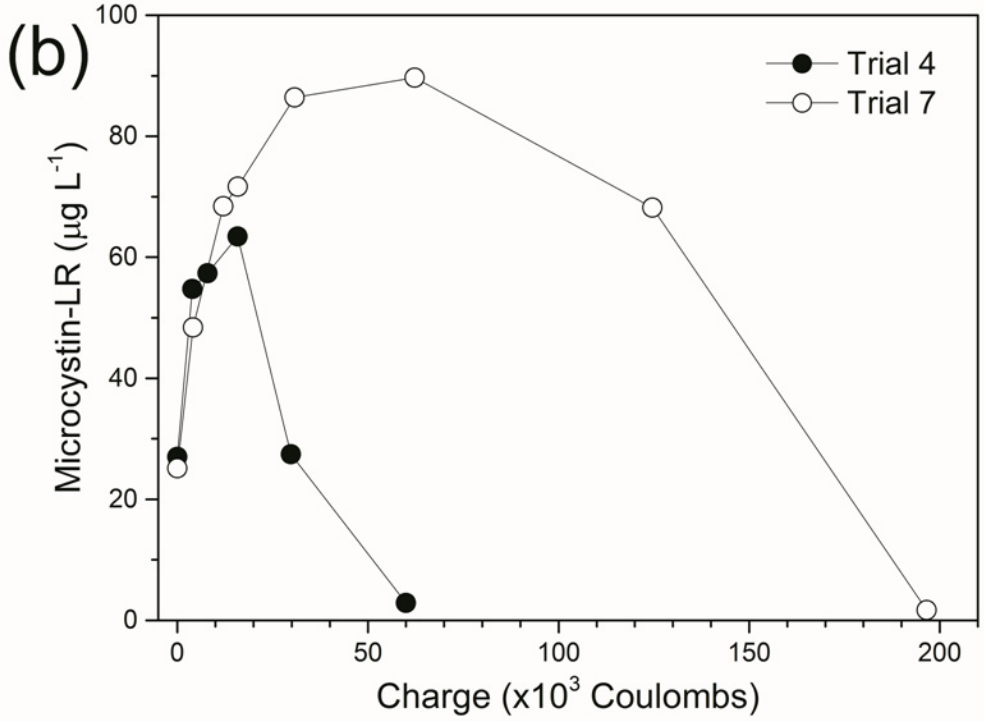
(b)
Trial 4
Trial 7
Microcystin-LR (µg L^-1)
Charge (x10^3 Coulombs)
0
20
40
60
80
100
0
50
100
150
200

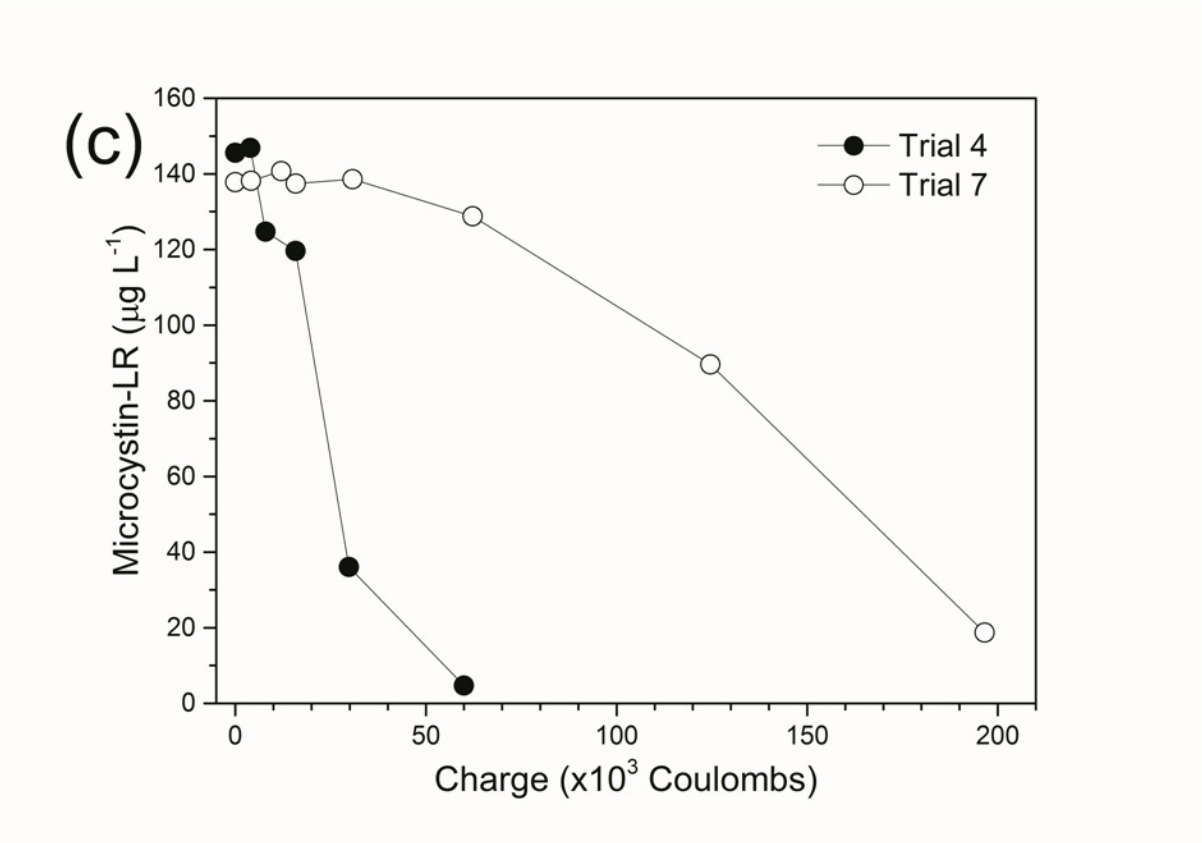

Fig. II-6. Effect of applied charge on (a) cell density and intracellular MC–LR concentration; (b) extracellular MC–LR concentration; and (c) total MC–LR concentration. Results are plotted for Trials 4 and 7 of Table II-2.

II.3.4 Variation in current density

As shown in Fig. II-7a, the current densities altered over time. Current density is known to be sensitive to factors such as voltage, electrode material and electrolyte conductivity. Therefore, given that the voltage and electrode materials were unchanged throughout the study, the current density was likely affected by the conductivity of the algal solution. In addition, the current density and the conductivity of the algal solution were highly correlated (Fig. II-7b). Conductivity is also affected by several factors. Liang et al. (2005) reported that conductivity was increased by electrolysis of bicine, which is added to MA medium as a buffering agent. Ionic matter released from the damaged *M. ichthyoblabe* cells would also raise the conductivity. Conversely, the released ionic matter could be deposited on the cathode surface, thereby reducing the conductivity.

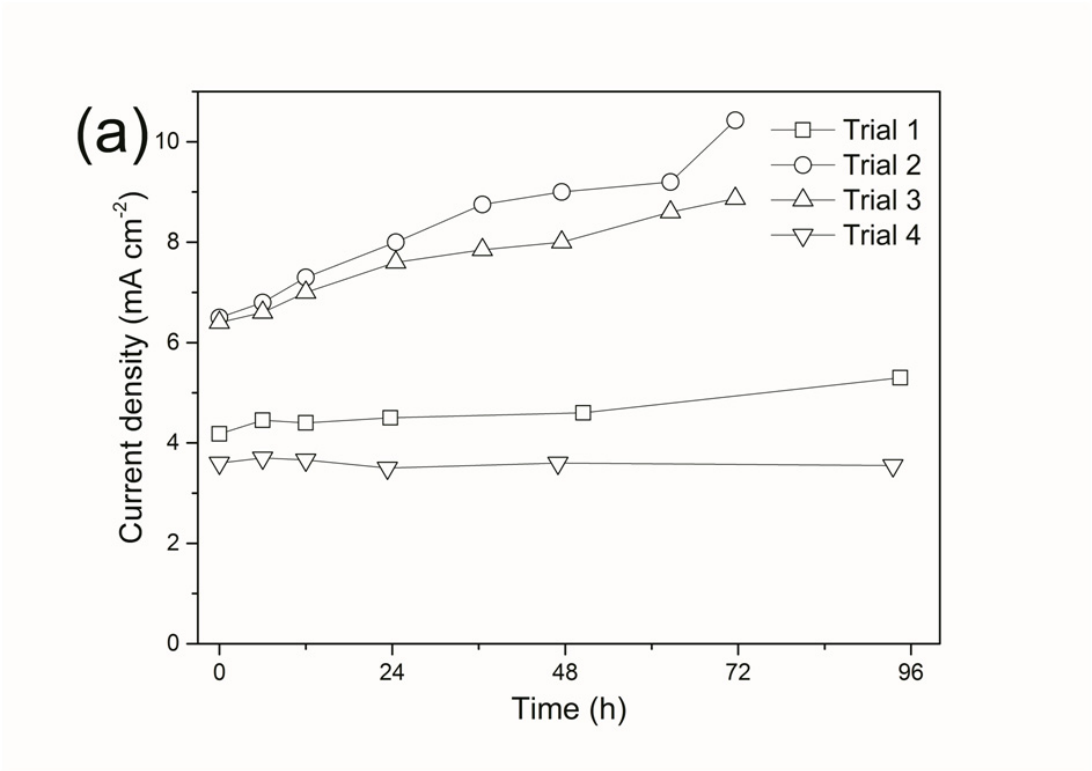

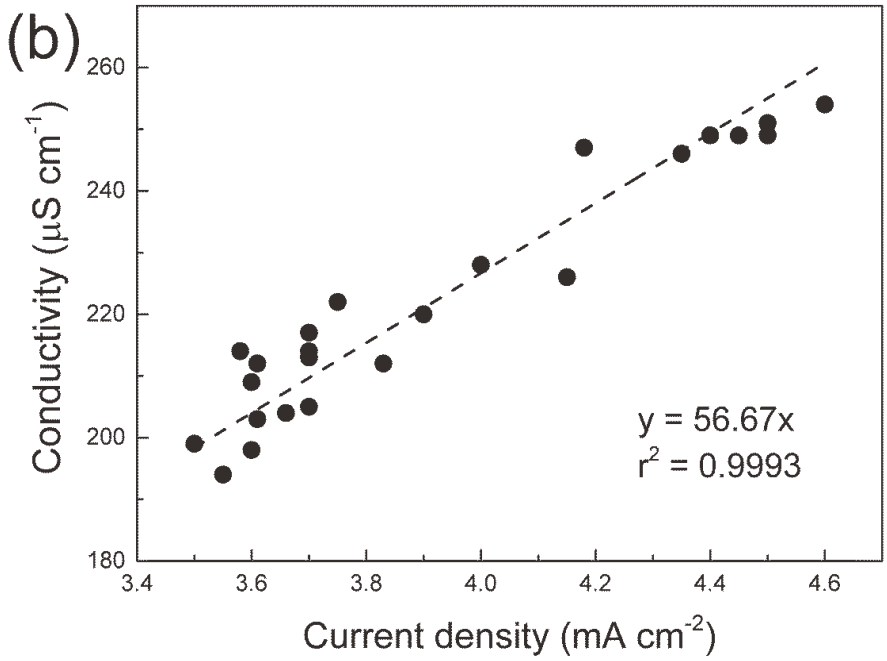

Fig. II-7. Analysis of the electrooxidation process: (a) temporal changes in current density, and (b) relationship between current density and conductivity.

References

Comninellis, Ch., Pulgarin, C. (1993) Electrochemical oxidation of phenol for wastewater treatment using SnO_2 anodes. J. Appl. Electrochem. 23 (2), 108–112.

Comninellis, Ch. (1994) Electrocatalysis in the electrochemical conversion/combustion of organic pollutants for waste water treatment. Electrochim. Acta 39 (11–12), 1857–1862.

Han, J.S., Jeon, B.S., Park, H.D. (2012) Cyanobacteria cell damage and cyanotoxin release in response to alum treatment. Water sci. Technol. 12 (5), 549–555.

Hoeger, S.J., Hitzfeld, B.C., Dietrich, D.R. (2005) Occurrence and elimination of cyanobacterial toxins in drinking water treatment plants. Toxicol. Appl. Phamacol. 203, 231–242.

Kerwick, M.I., Reddy, S.M., Chamberlain, A.H.L., Holt, D.M. (2005) Electrochemical disinfection, an environmentally acceptable method of drinking water disinfection? Electrochim. Acta 50 (25–26), 5270–5277.

Komárek, J. (1991) A review of water–bloom forming *Microcystis* species, with regard to populations from Japan. Algological Studies 64, 115–127.

Kraft, A., Stadelmann, M., Blaschke, M., Kreysig, D., Sandt, B., Schröder, F., Rennau, J. (1999) Electrochemical water disinfection Part I: Hypochlorite production from very dilute chloride solutions. J. Appl. Electrochem. 29 (7), 861–868.

Liang, W.Y., Qu, J.H., Chen, L.B., Liu, H.J., Lei, P.G. (2005)Inactivation of *Microcystis aeruginosa* by continuous electrochemical cycling process in tube using Ti/RuO_2

electrodes. Environ. Sci. Technol. 39 (12), 4633–4639.

Shi, H.X., Qu, J.H., Wang, A.M., Ge, J.T. (2005) Degradation of microcystins in aqueous solution with in situ electrogenerated active chlorine. Chemosphere 60 (3), 326–333.

Stucki, S., Kötz, R., Carcer, B., Suter, W. (1991) Electrochemical waste water treatment using high overvoltage anodes Part II: Anode performance and applications. J. Appl. Electrochem. 21 (2), 99–104.

Tanaka, S., Nakata, Y., Kimura, T., Yustiawati, Kawasaki, M., Kuramitz, H. (2002) Electrochemical decomposition of bisphenol A using Pt/Ti and SnO_2/Ti anodes. J. Appl. Electrochem. 32 (2), 197–201.

Tran, N., Drogui, P. (2013) To achieve more effective removal of harmful algal cells and their toxins. J. Environ. Manage. 114, 253–260.

Xie, L.Q., Yokoyama, A., Nakamura, K., Park, H.D. (2007) Accumulation of microcystins in various organs of the freshwater snail Sinotaia histrica and three fishes in a temperate lake, the eutrophic Lake Suwa, Japan. Toxicon 49 (5), 646–652.

Xu, Y.F., Yang, J., Ou, M.M., Wang, Y.L., Jia, J.P. (2007) Study of *Microcystis aeruginosa* inhibition by electrochemical method. Biochem. Eng. J. 36 (3), 215–220.

Yokoyama, A., Park, H.D. (2003) Depuration kinetics and persistence of the cyanobacterial toxin microcystin–LR in the freshwater bivalve *Unio douglasiae*. Environ. Toxicol. 18 (1), 61–67.

III. The variation in concentration of cations (Na^+, K^+ and Ca^{2+} ions) and nutrient species (N and P) during electrochemical treatment

III.1 Introduction

Nitrogen and phosphorus are nutrients that strongly influence the occurrence of a cyanobacteria bloom. Reyter et al. (2010) showed nitrate can be removed using copper and Ti/IrO_2 coupled electrodes by changing the anode/cathode surface area ratio. Kerwick et al. (2005) reported phosphate adsorption on the cathode. However, the mechanism was not revealed or elucidated.

Therefore, this study was conducted to evaluate the change of cations, nitrogen species and phosphorus species during electrochemical oxidation. In addition, I provide a possible mechanism for the removal of phosphorus.

III.2 Materials and methods

III.2.1 Algal culture

A unialgal culture of *Microcystis ichthyoblabe* (TAC95 strain; Tsukuba Algae Collection, National Science Museum) was used in this study. TAC95 was cultured in the late exponential growth phase or early stationary growth phase that corresponded to 14 days after inoculation in batch mode containing the sterilized 10 L MA medium (Table II-1) under illumination at approximetely 16 μmol m^{-2} s^{-1} and a 24 h light cycle at 23 ± 1 °C.

III.2.2 Apparatus

The electrochemical oxidation reactor was same with chapter 2 (see Fig. 2-1). The volume of the algal solutions (*Microcystis* cells + MA medium) to be treated was 4 L. The anode and cathode were made of Pt coated on a Ti substrate, and the dimensions of the electrode were 50 mm wide by 200 mm in diameter. The surface area immersed in the algal solution was 100 cm^2, and the distance between the anode and cathode was 5 mm. Agitation during treatment was provided by a magnetic stirrer (at about 200 rpm) and a potential of 10 V was maintained between the electrodes throughout the experiments with a DC power supply.

III.2.3 Concentraion of cations (Na^+, K^+ and Ca^{2+} ions)

Ten-mL aliquots were filtered through a glass-fiber filter (GF/C, Whatman, Maidstone, UK) and the filtered water was injected into a ion chromatograph (IC) for analysis.

The IC system consisted of a JASCO (Tokyo, Japan) PU-1580i pump with a column

(Shodex IC YK-421; 4.6 mm × 125 mm, Showa denko, Tokyo, Japan) coupled to a DG-1580-53 degasser, a CO-1565 oven, and a Showa Denko (Tokyo, Japan) Shodex CD-5 conductivity detector. The analytes were separated using a mobile phase consisting of 5 mM tartaric acid, 1 mM dipicolinic acid (pyridine-2,6-dicarboxylic acid) and 50 mM boric acid at a flow rate of 1 mL/min.

III.2.4 Nitrogen analysis

Total nitrogen (TN) and dissolved total nitrogen (DTN) were measured according to the method of Otsuki (1981). NH_4 ion was measured according to the method of Solorzano (1969). NO_2 and NO_3 ions were measured by ion chromatography (DX-500, DIONEX Co., Sunnyvale, US). Particulate organic nitrogen (PON) and dissolved organic nitrogen (DON) were calculated by the following equations:

$$PON = TN - DTN \qquad \text{(III-1)}$$

$$DON = DTN - (NH_4\text{-}N + NO_2\text{-}N + NO_3\text{-}N) \qquad \text{(III-2)}$$

III.2.5 Phosphorus analysis

Total phosphorus (TP) and dissolved total phosphorus (DTP) were measured according to the method of Menzel and Corwin (1965). Dissolved inorganic phosphorus (DIP) was measured according to the method of Murphy and Riley (1965). Particulate organic phosphorus (POP) and dissolved organic phosphorus (DOP) were calculated by the following equations:

$$POP = TP - DTP \quad \text{(III-3)}$$

$$DOP = DTP - DIP \quad \text{(III-4)}$$

III.2.6 Analysis of the deposits on the cathode

Deposits on the cathode were removed by scraping and dried at 60 °C for 48 h. The deposits were coated with osmium (Osmium coater Neo-AN, Meiwafosis Co., Ltd., Tokyo, Japan). The morphology and element compositions were investigated using a scanning electron microscope (SEM) (JSM-7600F, JEOL, Tokyo, Japan) coupled with energy-dispersive X-ray spectroscopy (EDS) (X-max, Oxford Instruments, Abingdon, Oxfordshire, UK).

To investigate the crystallinity of the deposits, X-ray diffraction (XRD) analysis was carried out. Half of each deposit sample was annealed at 550 °C for 2 h, and the other was analyzed without further treatment. They were then measured using an XRD (Ultima IV, Rigaku Co., Tokyo, Japan) and intensity data were collected over the 2θ range of 10–60° in steps of 0.02° (Cu Kα radiation).

III.3 Results and discussion

III.3.1 Variations in the concentration of cations (Na^+, K^+ and Ca^{2+} ions)

Fig. III-1 shows the variations in the concentration of cations of the solutions when separated from the living *Microcystis* cells with and without the electrochemical oxidation. The concentration of Na^+ ions and K^+ ions with the electrochemical oxidation increased gradually compared with the control (Fig. III-1a and b, respectively). The cell density of *Microcystis* cells decreased by 96% over 12 h (see Fig. II-2 in chapter II); however, the concentration of Na^+ ions and K^+ ions gradually increased after the same time period. K^+ ions are known to be released from damaged cell membranes (Zhou et al., 2013). In addition, particle analysis of the *Microcystis* cells shows that the size of the *Microcystis* cells with the electrochemical oxidation gradually decreased (see Fig II-4 in chapter II). Thus it appears that Na^+ ions and K^+ ions were extracted into the solution by the disintegration of the cells.

As shown in Fig. III-1c, the concentration of Ca^{2+} ions gradually decreased. They could be decreased because of deposition onto the cathode surface (Kraft et al. 1999):

$$Ca^{2+} + HCO_3^- + OH^- \rightarrow CaCO_3 + H_2O \qquad \text{(III-5)}$$

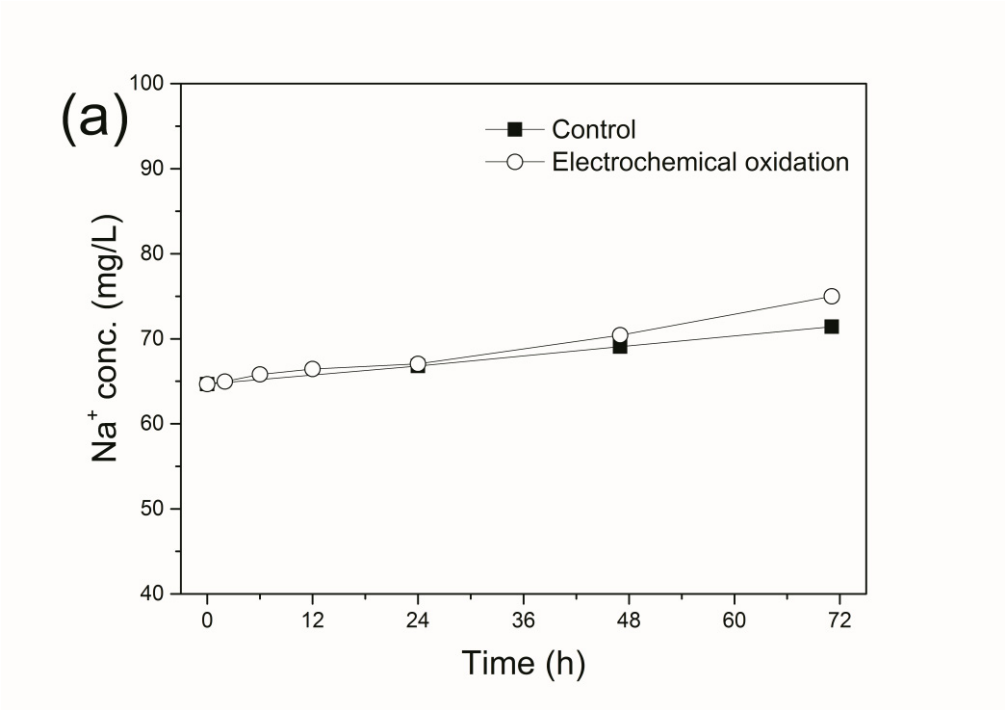
(a)
Control
Electrochemical oxidation
Na+ conc. (mg/L)
Time (h)
100
90
80
70
60
50
40
0
12
24
36
48
60
72

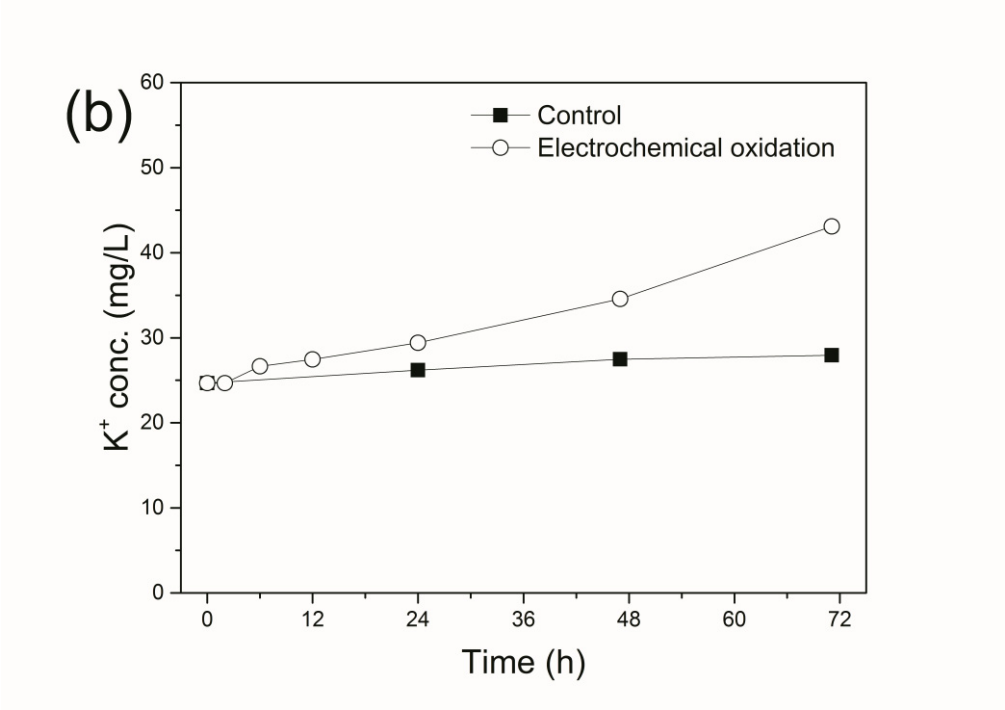
(b)
Control
Electrochemical oxidation
K+ conc. (mg/L)
Time (h)
60
50
40
30
20
10
0
0
12
24
36
48
60
72

(Continued)

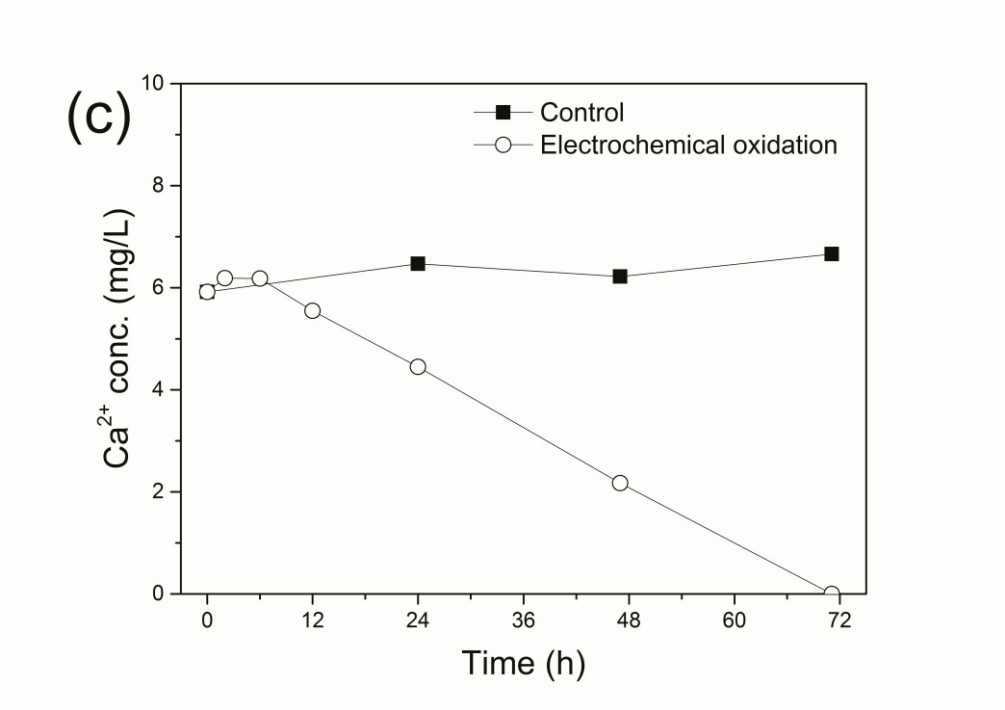

Fig III-1. Variation in concentration of cations. (a) Na^{+}, (b) K^{+} and (c) Ca^{2+}. The results are from a single experiment.

III.3.2 Variations in nitrogen species

Fig. III-2 shows the variations in nitrogen species. PON decreased gradually because of removal of the algal cells, in agreement with the cell density results (see Fig. II-2 in chapter II). TN is the sum of PON, DON, NO_3-N, NO_2-N and NH_4-N (Fig. III-2a). TN was maintained by the electrochemical oxidation.

As shown in Fig. III-2b, DON increased during initial treatment period (12 h) owing to cell degradation (PON→DON), after which it decreased. NO_2-N gradually decreased and was not detectable after 12 h. NO_3-N rapidly increased during 12 h compared with the increase after 12 h. NO_2-N could be oxidized to NO_3-N on the anode surface. After 12 h, DON gradually decreased. On the other hand, NO_3-N and NH_4-N gradually increased. DON could be oxidized to NO_3-N on the anode surface and deoxidized to NH_4-N on the cathode surface.

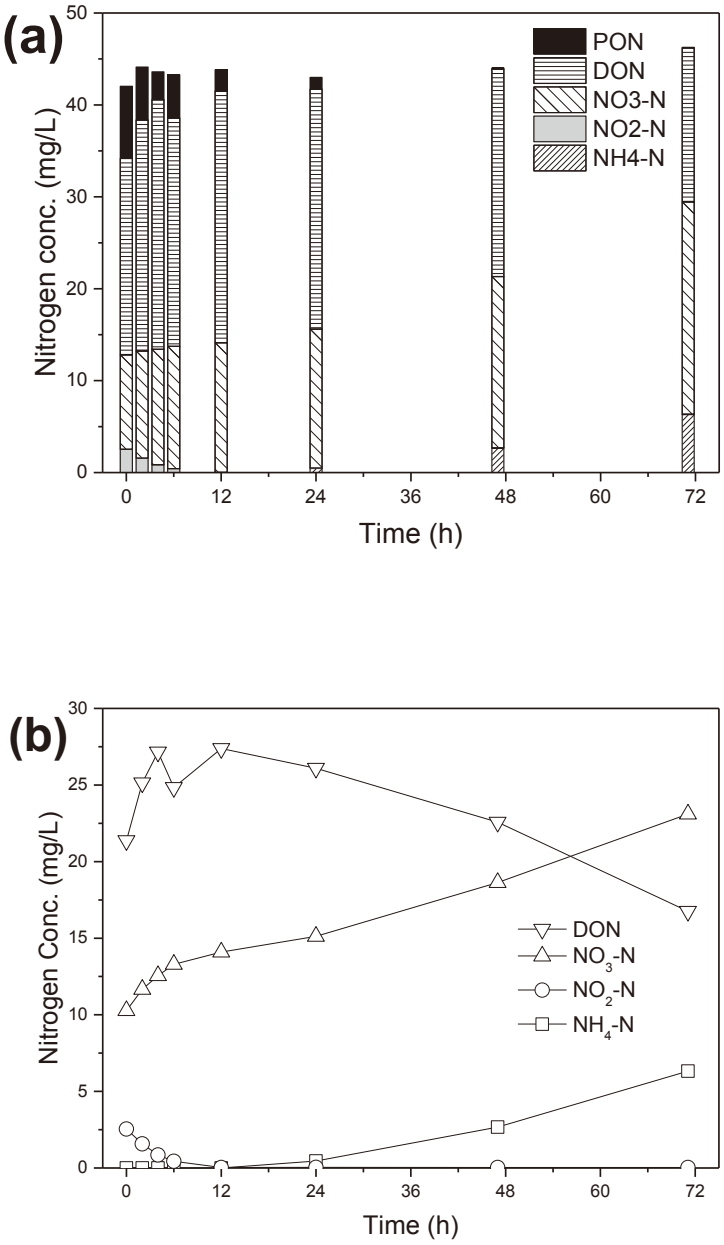

Fig. III-2. Variation in nitrogen species. (a); PON, DON, NO_3-N, NO_2-N and NH_4-N, TN is the sum of PON, DON, NO_3-N, NO_2-N and NH_4-N. (b); DON, NO_3-N, NO_2-N and NH_4-N. The results are from a single experiment.

III.3.3 Variations in phosphorus species

Fig. III-3 shows the variations in TP, POP, DOP and DIP. TP is the sum of POP, DOP and DIP. TP decreased by 29% over 71 h. POP was not detected in the samples after 6 h in agreement with the cell density results (see Fig. II-2 in chapter II).

DIP increased from 3.92 to 4.83 mg/L during the initial 12-h period, and then decreased. DOP increased from 2.72 to 3.09 mg/L during the initial 24 h period, and then remained constant. The increase of DIP and DOP in the initial treatment period is most likely due to release from the disintegration of the algal cells.

Overall, the decrease in phosphorous caused by the decrease of DIP resulted from the deposit on the cathode surface.

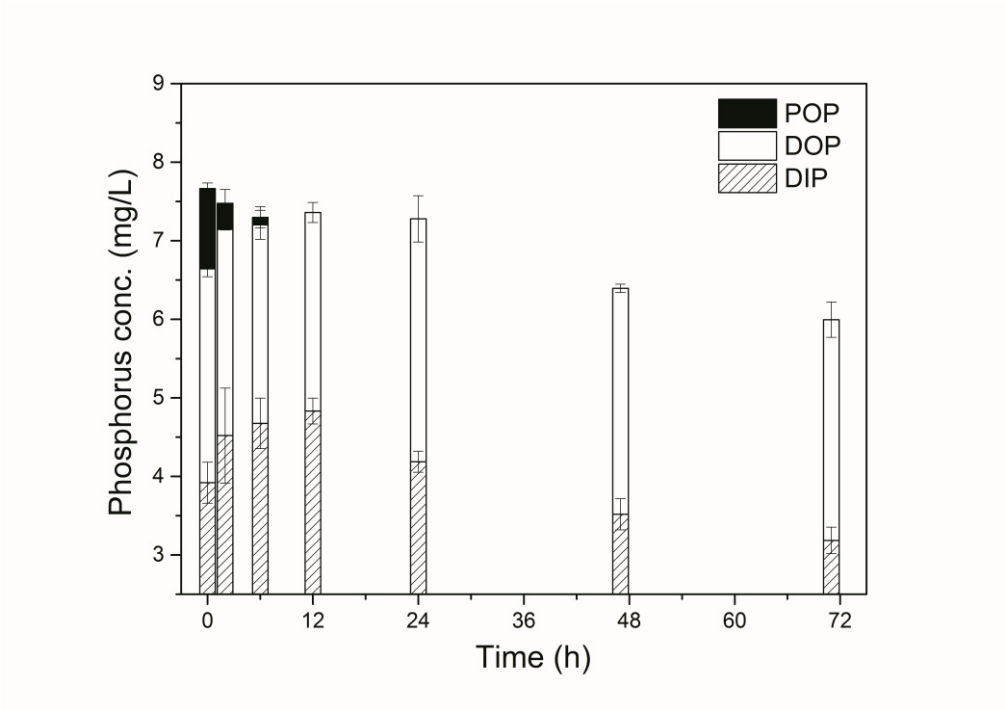

Fig. III-3. Variation in POP, DOP and DIP. TP is the sum of POP, DOP and DIP. The results shown are mean data from triplicate experiments, and error bars indicate standard deviations.

III.3.4 Analysis of the deposits on the cathode surface

Fig. III-4 shows the SEM image of the deposits from the cathode surface. Table III-1 shows the elemental composition (C, O, P and Ca) for each spectrum collected from the sample. As shown in Fig. III-4 and Table III-1, Ca was not distributed uniformly, with high levels of Ca detected in spectra 1, 4 and 5. Therefore, Ca was deposited in grains on the cathode electrode.

High levels of P were detected in spectra 4 and 5, which also contained high levels of Ca and O. This implies P is being deposited as calcium phosphates. As the solubility of calcium phosphates decreases with increasing pH, calcium phosphates deposit on the cathode because the pH increases in turn because of the reduction of H^+ ions (Monma, 1994). The pH of the algal solutions during the electrochemical oxidation was maintained at 8.0 to 8.3 throughout the experiment. However, the pH in the vicinity of the anode and cathode were below 3 and greater than 12, respectively.

The materials seen in spectra 2 and 3 contained high levels of C. Therefore, they could be derived from algal cells and deposited on the cathode.

XRD analysis was conducted to investigate the crystallinity of the deposits. Fig. III-5 shows the XRD patterns of the deposits from the cathode, with and without annealing at 550 °C for 2 h. The deposits appeared to be amorphous. To investigate any potential crystallinity of the deposits, they were annealed at 550 °C for 2 h. $CaCO_3$ and $CaHPO_4$ (monetite) were detected in the annealed samples. $CaHPO_4$ (monetite) and/or $CaHPO_4{\cdot}2H_2O$ (brushite) can be deposited electrochemically on the cathode surface according to the equations:

$$Ca^{2+} + HPO_4^{2-} \rightarrow CaHPO_4 \qquad \text{(III-6)}$$

$$Ca^{2+} + HPO_4^{2-} + 2H_2O \rightarrow CaHPO_4{\cdot}2H_2O \qquad \text{(III-7)}$$

However, monetite was detected only in the annealed sample, most likely because brushite converts to monetite at approximately 220 °C (Dosen and Giese, 2011).

Overall, P and Ca were deposited as $CaHPO_4$ and/or $CaHPO_4{\cdot}2H_2O$. On the other hand, Ca was deposited not only as $CaHPO_4$ and/or $CaHPO_4{\cdot}2H_2O$, but also as $CaCO_3$ on the cathode surface. The removal rate of phosphorus was 0.03 mg/L/h (0.13 μg/L/C).

Table III-1. The contents of components for the spectra 1-5 of Fig. III-4.

Spectra	Components (wt%)			
	C	O	P	Ca
1	+	++	-	++
2	+++	++	-	-
3	+++	++	-	-
4	++	+	+	++
5	++	+	+	++

-, $x \leq 1$;

+, $1 < x \leq 20$;

++, $20 < x \leq 50$;

+++, $50 < x$.

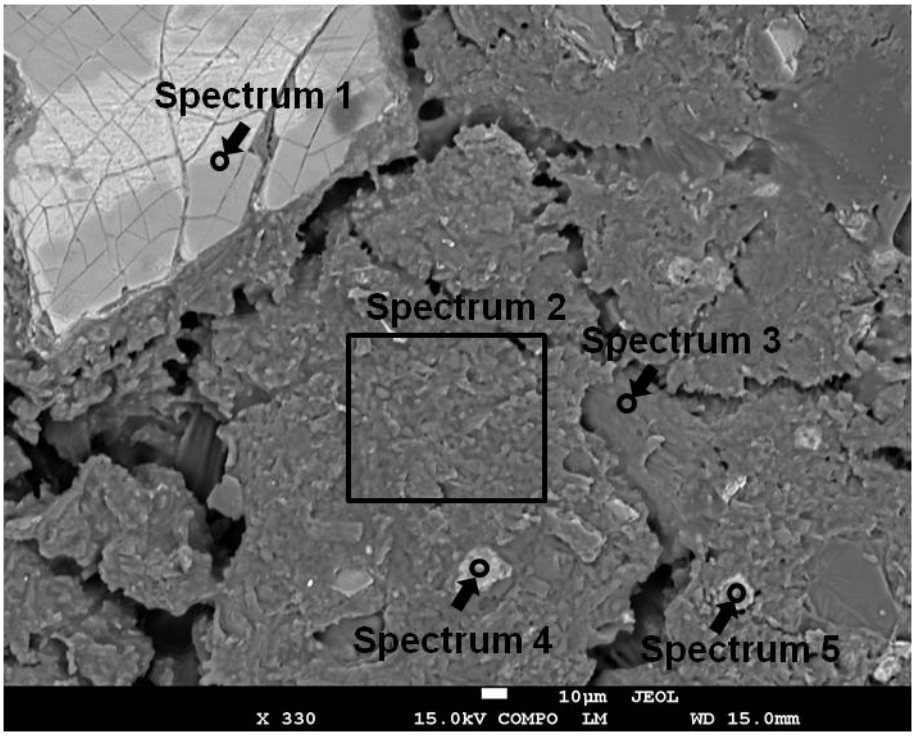

Fig. III-4. SEM image of the deposits from the cathode surface. Spectra 1 to 5 were analyzed by EDS, and the results are shown in Table III-1.

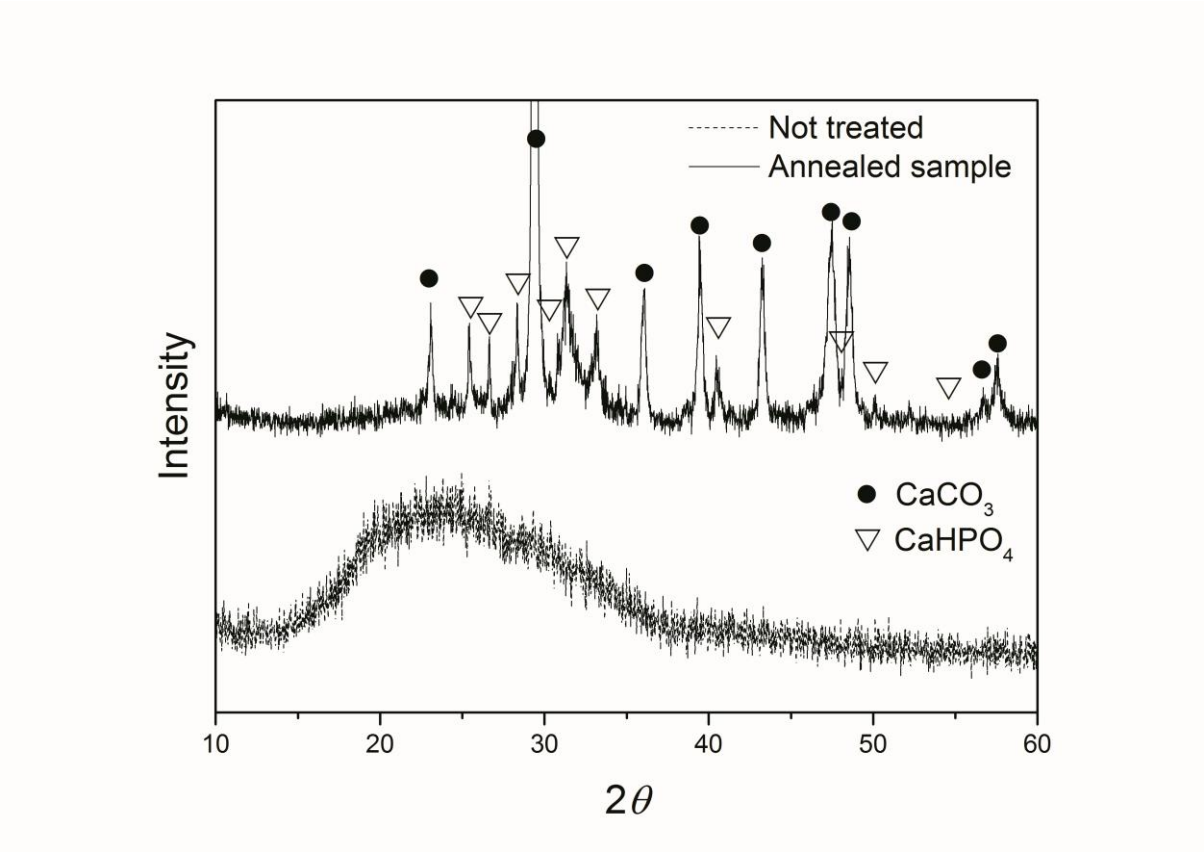

Fig. III-5. XRD patterns of the deposits from the cathode with and without annealing at 550 °C for 2 h.

References

Dosen, A., Giese, R.F. (2011). Thermal decomposition of brushite, $CaHPO_4 \cdot 2H_2O$ to monetite $CaHPO_4$ and the formation of an amorphous phase. American Mineralogist 96, 368-373.

Kerwick, M.I., Reddy, S.M., Chamberlain, A.H.L., Holt, D.M. (2005) Electrochemical disinfection, an environmentally acceptable method of drinking water disinfection?. Electrochimica Acta 50, 5270-5277.

Menzel, D.W., Cowin, N. (1965) The measurement of total phosphorus in seawater based on the liberation of organically bound fractions by persulfate oxidation. Limnology and Oceanography 10, 280-282.

Monma, H. (1994) Electrolytic depositions of calcium phosphates on substrate. Journal of Materials Science 29, 949-953.

Murphy, J., Riley, J.P. (1965) A modified single-solution method for the determination of phosphate in natural waters. Analytica Chimica Acta. 27, 31-36.

Otsuki, A. (1981) Use of ultraviolet spectrophotometric determination of nitrate for the determination of total nitrogen in environmental water samples using alkaline persulfate digestion [in Japanese]. Japan Analyst 30, 688-689.

Reyter, D., Bélanger, D., Roué, L. (2010) Nitrate removal by a paired electrolysis on copper and Ti/IrO_2 coupled electrodes – Influence of the anode/cathode surface area ratio. Water Research 44, 1918-1926.

Solózano, L. (1969) Determination of ammonia in natural waters by the phenol hypochlorite method. Limnology and Oceanography 14, 799-801.

Zhou, S., Shao, Y., Gao, N., Deng, Y., Qiao, J., Ou, H., Deng, J. (2013) Effects of different algaecides on the photosynthetic capacity, cell integrity and mirocystin-LR release of *Microcystis aeruginosa*. Science of The Total Environment 463-464, 111-119.

IV. The effect of electrode material for removal of *Microcystis* sp. by electrochemical oxidation

IV.1 Introduction

Microcystis sp. often occurs as large colonies. Colony formation plays an important role for the domination the freshwater phytoplankton community (Oliver, 1994). However, after isolation from the lake and cultivation in laboratory, the colony disaggregates and develops into unicellular cell (Reynolds et al., 1981; Bolch and Blackburn, 1996). Thus, the results of laboratory studies using unicellular strain could not explain natural environmental phenomenon.

Many factors (such as current density, concentration of chlorine ion, pH, reactor volume and electrode material) affects to the removal efficiency of electrochemical oxidation. The electrode material has a significant impact on the electrochemical kinetics and the reactions occurring. Tanaka et al. (2002) reported that bisphenol A was rapidly oxidized using oxide anode (SnO_2/Ti) compared with Pt/Ti anode.

Therefore, this study was conducted to evaluate the possibility of removal for colonial *Microcystis* cells using electrochemical oxidation and removal efficiency of *Microcystis* sp. (colonial cells) by electrode material (Pt/Ti electrode and oxide electrode) of electrochemical oxidation.

IV.2 Materials and methods

IV.2.1 *Microcystis* cells

Colonial *Microcystis* cells were collected from Chikato pond (Matsumoto, Japan) in September, 2010 using 40 μm plankton net.

IV.2.2 Apparatus

The electrochemical oxidation reactor was same with chapter II (see Fig. II-1). *Microcystis* sp. from Chikato pond and Chikato pond water was used as a algal solution for treatment. The volume of the algal solutions to be treated was 40 L. The anode and cathode were made of Pt coated on a Ti substrate and DSE (based on ferrite oxide electrode; Dimensionally Stable Electrode, PERMELEC ELECTRODE LTD., Hujisawa, Japan). The dimensions of the Pt/Ti and DSE were 50 mm wide by 200 mm in diameter and 100 mm wide by 100 mm in diameter, respectively. The surface area immersed in the algal solution was 100 cm^2, and the anode-cathode separation was 5 mm. Conductivity of algal solution was measured using a electrical conductivity meter (HEC-110, DKK-TOA Co., Tokyo, Japan). Agitation during treatment was provided by a magnetic stirrer (at about 200 rpm) and a potential of 10 V was maintained between the electrodes throughout the experiments with a DC power supply. The experiments were performed in duplicate.

IV.2.3 Cell and colony counting

The 10 mL aliquots were fixed with formaldehyde (final concentration = 2%) (Han et al. 2012). Next, a small amount of the fixed 10 mL samples were placed on a Sedgwick-Rafter, and the cells and the colonies (over 10 cells) were counted by microscopic examination at 400× (BK51, Olympus, Tokyo, Japan).

IV.3 Results and discussion

Fig. IV-1 shows the variations in electric potential and current using the Pt/Ti electrodes and DSE electrodes during the electrochemical oxidation. The electric potentials were maintained 10 to 10.5 V during the electrochemical oxidation regardless of electrode materials (Fig. IV-1 (a)). As shown in Fig. IV-1 (b), The current of the electrochemical oxidation using Pt/Ti electrode was decreased (30 to 27 mA; 1st experiment and 25 to 22 mA; 2nd experiment). There were some spikes of the electrochemical oxidation using DSE electrode. However, there was not a big difference of change of current between Pt/Ti electrode and DSE electrode (Fig. IV-1 (b)).

As shown in Fig. IV-2, the conductivity of algal solution using the Pt/Ti electrodes and DSE electrodes during the electrochemical oxidation was gradually decreased. The released ionic matter could be deposited on the cathode surface, thereby reducing the conductivity

Fig. IV-3 shows the variations in cell density and colony density using the Pt/Ti electrodes and DSE electrodes during the electrochemical oxidation. The cell degradation trends are similar to the colony degradation trends. The cells and colonies were decreased simultaneously. The cell density and colony density using the Pt/Ti electrode were reduced by 82% and 73% at an applied charge of approximately 14.0×10^4 C, respectively. However, the cell density and colony density using the DSE electrode were reduced by 99% and undetectable at an applied charge of approximately 5.2×10^4 C, respectively.

Changes in cell morphology resulting from the electrooxidation process were investigated by SEM analysis. As shown in Fig. IV-4a, the surfaces of colonial cells in the control group were undamaged, and covered with a film. Yang and Kong (2012) reported that the content of extracellular polysaccharide of colonial *M. aeruginosa* was approximately two

times compared with unicellular *M. aeruginosa*. It is considered that the film in Fig. IV-4a was polysaccharide. The electrochemically oxidized cells were broken, and in some cases only the cell membranes remained (indicated by arrows in Fig. IV-4b and c). The trends of broken aspects of colonial cells were similar to the trends of unicellular cells (Fig. II-3b, c and d).

Overall, the removal of *Microcystis* sp. cells and colonies using electrochemical oxidation was possible. The removal efficiency for *Microcystis* sp. cells and colonies of DSE electrodes were better than Pt/Ti electrodes. The evolution of oxygen and hydroxyl radical on the anode surface of electrolysis of water can be briefly described by following equations;

$$2H_2O \rightarrow 2OH^{\bullet} + 2H^{+} + 2e^{-} \qquad \text{(IV-1)}$$

$$2OH^{\bullet} \rightarrow 2H^{+} + O_2 + 2e^{-} \qquad \text{(IV-2)}$$

If anode material has a property which overpotential is low for equation IV-1 and/or high for equation IV-2, the range of generation of $OH^{\bullet}$ can be wide, then the anode effectively removed organic (Polcaro et al., 2000; Tanaka et al., 2002). The overpotential of oxide anode for oxygen evolution is high compared with Pt anode (Comninellis and Pulgarin, 1993). Therefore, the effective removal for *Microcystis* sp. cells and colonies using DSE electrode (based on ferrite oxide electrode) is possible.

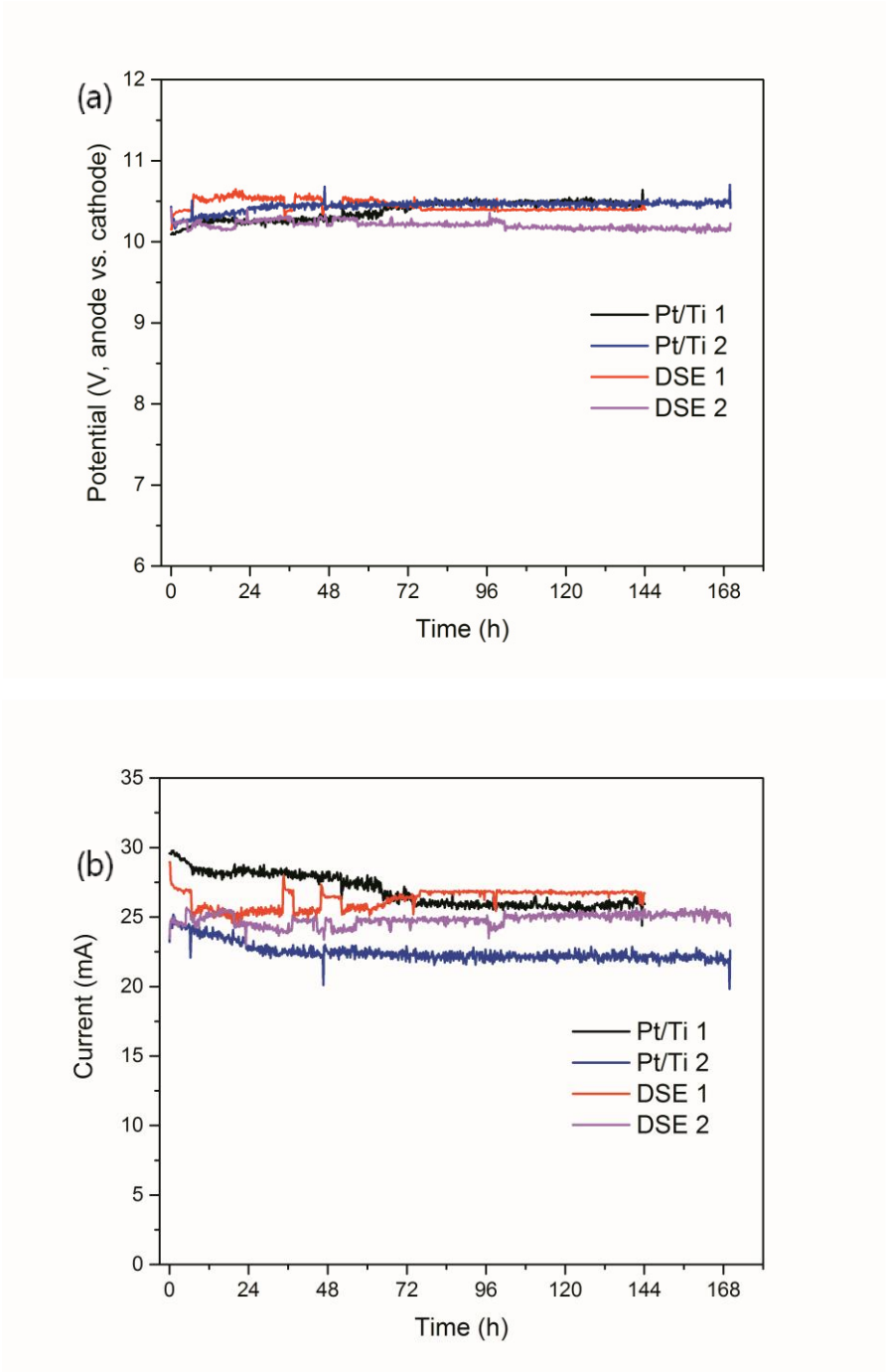

Fig. IV-1. Variations in electric potential (a) and current (b) using the Pt/Ti electrodes and DSE electrodes during the electrochemical oxidation. The experiments were performed in duplicate.

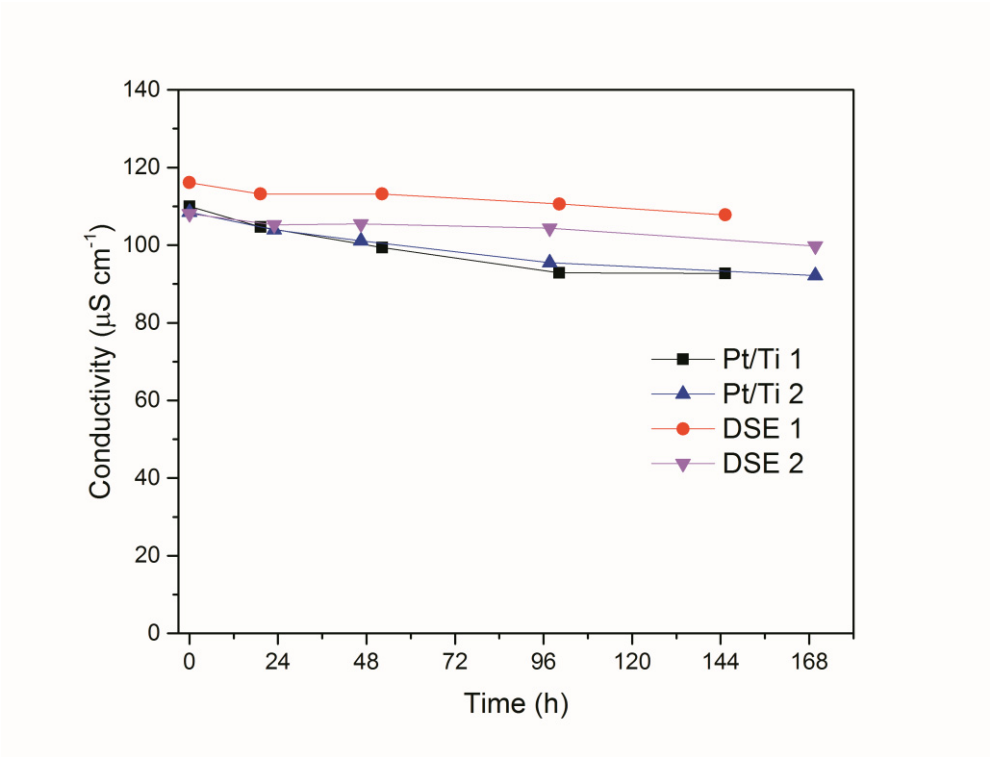

Fig. IV-2. Variations in conductivity of algal solution using the Pt/Ti electrodes and DSE electrodes during the electrochemical oxidation. The experiments were performed in duplicate.

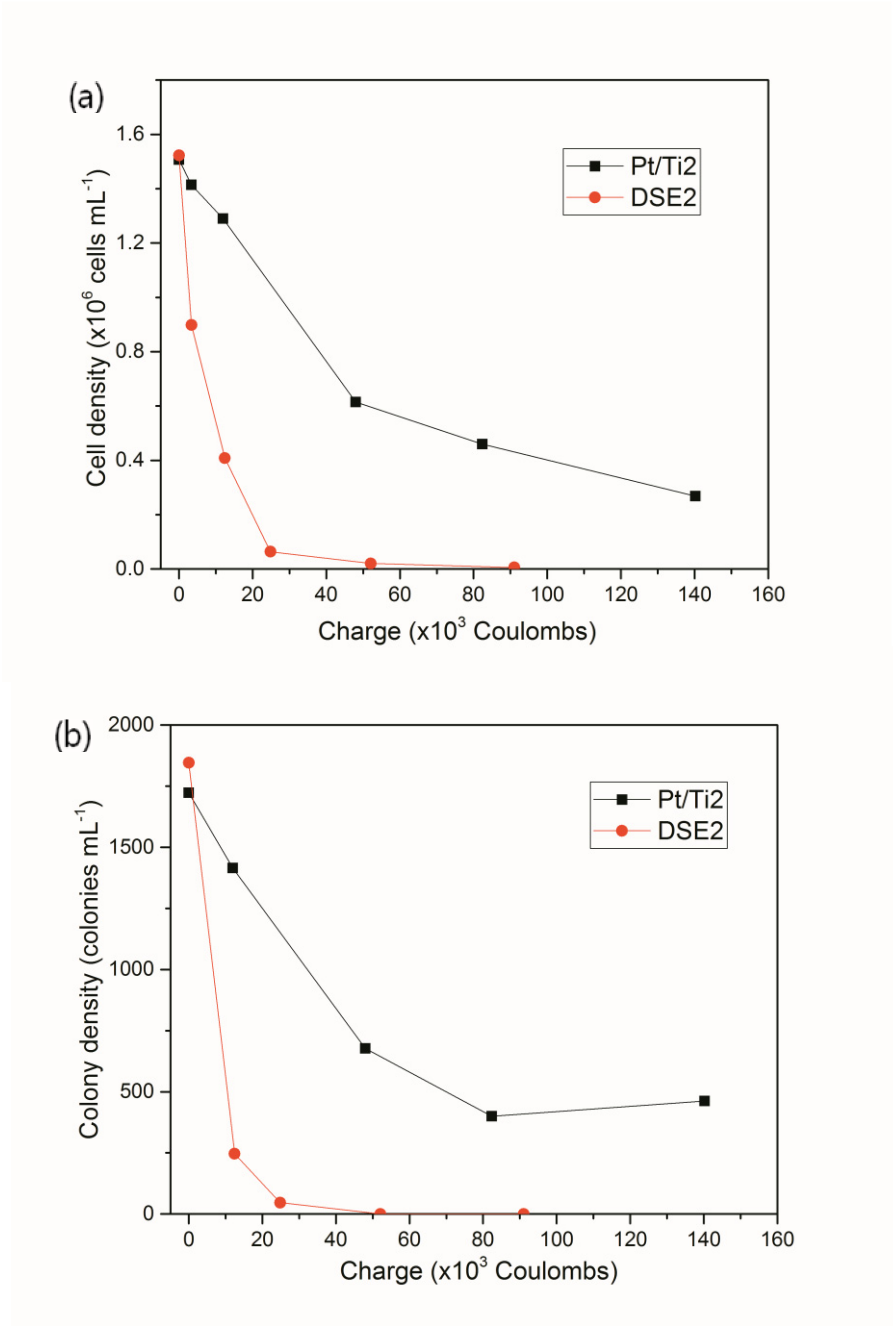

Fig. IV-3. Variations in cell density (a) and colony density (b) using the Pt/Ti electrodes and DSE electrodes during the electrochemical oxidation. The results are the sum of MC-LR and MC-RR. The results are from a single experiment.

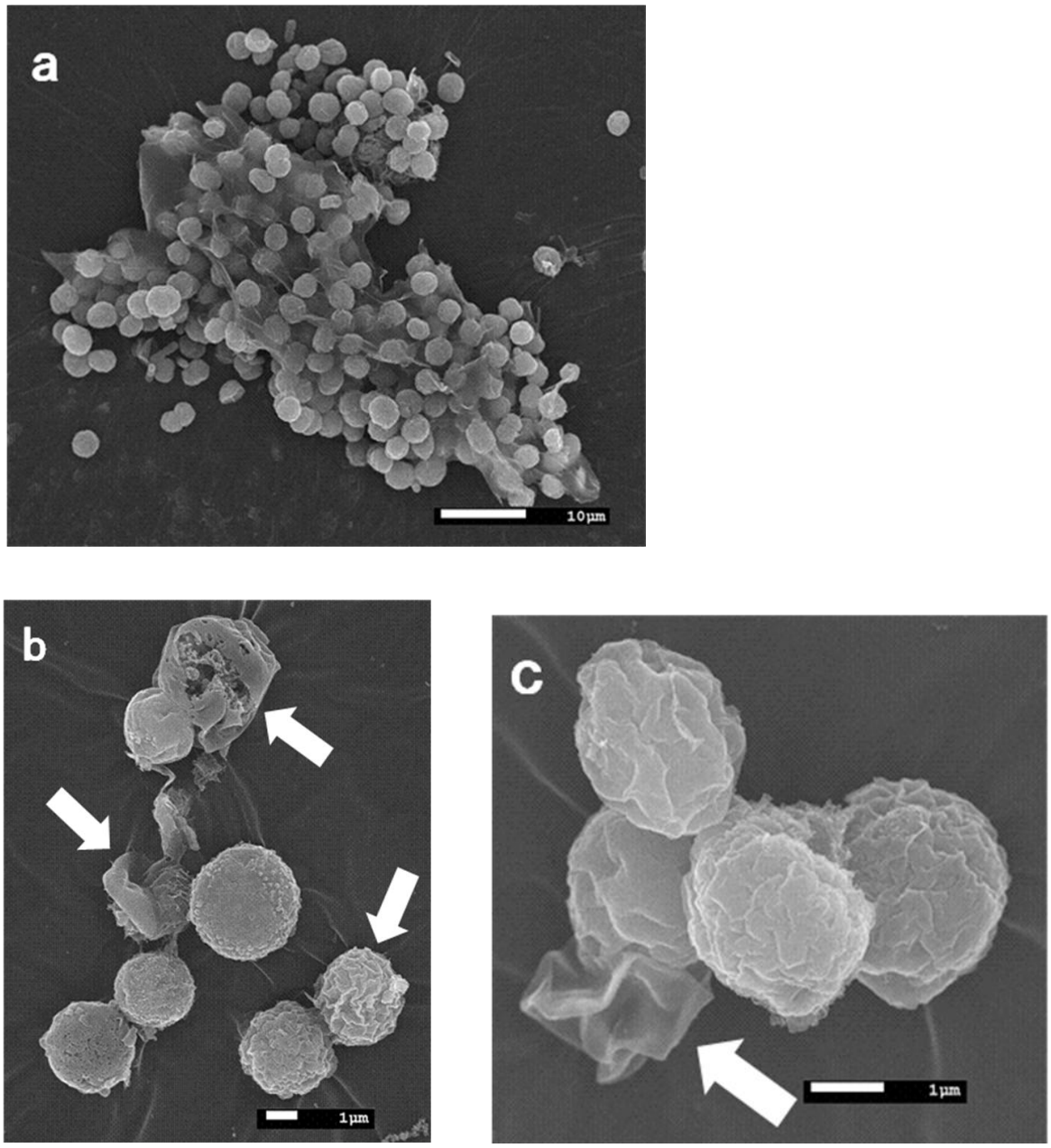

Fig. IV-4. SEM images of untreated cells (a) and treated cells (b and c). The arrows point to broken cells.

References

Comninellis, C., Pulgarin, C. (1993) Electrochemical oxidation of phenol for wastewater treatment using SnO_2 anodes. Journal of Applied Electrochemistry 23, 108-112.

Oliver, R.L. (1994) Floating and sinking in gas vacuolaterd cyanobacteria. Journal of Phycology 30, 161-173.

Polcaro, A.M., Palmas, S., Renoldi, F., Mascia, M. (2000) Three-dimensional electrodes for the electrochemical combustion of organic pollutants. Electrochimica Acta 46, 389-394.

Reynolds, C.S., Jaworski, G.H.M., Cmiech, H.A., Leedale, G.F. (1981) On the annual cycle of the Blue-Green-Alga *Microcystis aeruginosa* Kutz emend Elenkin. Philosophical Transactions of the Royal Society B. 293, 419-477.

Tanaka, S., Nakata, Y., Kimura, T., Yustiawati, Kawasaki, M. Kuramitz, H. (2002) Electrochemical decomposition of bisphenol A using Pt/Ti and SnO_2/Ti anodes. Journal of Applied Electrochemistry 32, 197-201.

Yang, Z., Kong, F. (2012) Formation of large colonies: a defense mechanism of *Microcystis aeruginosa* under continuous grazing pressure by flagellate *Ochromonas* sp.. Journal of Limnology 71, 61-66.

V. Application of electrochemical treatment in a pond

V.1 Introduction

From the results of chapter 2 and 3, it is possible that removal of *Microcystis* cells, microcystins and phosphorus. In addition, colonial cells also could be removed by electrochemical treatment (chapter 4).

By dissolution of anode (such as Al and Fe) using an electrochemical method, electro-coagulation of pollutants is possible. Electrogenerated ferric ions may form monomeric ions, ferric hydroxo complexes with hydroxide ions and polymeric species, depending on the pH range. They are transformed finally into $Fe(OH)_3$ (Kobya et al., 2003).

When algae die they sink to the bottom where they are decomposed and the nutrients contained in cells are converted into inorganic form by bacteria. The range of anaerobic sediment and deeper water extend because the decomposition process uses oxygen. Inorganic nutrients (such as phosphorus) are released into the water bodies (Wetzel, 2001) (Fig. I-2 in chapter I).

Oxygen is generated by electrochemical treatment (chapter I). Therefore, in this study, an electrochemical treatment equipment with a Fe electrodes and particular propeller (W-motion) was established in a pond (Chikato pond, Matsumoto, Japan) and evaluated the change of biomass, nutrient (N and P) and concentration of dissolved oxygen.

V.2 Materials and methods

V.2.1 Chikato pond

Chikato pond is located in Matsumoto, Japan and an eutrophic pond which produces cyanobacteria blooms annually. Fig. V-1 shows the image of Chikato pond. The area and water volume of Chikato pond are approximately 26×10^3 m^2 and 60×10^3 m^3, respectively.

V.2.2 Electrochemical treatment equipment

Fig. V-2 shows the photograph of the electrochemical equipment. It was composed with 4 floaters, 2 electrodes set and 2 W-motion (Fig. V-2c). Fig. V-3 shows the schematic diagram of the water flow by rotating W-motion. The water moves downward by rotating counter-clock direction. As shown in Table V-1, the electrodes set 1 and 2 were composed with 7 Pt/Ti electrodes and 7 Fe electrodes and 14 Pt/Ti electrodes as anode and 14 stainless steels as cathode, respectively. The distance between anode and cathode was 5 mm. The electrodes were set in 0.9 and 1.38 m depth from surface water, respectively. The W-motions were set in 0.4 and 1.8 m depth. The pH meter was set in 0.46 m. The dissolved oxygen meters were set in 0.73, 1.35 and 2.21 m. The experiment was carried out from August 21 to October 19 in 2009. Fig. V-4 shows the photograph of installation in pond.

V.2.3 Dissolved oxygen, OD_{405nm}, temperature, pH, conductivity of water and concentration of N and P species

Dissolved oxygen, OD_{405nm}, V.2.3 Temperature, pH and conductivity of water were measured in St. a, b and c during the experiment.

200 mL of water samples were collected at St. a, b and c during the experiment and

100 mL of water samples were filtered through a glass-fiber filter (GF/C, Whatman, Maidstone, UK). Total nitrogen (TN) and total phosphorus (TP) were measured from the unfiltered 100 mL of water samples. Dissolved total nitrogen (DTN) and dissolved total phosphorus (DTP) were measured from the filtered 100 mL of water samples. TN and DTN were measured according to the method of Otsuki (1981). TP and DTP were measured according to the method of Menzel and Corwin (1965).

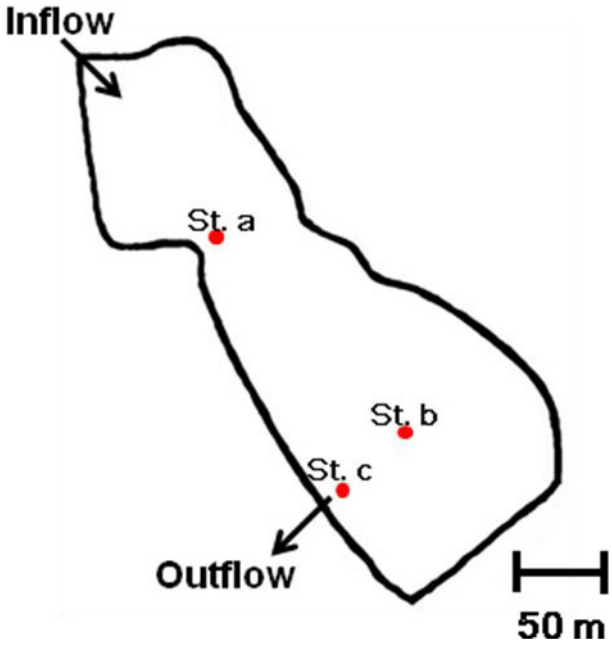

Fig. V-1. Image of Chikato pond (Matsumoto, Japan) and sampling station. The electrochemical treatment equipment was installed at St. b.

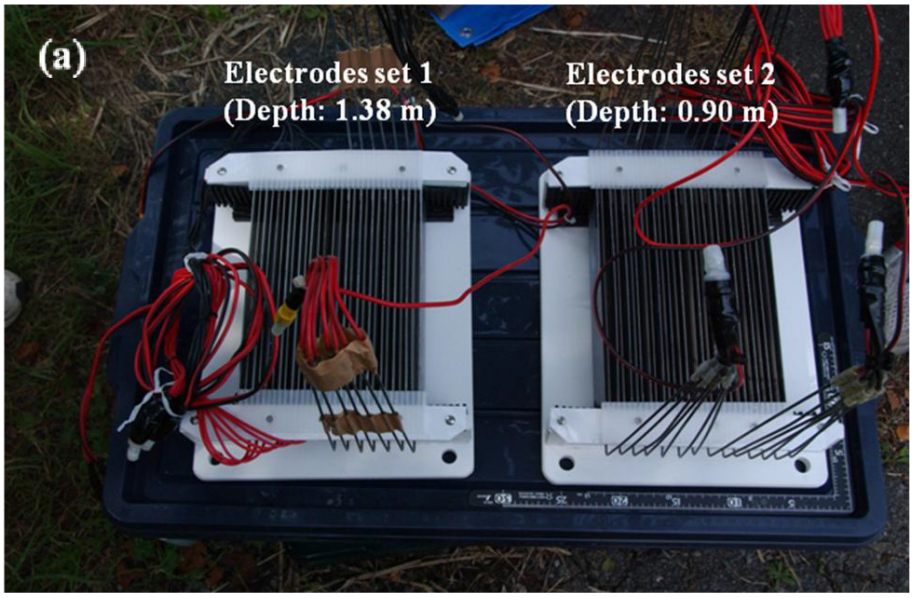

(Continued)

Fig. V-2. Photograph of the electrochemical treatment equipment. (a) electrodes set 1 and 2; (b) W-motion; and (c) electrochemical treatment equipment.

Table V-1. Components of electrodes set 1 and 2.

Electrodes set 1		Electrodes set 2	
Anode	**Cathode**	**Anode**	**Cathode**
Pt/Ti (7 ea) **Fe (7 ea)**	**Stainless Steel** **(SUS304 14 ea)**	**Pt/Ti (14 ea)**	**Stainless Steel** **(SUS304 14 ea)**

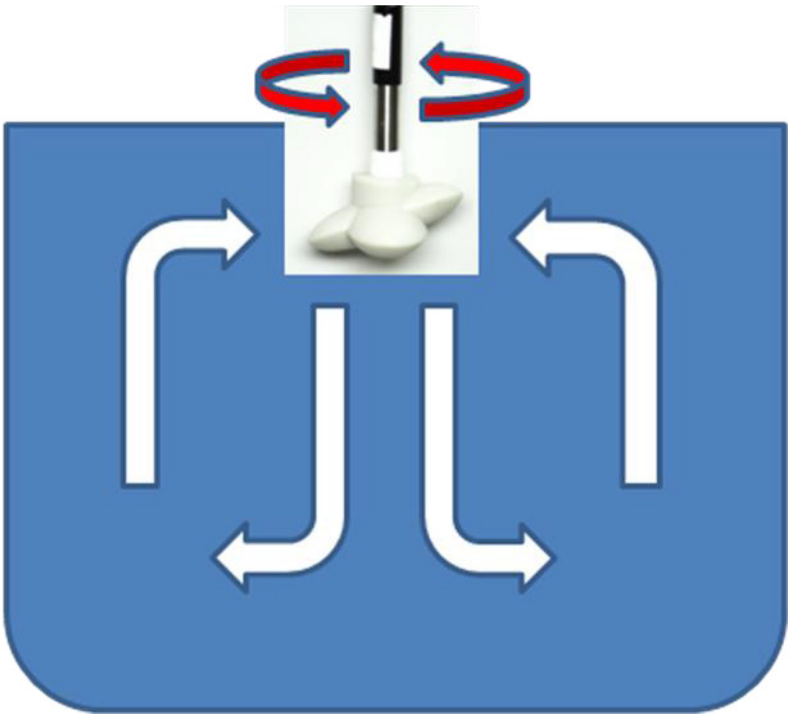

Fig. V-3. Schematic diagram of the water flow by rotating W-motion.

Fig. V-4. Photograph of the electrochemical treatment equipment installation.

V.3 Results and discussion

Fig. V-5 shows the variations in voltage and current of the electrodes set in depth 0.9 m. The voltage maintained 10.0 to 10.5 V. However, the current gradually decreased. The current could be dropped by the dissolution of the Fe electrodes of electrodes set 1 and deposition of organic and/or inorganic anions on the cathode surface.

Fig. V-6 shows the variations in temperature. The results of temperature were decreased approximately 24°C to 14°C during treatment by seasonal change (summer to autumn) and there was not a big difference between station and depth of water. Daily water temperature range of 2.21 m depth in the equipment was smaller than 0.73 and 1.35 m depth.

As shown in Fig. V-7, the results of pH were changed in the range of approximately 7.5 to 7.5 and there was not a big difference by station.

The values of conductivity in St. a, b and c were maintained in 0.12 mS cm^{-1} during treatment (Fig. V-8).

Fig. V-9 shows the variations in dissolved oxygen. There was not a big difference between St. a, b and c. The results of dissolved oxygen in equipment (depth of 0.73, 1.35 and 2.21 m) were smaller than the results of St. a, b and c (water surface). The dissolved oxygen in depth of 2.21 m (9.9 mg O_2 L^{-1}) was smaller than the dissolved oxygen in depth of 0.73 (12.2 mg O_2 L^{-1}) and 1.35 m (10.8 mg O_2 L^{-1}), however it was gradually increased and overturned in September 10th. Finally, the dissolved oxygen in depth of 2.21 m became equal to the dissolved oxygen of surface water in October 16th. It is considered that oxygen generated from the electrodes was carried into deeper water by the rotating W-motion.

Fig. V-10 shows the variations of nitrogen species in St. a, b and c. The results of TN, DTN and PON were not a big difference between St. a, b and c. The DTN of St. a, b and c were maintained approximately 0.1 mg L^{-1} (Fig. V-10b) and the change of TN was dependence on the change of PON (Fig. V-10a and c).

Fig. V-11 shows the variations of phosphorus species in St. a, b and c. The trends of the change of phosphorus species were similar than the change of nitrogen species. The results of TP, DTP and POP were not a big difference between St. a, b and c. The change of TP was dependence on the change of POP (Fig. V-11a and c).

From the results of PON (Fig. V-10c) and POP (Fig. V-11c), the removal of *Microcystis* cells by the electrochemical treatment equipment was not efficient. The removal efficiency of *Microcystis* cells was greatly reduced at the higher algal suspension volume (Chapter II). However, it is possible that oxygen generated from the electrodes was carried into deeper water by the rotating W-motion (Fig. V-9).

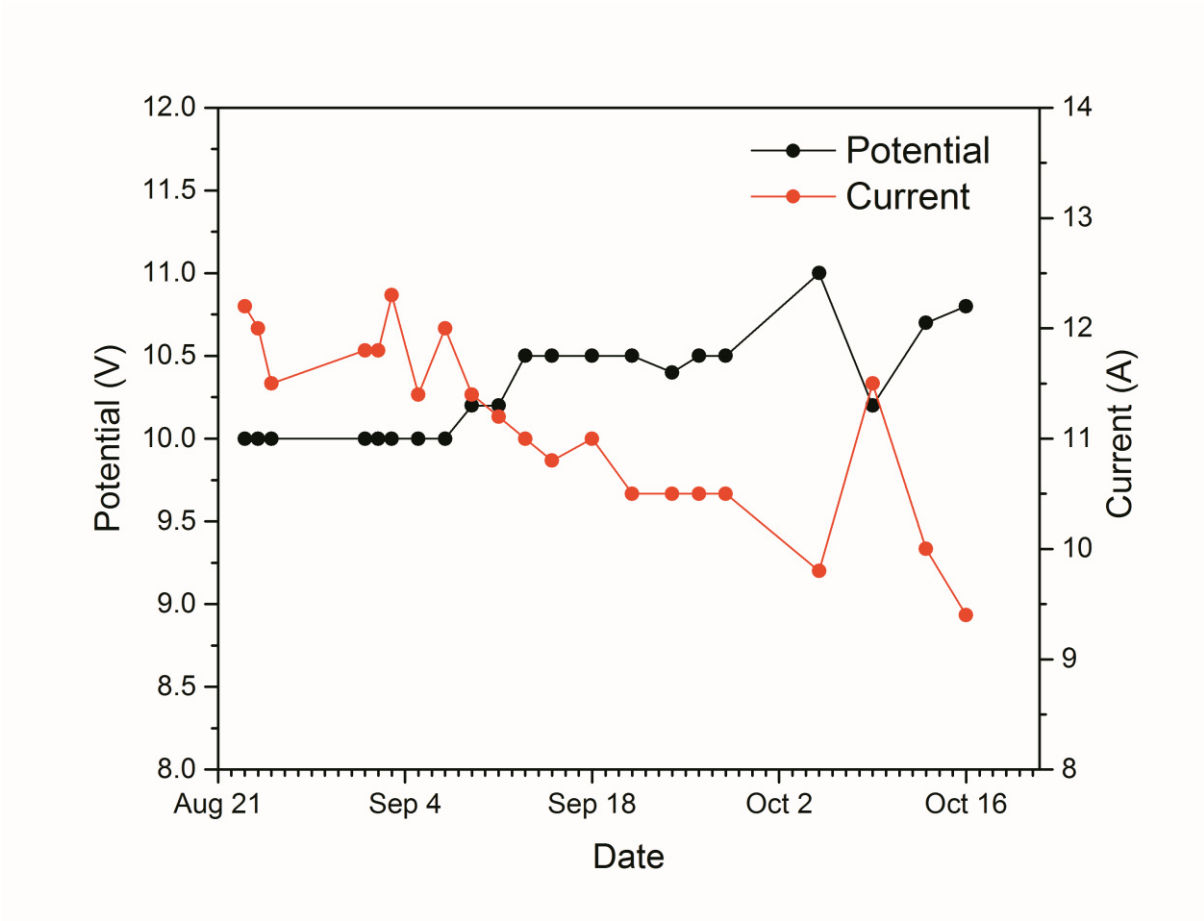

Fig. V-5. Variations in electric potential and current of the electrodes set in 0.9 m depth.

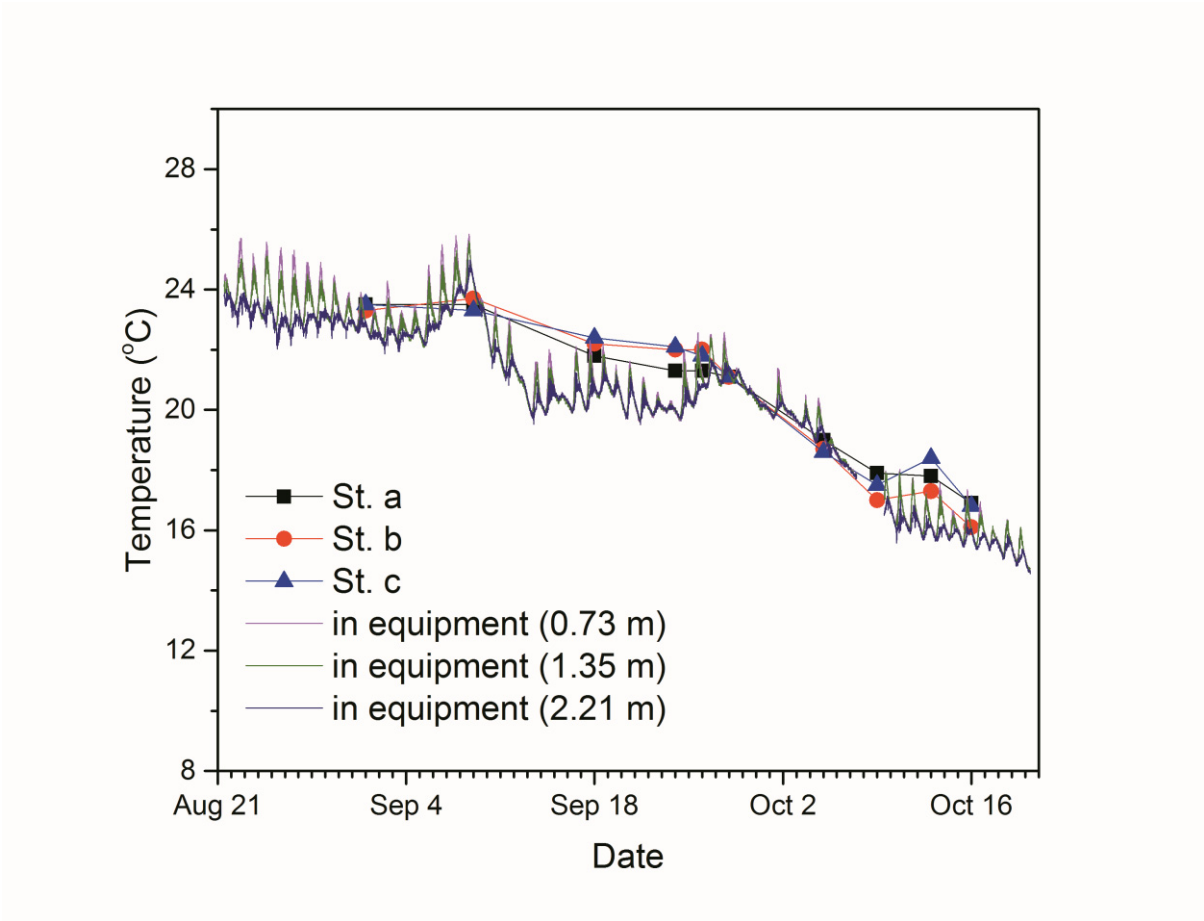

Fig. V-6. Variations in temperature in St. a, b, c and equipment in 0.73, 1.35 and 2.21 m depth. The lack of data from October 7 to October 9 was caused by the stop operation of the electrochemical equipment because of typhoon.

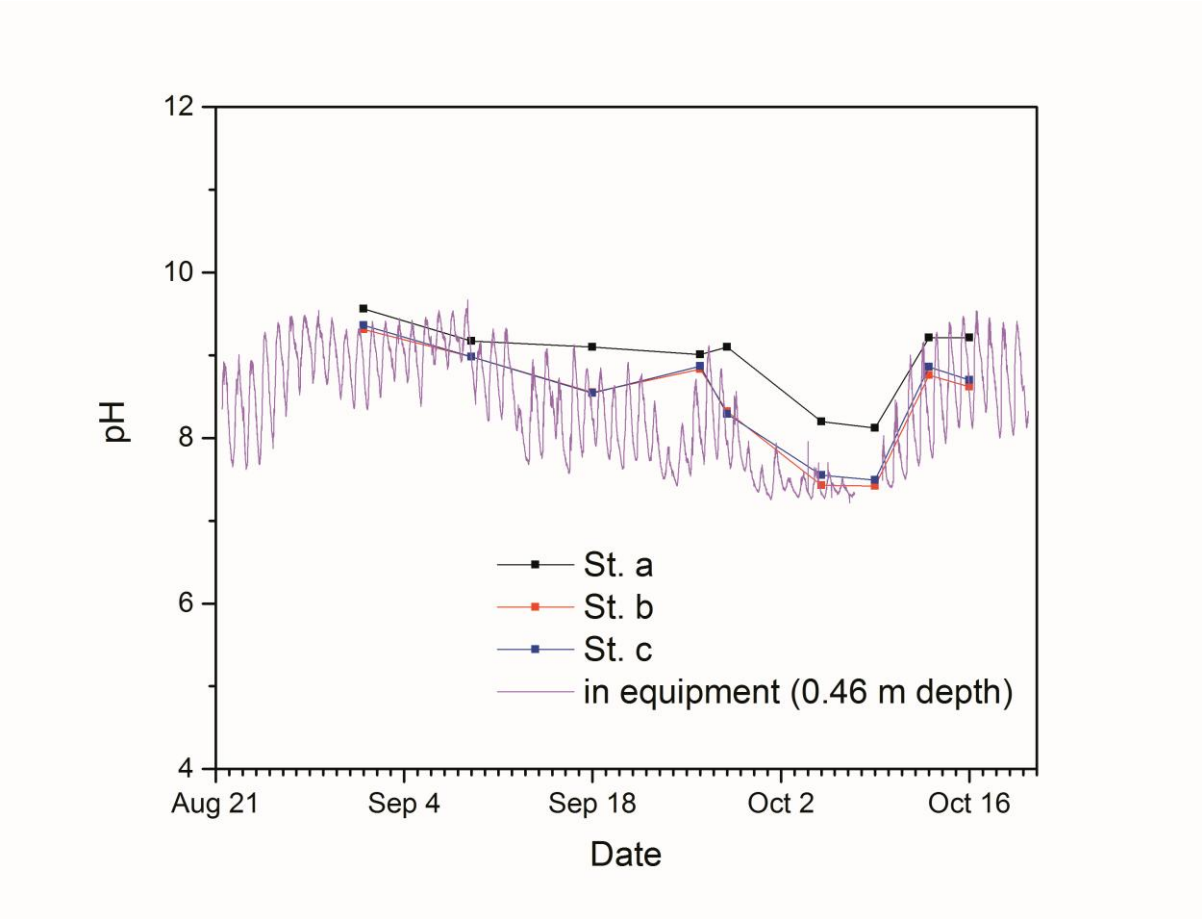

Fig. V-7. Variations in pH in St. a, b, c and equipment in 0.46 m depth. The lack of data from October 7 to October 9 was caused by the stop operation of the electrochemical equipment because of typhoon.

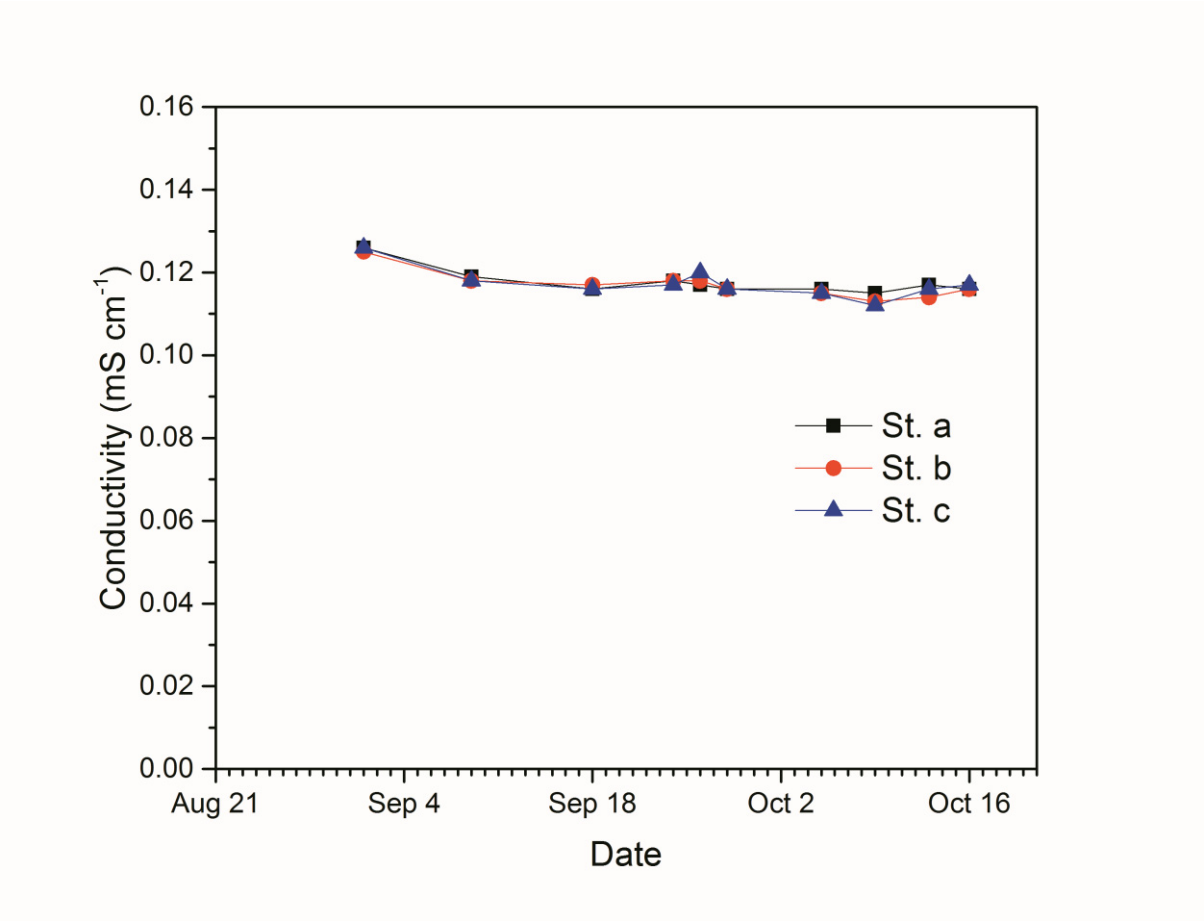

Fig. V-8. Variations in conductivity in St. a, b and c.

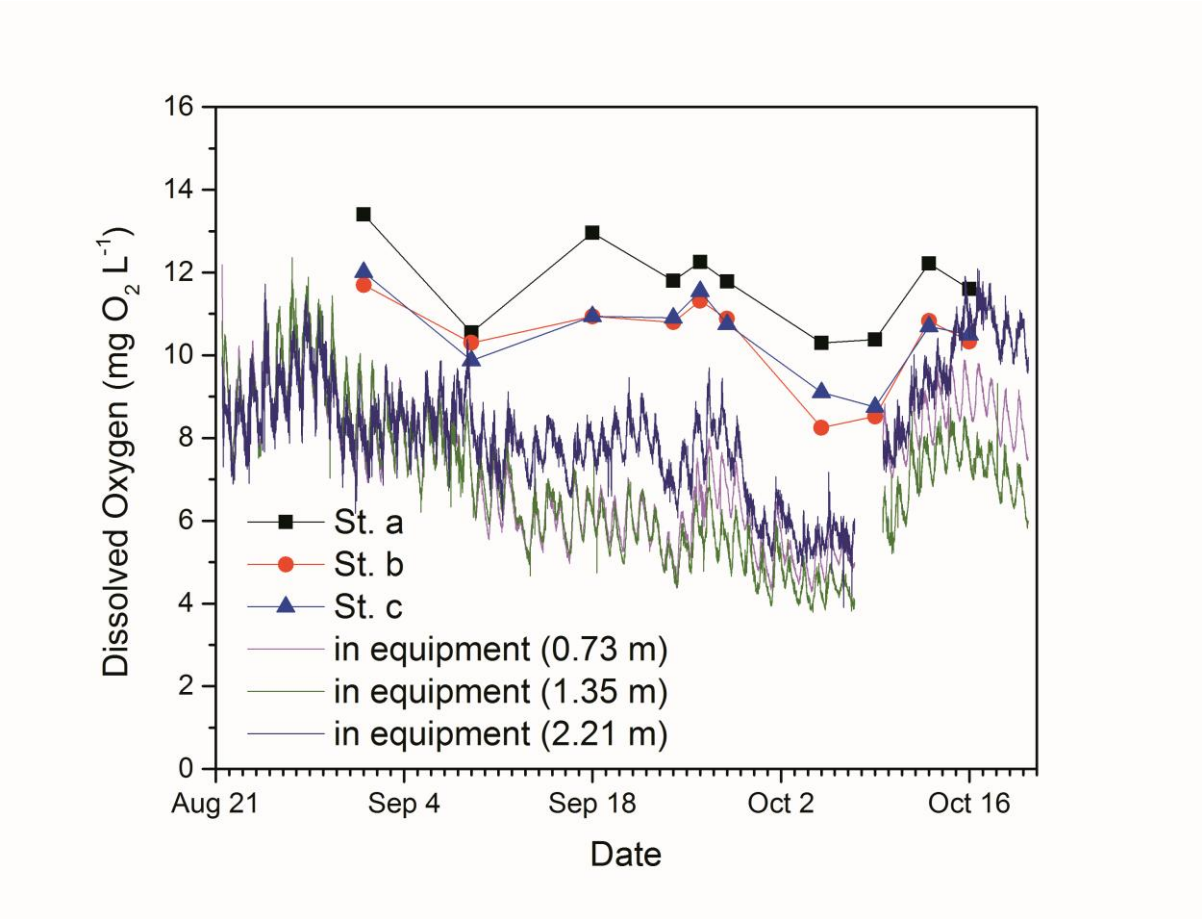

Fig. V-9. Variations in dissolved oxygen in St. a, b, c and equipment in 0.73, 1.35 and 2.21 m depth. The lack of data from October 7 to October 9 was caused by the stop operation of the electrochemical equipment because of typhoon.

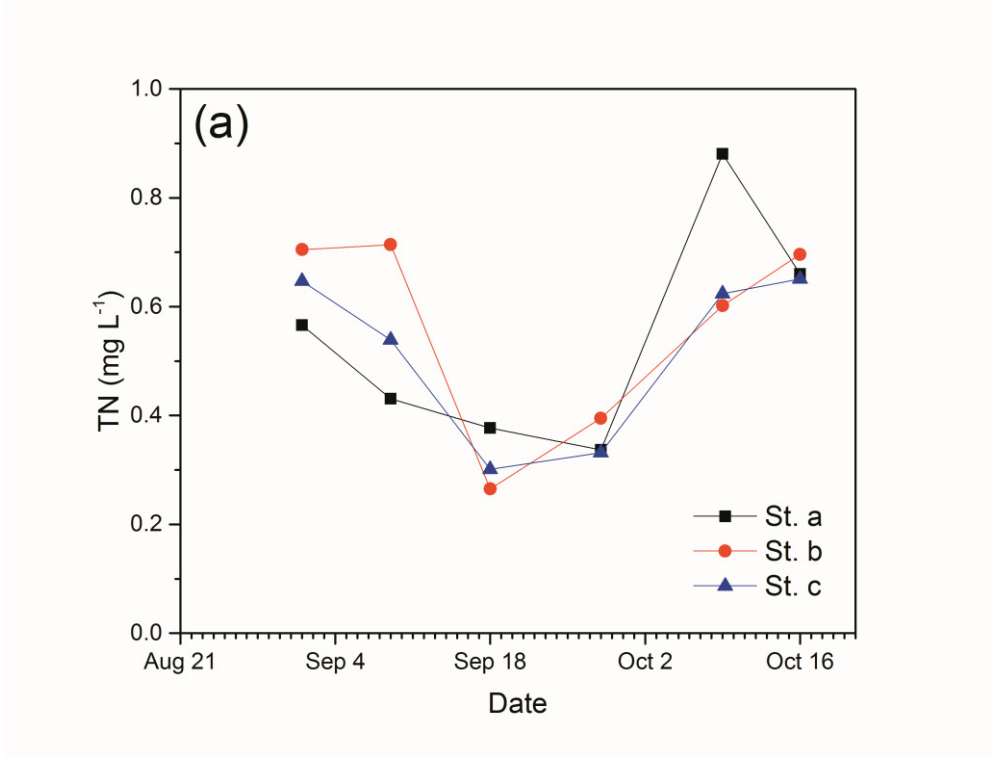
(a)
TN (mg L-1)
1.0
0.8
0.6
0.4
0.2
0.0
Aug 21
Sep 4
Sep 18
Oct 2
Oct 16
Date
St. a
St. b
St. c

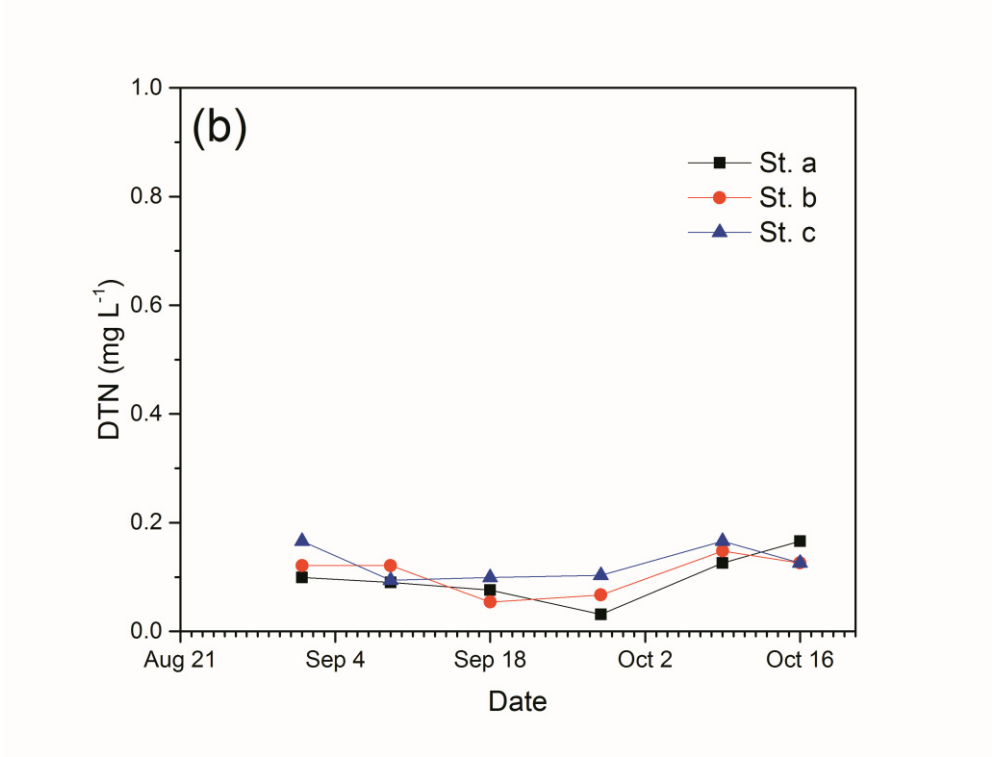
(b)
DTN (mg L-1)
1.0
0.8
0.6
0.4
0.2
0.0
Aug 21
Sep 4
Sep 18
Oct 2
Oct 16
Date
St. a
St. b
St. c

(Continued)

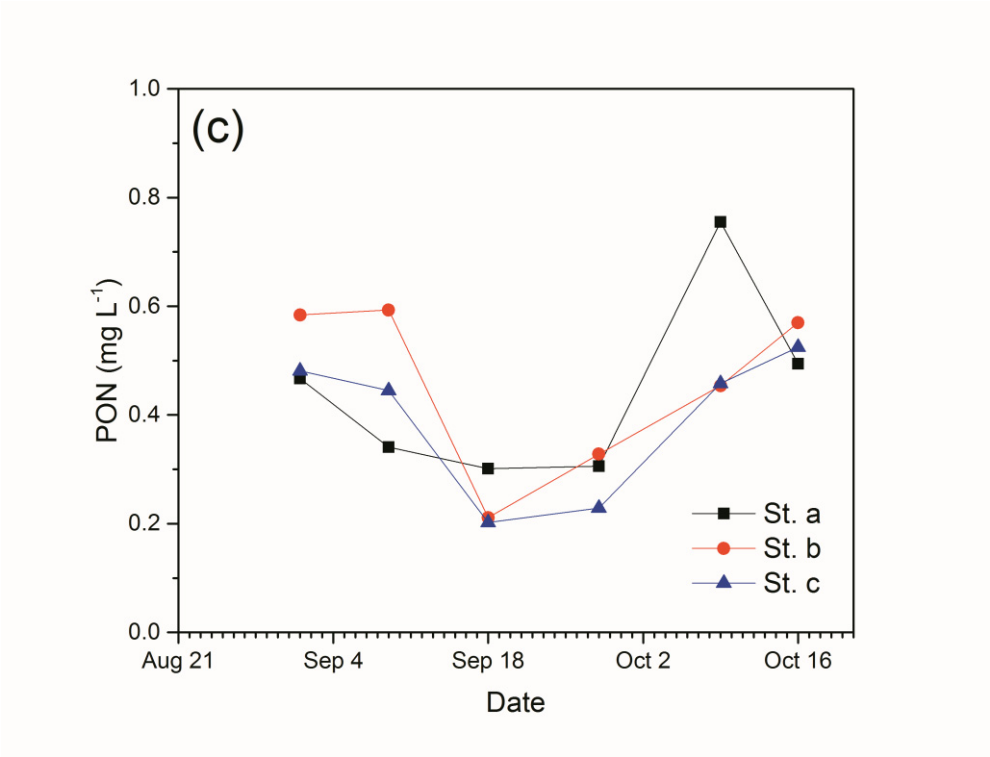

Fig. V-10. Variations in total nitrogen (a), dissolved total nitrogen (b) and particulate organic nitrogen (c) in St. a, b and c.

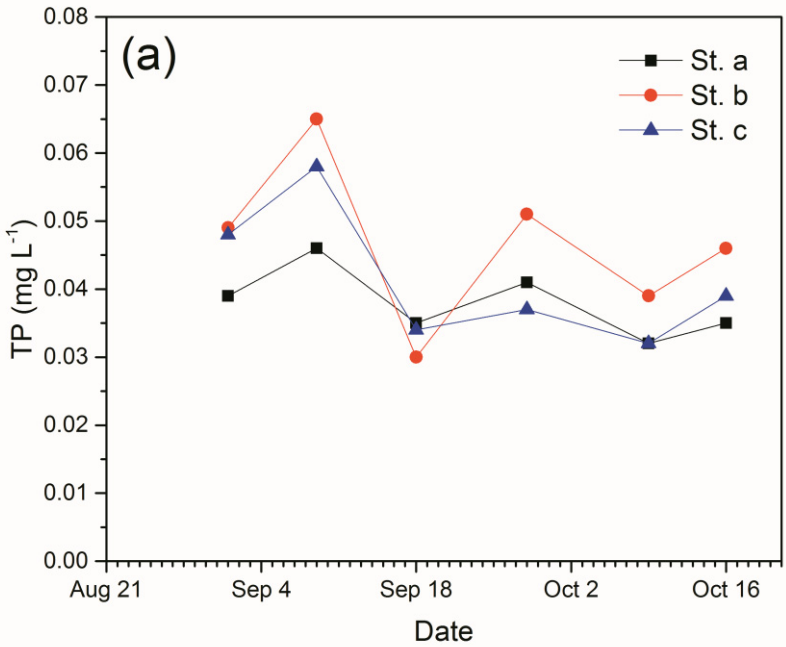
(a)
St. a
St. b
St. c
TP (mg L-1)
0.08
0.07
0.06
0.05
0.04
0.03
0.02
0.01
0.00
Aug 21
Sep 4
Sep 18
Oct 2
Oct 16
Date

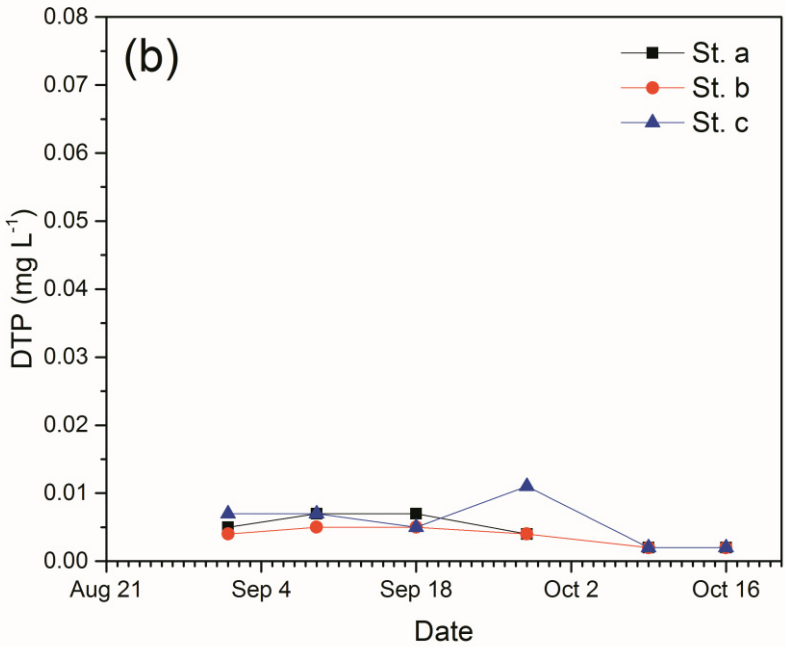
(b)
St. a
St. b
St. c
DTP (mg L-1)
0.08
0.07
0.06
0.05
0.04
0.03
0.02
0.01
0.00
Aug 21
Sep 4
Sep 18
Oct 2
Oct 16
Date

(Continued)

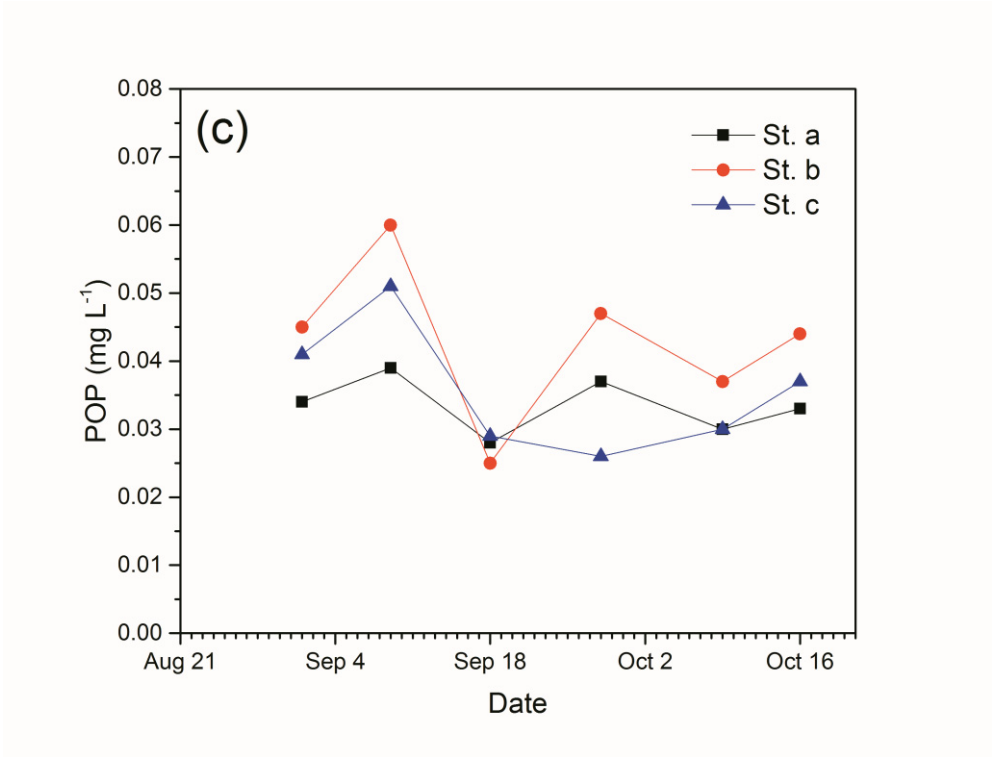

Fig. V-11. Variations in total phosphorus (a), dissolved total phosphorus (b) and particulate organic phosphorus (c) in St. a, b and c.

References

Kobya, M., Can, O.T., Bayramoglu, M. (2003) Treatment of textile wastewaters by electrocoagulation using iron and aluminum electrodes. Journal of Hazardous Materials B 100, 163-178.

Menzel, D.W., Cowin, N. (1965) The measurement of total phosphorus in seawater based on the liberation of organically bound fractions by persulfate oxidation. Limnology and Oceanography 10, 280-282.

Otsuki, A. (1981) Use of ultraviolet spectrophotometric determination of nitrate for the determination of total nitrogen in environmental water samples using alkaline persulfate digestion [in Japanese]. Japan Analyst 30, 688-689.

Wetzel, R. (2001) Limnology, 3 E. Lake and River Ecosystems. Academic Press, 525 B Street, Ste. 1900, San Diego, CA 92101, USA.

VI. General discussion and conclusions

VI.1 The removal of *Microcystis ichthyoblabe* cells and its hepatotoxin microcystin-LR during electrooxidation process using Pt/Ti electrodes

This study evaluated the removal of *Microcystis* cells and their toxic MC–LR by the electrooxidation process. Damaged *Microcystis* cells released their intracellular MC–LR into the medium, temporarily increasing the extracellular MC–LR concentration during the initial stage of electrooxidation.

In the 4 L volume, the cells and MC–LR were removed at applied charges of 3×10^4 C and 6×10^4 C, respectively. The removal efficiency of *M. ichthyoblabe* cells and MC–LR was unaffected by initial cell density, initial MC–LR concentration and solution conductivity, but was heavily compromised by large algal suspension volume.

There was a good correlation between the current density and the conductivity of the algal solution.

VI.2 The variation in concentration of cations (Na^+, K^+ and Ca^{2+} ions) and nutrient species (N and P) during electrochemical treatment

The concentration of Na^+ ions and K^+ ions gradually increased with the electrochemical oxidation. Ca^{2+} ions decreased because of their deposition on the cathode

surface.

DON increased during initial treatment period (12 h) owing to cell degradation (PON→DON), after which it decreased. NO_2-N could be oxidized to NO_3-N on the anode surface. NO_3-N and NH_4-N gradually increased. DON could be oxidized to NO_3-N on the anode surface and deoxidized to NH_4-N on the cathode surface.

TP decreased by 29.2% after 71 h as a result of the decrease in DIP, in turn because of the deposition on the cathode surface. Phosphorus was deposited on the cathode surface with calcium ions as a precursor of $CaHPO_4$ (monetite) and/or $CaHPO_4 \cdot 2H_2O$ (brushite).

The degradation of organic matter could be influenced by the anode materials in electrochemical oxidation treatments (Stucki et al., 1991).

VI.3 The effect of electrode material for removal of *Microcystis* sp. by electrochemical oxidation

After isolation from the lake and cultivation in laboratory, the colony disaggregates and develops into unicellular cell (Reynolds et al., 1981; Bolch and Blackburn, 1996). Thus, the results of laboratory studies using unicellular strain could not explain natural environmental phenomenon. Therefore, this study was conducted to evaluate the removal efficiency for unicellular and colonial *Microcystis* cells by electrochemical oxidation.

This study was conducted to evaluate the possibility of removal for colonial *Microcystis* cells using electrochemical oxidation and removal efficiency of *Microcystis* sp. (colonial cells) by electrode material (Pt/Ti electrode and DSE electrode) of electrochemical oxidation.

The removal of *Microcystis* sp. cells and colonies using electrochemical oxidation

was possible. The removal efficiency for *Microcystis* sp. cells and microcystins of DSE electrodes were better than Pt/Ti electrodes. The SnO_2/Ti anode (dimensionally stable anode; DSA) was more effective in removal of bisphenol A than Pt/Ti anode (Tanaka et al., 2002). The overpotential of oxide anode for oxygen evolution is high compared with Pt anode (Comninellis and Pulgarin, 1993). Therefore, the effective removal for *Microcystis* sp. cells and microcystins using DSE electrode (based on ferrite oxide electrode) is possible.

VI.4 Application of electrochemical treatment in a pond

By dissolution of anode (such as Al and Fe) using an electrochemical method, electro-coagulation of pollutants is possible.

When algae die they sink to the bottom where they are decomposed and the nutrients contained in cells are converted into inorganic forms by bacteria. The range of anaerobic sediment and deeper water extend because the decomposition process uses oxygen. Inorganic nutrients (such as phosphorus) are released into the water bodies (Wetzel, 2001). Therefore, in this study, an electrochemical treatment equipment with a Fe electrodes and particular propeller (W-motion) was established in a pond (Chikato pond, Matsumoto, Japan) and evaluated the change of biomass, nutrient (N and P) and concentration of dissolved oxygen.

The removal of *Microcystis* cells by the electrochemical treatment equipment was not efficient in Chikato pond. However, it is possible that oxygen generated from the electrodes was carried into deeper water by the rotating W-motion.

VI.5 Conclusions

Microcystis cells and its microcystins could be removed by electrochemical oxidation treatment (chapter II). Colonial *Microcystis* cells also could be removed by electrochemical oxidation treatment (chapter IV). Phosphorus could be removed by the electrochemical treatment (chapter III). Oxygen generated from the electrodes was carried into deeper water by the rotating W-motion (chater V). From these results, the problem of eutrophication of lake could be solved (Fig. VI-1). Fig. VI-2 shows the schematic diagram of purification of eutrophic lake by electrochemical treatment. Hydrogen generate from the cathode and it can be used in fuel cell, then electric cost will be reduced.

Despite this, there remains much to be solved.

From the results of chapter III, nitrogen was not removed though internal species are changed. Reyter et al. (2010) suggested that the anode and cathode potential must be around 2.3 V and -1.5 V, respectively, and copper electrode used as cathode.

Phosphorus could be removed by the electrochemical treatment. However, the removal efficiency was low compared with the removal of *Microcystis* cells and microcystins. To remove *Microcystis* cells and phosphorus simultaneously, chemical and electrochemical methods using Al^{3+} and Fe^{3+} ions have been studied (Bektaş et al., 2004; Dosen and Giese, 2011; Cooke et al., 2005) where the algal cells and phosphate are coagulated. However, phosphorus can be returned to the solution when precipitated by Fe^{3+} ions (Cooke et al., 2005). A method using Al^{3+} ions was highly efficient at removing phosphorus (Bektaş et al., 2004). However, when removing both algae and phosphorus, microcystin can be released from the *Microcystis* cells because of damage to the algal cell (Han et al., 2013). In addition, the removal efficiency of *Microcystis* cells was greatly reduced at the higher algal suspension volume.

To solve this problem, I suggest the continuous mixture of Al and oxide anode

system at site of inflow. The Al anode might be dissolved to Al^{3+} ions during treatment, Al^{3+} ions coagulated with algal cells and phosphate, after which the flocs might sunk on the oxide anode surface. The algal cells and its metabolites might be immediately removed because the flocs contact with the oxide anode. Phosphate could be easily removed by recovery of the flocs because phosphate still remained to the flocs.

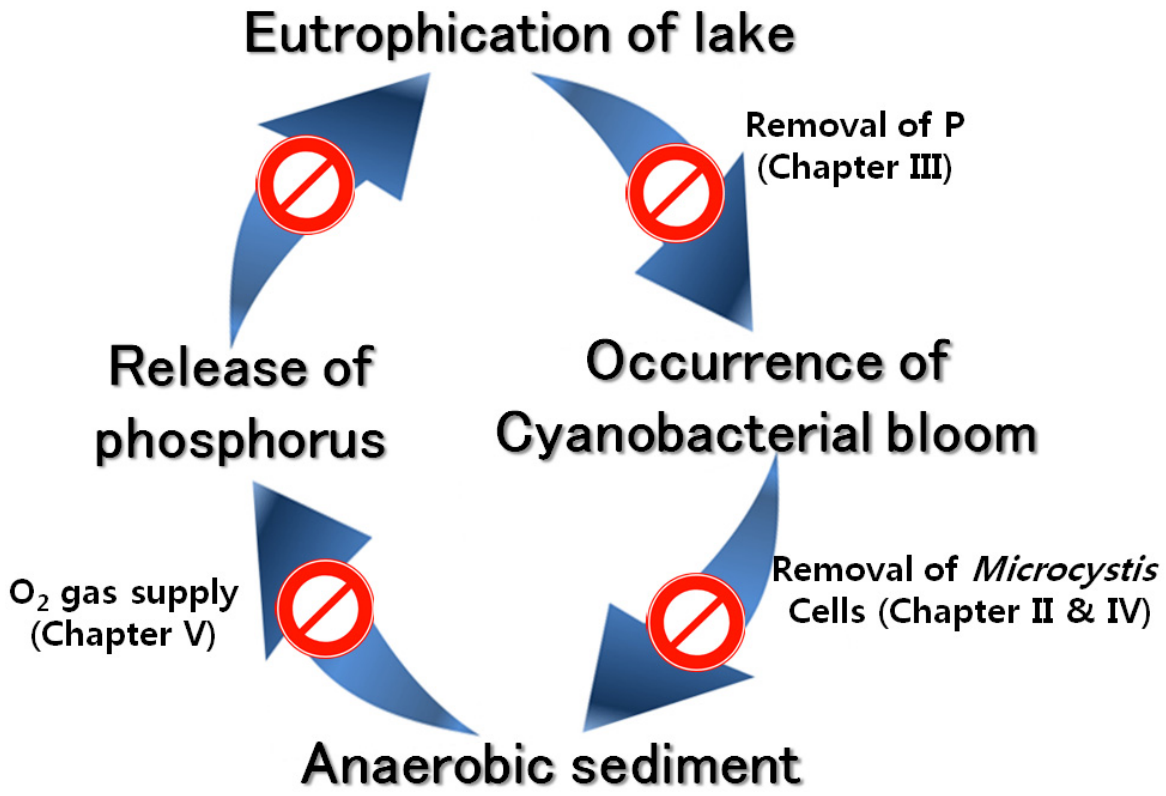

Fig. VI-1. Purification of eutrophic lake by electrochemical treatment.

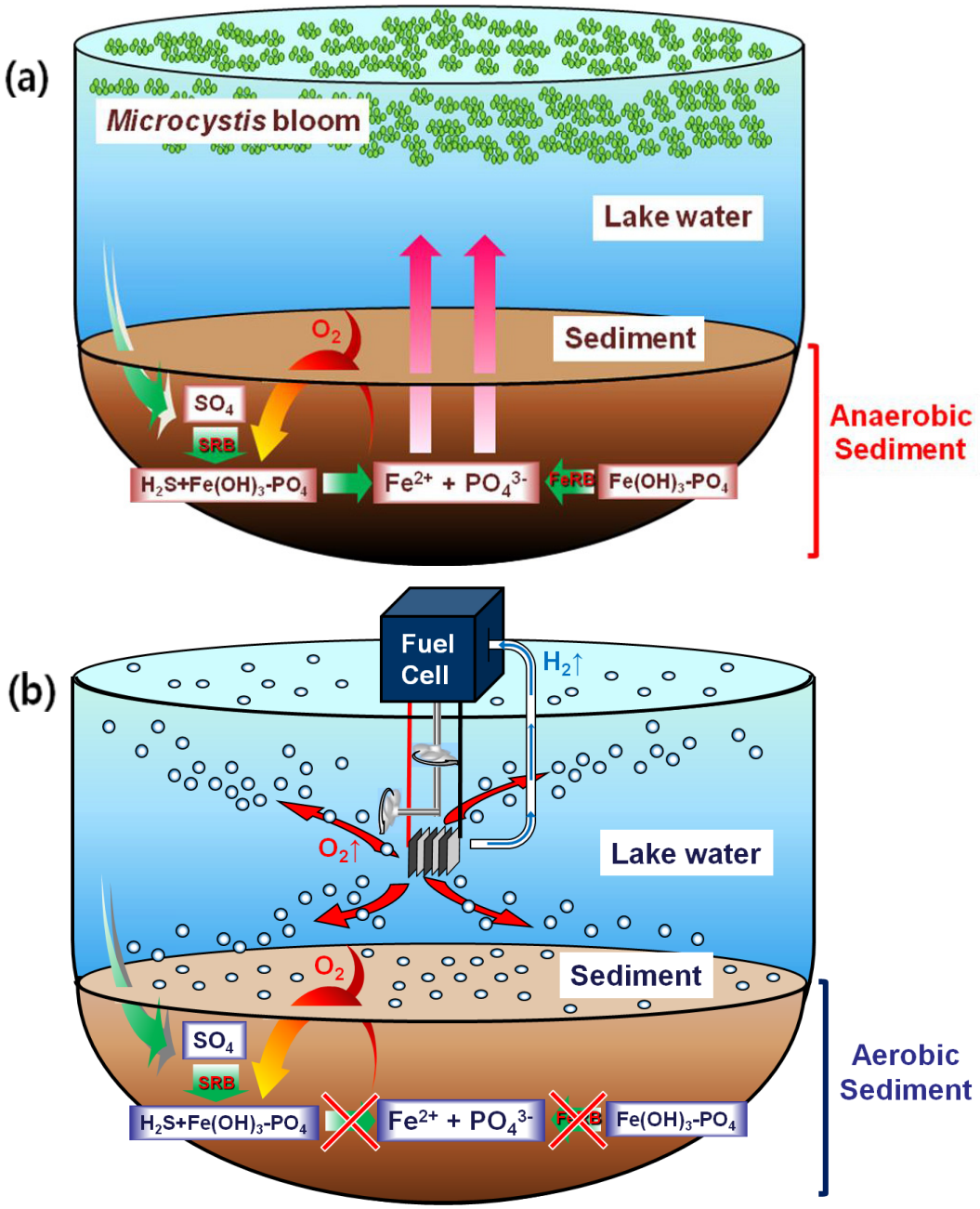

Fig. VI-2. Schematic diagram of purification of eutrophic lake by electrochemical treatment; (a) before treatment (modified Wetzel, 2001) and (b) after treatment. SRB and FeRB indicate sulfate-reducing bacteria and ferric-reducing bacteria.

References

Bektaş, N., Akbulut, H., Inan, H., Dimoglo, A. (2004) Removal of phosphate from aqueous solutions by electro-coagulation. Journal of Hazardous Materials 106B, 101-105.

Bolch, C.J.S., Blackburn, S.I. (1996) Isolation and purification of Australian isolates of the toxic cyanobacterium *Microcystis aeruginosa* Kutz. Journal of Applied Phycology 8: 5-13.

Comninellis, C., Pulgarin, C. (1993) Electrochemical oxidation of phenol for wastewater treatment using SnO_2 anodes. Journal of Applied Electrochemistry 23, 108-112.

Cooke, G.D., Welch, E.B., Peterson, S.A., Nichols, S.A. (2005) Restoration and Management of Lakes and Reservoirs. CRC Press, Inc., Boca Raton, Florida, USA.

Dosen, A., Giese, R.F. (2011). Thermal decomposition of brushite, $CaHPO_4 \cdot 2H_2O$ to monetite $CaHPO_4$ and the formation of an amorphous phase. American Mineralogist 96, 368-373.

Han, J.S., Jeon, B.S., Futatsugi, N., Park, H.D. (2013) The effect of alum coagulation for in-lake treatment of toxic *Microcystis* and other cyanobacteria related organisms in microcosm experiments. Ecotoxicology and Environmental Safety 96, 17-23.

Kerwick, M.I., Reddy, S.M., Chamberlain, A.H.L., Holt, D.M. (2005) Electrochemical disinfection, an environmentally acceptable method of drinking water disinfection?. Electrochimica Acta 50, 5270-5277.

Reynolds, C.S., Jaworski, G.H.M., Cmiech, H.A., Leedale, G.F. (1981) On the annual cycle of the Blue-Green-Alga *Microcystis aeruginosa* Kutz emend Elenkin. Philosophical

Transactions of the Royal Society B. 293, 419-477.

Reyter, D., Bélanger, D., Roué, L. (2010) Nitrate removal by a paired electrolysis on copper and Ti/IrO_2 coupled electrodes – Influence of the anode/cathode surface area ratio. Water Research 44, 1918-1926.

Stucki, S., Kötz, R., Carcer, B., Suter, W. (1991). Electrochemical waste water treatment using high overvoltage anodes Part II: Anode performance and applications. *J. Appl. Electrochem.* 21, 99.

Tanaka, S., Nakata, Y., Kimura, T., Yustiawati, Kawasaki, M. Kuramitz, H. (2002) Electrochemical decomposition of bisphenol A using Pt/Ti and SnO_2/Ti anodes. Journal of Applied Electrochemistry 32, 197-201.

Wetzel, R. (2001) Limnology, 3 E. Lake and River Ecosystems. Academic Press, 525 B Street, Ste. 1900, San Diego, CA 92101, USA.

Yang, Z., Kong, F. (2012) Formation of large colonies: a defense mechanism of *Microcystis aeruginosa* under continuous grazing pressure by flagellate *Ochromonas* sp.. Journal of Limnology 71, 61-66.

Appendix

Microcystin extraction from *Microcystis* cells using boiling treatment

1. Introduction

Several solvents, such as 0.1 M ammonium bicarbonate (pH 8.4) (Botes et al., 1982), butanol:methanol:water (5:20:75, v/v) (Krishnamurthy et al., 1986), 5% acetic acid (Harada et al., 1988) and 70% methanol (Gjølme and Utkilen, 1996), are used for the extraction of microcystins from cyanobacteria cells. Metcalf and Codd (2000) suggested the extraction of microcystins using boiling waterbath and a microwave oven. However, to the best of our knowledge, no studies have been investigated the loss of microcystins during extraction process.

In this study, three extraction methods (homogenizing+5% acetic acid treatment, boiling+ultrasonic treatment and boiling water treatment) of microcystins were compared. In addition, internal standard was added in the extraction methods and evaluated the loss of microcystins during process. From the results of the extracted microcystins concentration and the loss of microcystins concentration, the ability of microcystin extraction could be calculated. Furthermore, heat stability of MC-LR was evaluated.

2. Materials and methods

2.1. Algal culture

A unialgal culture of *Microcystis ichthyoblabe* (TAC95 strain; Tsukuba Algae Collection, National Science Museum) was used in this study. TAC95 was cultured in the late exponential growth phase or early stationary growth phase that corresponded to 14 days after inoculation in batch mode containing the sterilized 10 L MA medium (Table II-1) under illumination at approximetely 16 μmol m^{-2} s^{-1} and a 24 h light cycle at 23 ± 1 °C. TAC95 strain is known to produce only MC-LR (Yokoyama and Park, 2003).

A small amount of the cultured TAC95 solution was pipetted into a Fuchs-Rosenthal hemocytometer, and the cells were counted under the microscope at 400× magnification (BK51, Olympus, Tokyo, Japan). The cell density of the cultured TAC95 solution was 1.43×10^{7} cells mL^{-1}.

The 30 mL sample aliquots were filtered through a glass-fiber filter (GF/C, Whatman, Maidstone, UK) and immediately freeze-dried at -80°C (FDU-2100, EYELA, Tokyo, Japan) and kept in a desiccator until treatment.

2.2. Heat stability of MC-LR

MC-LR was purified from TAC95 strain, and purified MC-LR was dissolved in 100% MeOH. The concentration of purified MC-LR was 9.30 μg mL^{-1}. A 100 μL of purified MC-LR was put in a glass micro tube (3 mL) and Methanol was evaporated using a rotary evaporator. Oven (TS-42S, Toyo Roshi Kaisha, LTD., Tokyo, Japan) was pre-heated to 100, 150, 175, 200, 225 and 250ºC. The temperature was measured by a radiation thermometer (SIK-300, Sansyo, Tokyo, Japan). The MC-LR samples were put in the pre-heated oven, then, kept during 10 and 60 min, after which the samples were taken out and cooled down at room temperature (25ºC). The remained MC-LR was dissolved in MeOH (100 μL). The MeOH solution containing MC-LR was injected into a high-performance liquid chromatography (HPLC) machine for analysis. All experiments were performed in triplicate.

2.3. MC-LR extraction methods

2.3.1. Treatment 1

The glass-fiber filter sample filtered TAC95 solution (30 mL) was homogenized by a mortar and a pestle. 5% aqueous acetic acid of 10 mL was added in the sample and stirred

during 30 min. The stirred sample was centrifuged at 2380 ×g during 15 min, after which the supernatant was separated. 5% aqueous acetic acid of 10 mL was added in the precipitate and stirred during 30 min then it was centrifuged and the supernatant was separated. The process from adding of 5% aqueous acetic acid of 10 mL to separation of supernatant was repeated one more time. Through the process, total 30 mL of supernatant was gathered. All experiments were performed in triplicate.

2.3.2. Treatment 2

The glass-fiber filter sample which filtered TAC95 solution (30 mL) was put in a centrifuge tube. 10 mL water was added in the centrifuge tube and heated in boiling water during 10 min. All water used was purified using Milli-Q system (Millipore, Tokyo, Japan). The sample was centrifuged at 2380 ×g during 15 min, after which the supernatant was separated. 10 mL water was added in the centrifuge tube and ultrasonic treated during 10 min using ultrasonic cleaner (IUC-7321N, Yamato Scientific co., LTD., Tokyo, Japan). The sample was then centrifuged at 2380 ×g during 15 min, after which the supernatant was separated. The process from adding 10 mL water to separation of supernatant was repeated one more time. Through the process, total 30 mL of supernatant was gathered. All experiments were performed in triplicate.

2.3.3.Treatment 3

The glass-fiber filter sample which filtered TAC95 solution (30 mL) was put in a centrifuge tube. Boiling water of 10 mL was added in the centrifuge tube and kept during 5 min room temperature (25ºC). The sample was centrifuged at 2380 ×g during 15 min, after which the supernatant was separated. This process were performed in triplicate, then total 30

mL of supernatant was gathered. All experiments were performed in triplicate.

2.4. Recovery for methods

To investigate the effect of recovery for treatments, TAC 95 strain which produce only MC-LR was selected (Yokoyama and Park, 2003) and added MC-RR as internal standard before treatments. MC-RR was purified from *Microcystis* cells of Chikato pond, Matsumoto, Japan in 2010. The purified MC-RR was dissolved in water and the concentration was 3.05 μg mL^{-1}. 200 μL of MC-RR solutions were added in the mortar before homogenizing (Treatment 1), in the centrifuge tube before boiling (Treatment 2) and in the centrifuge tube before adding boiling water (Treatment 3).

2.5. Analysis of MC-LR and MC-RR

The supernatants of treatment 1, 2 and 3 with MC-RR were applied to an HLB cartridge (0.5 g, Oasis, Waters, Milford, MA, USA) preconditioned with MeOH (10 mL) and water (10 mL). The MC-LR and MC-RR were eluted from the HLB cartridge by MeOH (200 μL). The MeOH solution containing MC-LR and MC-RR was injected into a high-performance liquid chromatography (HPLC) machine for analysis.

The HPLC system consisted of a Shimadzu (Kyoto, Japan) LC-9A pump coupled to a SPD-10A set to 238 nm, an SPD-M10A photodiode array detector, and a C-R6A integrator and ODS column (Cosmosil 5C18-MS-II; 4.6 mm × 150 mm, Nacalai Tesque, Kyoto, Japan). The sample was separated using a mobile phase of methanol:0.05 M phosphate buffer (pH 3.0, 58:42) applied at a flow rate of 1 mL/min. The MC-LR concentration was quantified against MC-LR standards (Kanto Ltd., Tokyo, Japan).

2.6. Statistical analysis

Statistical analysis for MC-LR by the extraction methods and MC-RR recovery was performed using R version 3.0.2 (R Core Team 2013). We confirmed that all data were normaly destributed ($p > 0.05$ with Shapiro-Wilk test). And thus, the differences between treatments were tested using Tukey HSD test following one-way ANOVA.

3. Results and discussion

3.1. Heat stability of MC-LR

To investigate the heat stability of MC-LR, heat experiments were performed. The MC-LR samples were heated at 100, 150, 175, 200, 225 and 250ºC during 10 min and 1 h, respectively (Fig. 1). MC-LR concentration was not changed at 100ºC and not detected at 250ºC during 10 min heat treatment (Fig. 1 (a)). The results of MC-LR concentration which heated at 100 and 150ºC during 10 min were not significantly differed with the result of 25ºC MC-LR concentration (not treated). MC-LR concentration was decreased by approximately 5.5% at 100ºC during 1 h heat treatment (Fig. 1 (b)). However, this result was not significantly differed with the result of 25ºC MC-LR concentration (not treated). Yu et al. (2009) reported that MC-LR was stable when the temperature was less than 100ºC during 6 h.

3.2. Effect of extraction efficiency of MC-LR for treatments

The MC-LR concentration of treatment 1, 2 and 3 were 621.0, 672.7 and 584.3 $\mu g\ L^{-1}$, respectively (Fig. 2). The highest MC-LR concentration was extracted by treatment 2. However, there was not significant difference between treatment 1 and 2. The lowest MC-LR

concentration was extracted by treatment 3 and it was significantly differed with the result of treatment 2.

3.3. Effect of recovery for methods

Fig. 3 shows the recovery of MC-RR for methods. The recovery of MC-RR of treatment 1, 2 and 3 were 70.5, 88.9 and 80.0%, respectively, compared with not treated MC-RR (control). These results indicate a loss of microcystins by treatment and the loss of MC-RR by treatment 1, 2 and 3 were 29.5, 11.1 and 20.0%, respectively. It is considered that the loss of treatment 1 caused by the homogenizing process using mortar and pestle and the transferring. However, the recovery of treatment 2 was lower than control, but there was not significant difference. On the other hand, the result of treatment 3 was lower than the result of treatment 2 but there was not significant difference. These results indicate that the use of homogenizing process can cause a lot of loss of extracted microcystins whereas the loss by the boiling/ultrasonic treatment is little.

From the results of Fig. 2 and Fig. 3, the MC-LR concentration without loss during process can be calculated by the following equation and this value means the MC-LR extraction ability from *Microcystis* cells of treatment 1, 2 and 3.

MC-LR concentration without loss during process =

MC-LR concentration (results of Fig. 2) × 100 / (Recovery (results of Fig. 3)) (1)

The calculated MC-LR concentration of treatment 1, 2 and 3 were 881.9, 756.8 and 730.3 μg

L^{-1}, respectively (Fig. 4). The result of treatment 1 was highest, and it is significantly differed with the results of treatment 2 and 3. The extraction method using mortar and pestle with 5% acetic acid (treatment 1) had good microcystin extraction ability from *Microcystis* cells compared with treatment 2 and 3 however, the loss of microcystins during process was great (Fig. 3), thereby actually extracted MC-LR concentration was lower than treatment 2 (Fig. 2).

The MC-LR extraction ability of treatment 3 was a little lower than treatment 2, but there was not significant difference. It means that the microcystin extraction ability was not influenced by the ultrasonic cleaning process but influenced by the boiling/boiled water.

The MC-LR extraction ability of treatment 2 was lower than treatment 1, however actually extracted MC-LR concentration was higher because it had good recovery of microcystins.

4. Conclusions

In this study, heat stability of MC-LR was evaluated. In addition, MC-LR extraction efficiency and recovery of three extraction methods (the homogenizing+5% acetic acid treatment, the boiling+ultrasonic treatment and the boiling water treatment) were compared. From these results, the microcystin extraction ability was evaluated.

The homogenizing+5% acetic acid treatment had highest microcystin extraction ability among three methods. However, the loss of microcystins during process also was highest. The MC-LR extraction ability of the boiling+ultrasonic treatment was lower than the homogenizing+5% acetic acid treatment, however actually extracted MC-LR concentration was higher because it had good recovery of microcystins. The boiling water treatment was the simplest method among three methods. However, the extraction efficiency of MC-LR was

lowest.

The samples must be homogenized one at a time by the homogenizing+5% acetic acid treatment. However, the samples can be treated at once by the boiling+ultrasonic treatment. Therefore, the boiling+ultrasonic treatment is adaptable to precise analysis of many samples. The boiling water treatment is simple method, therefore it can be applied for on-site analysis.

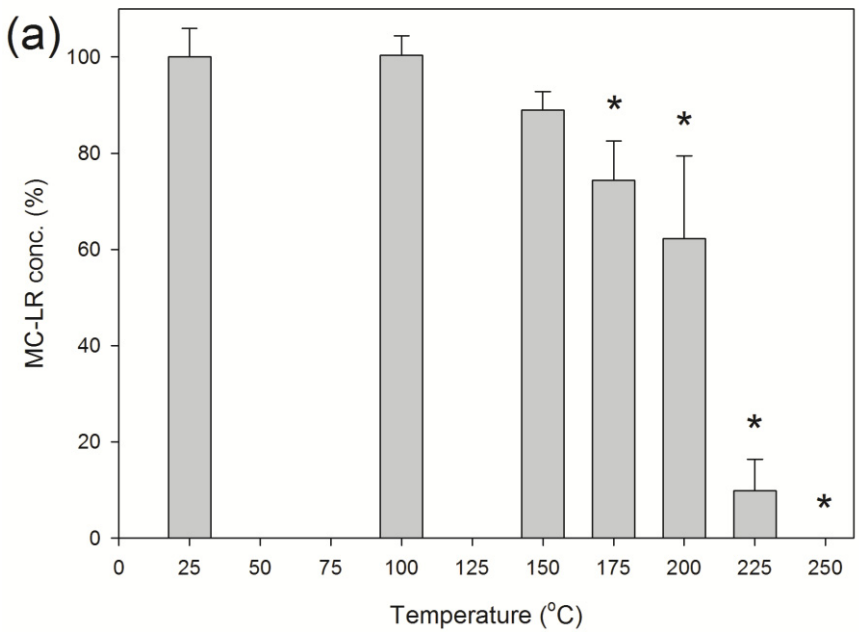

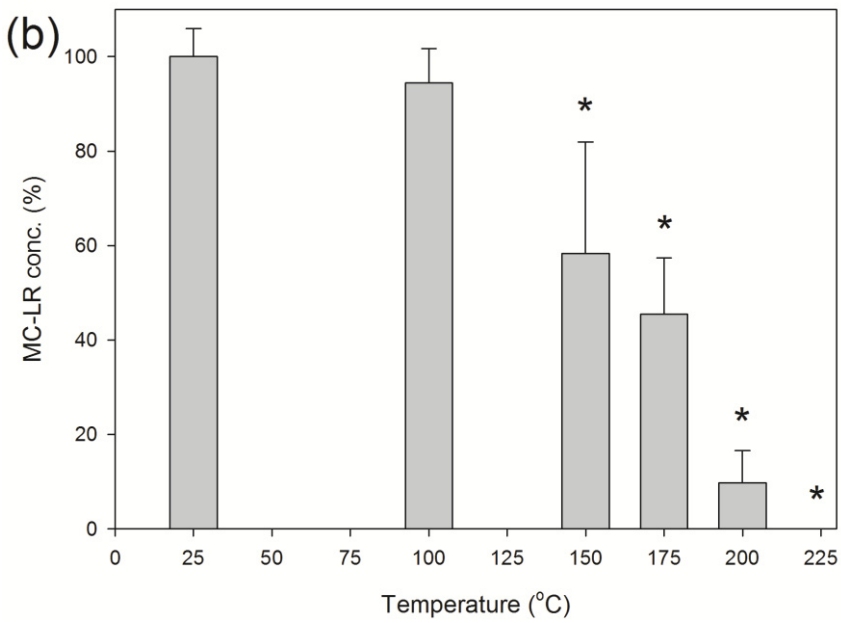

Fig. 1. The MC-LR concentration heated during 10 min (a) and 1 h (b). Asterisk (*) represent significant differences with 25ºC treated sample (Tukey's multiple-comparison test, $p < 0.05$).

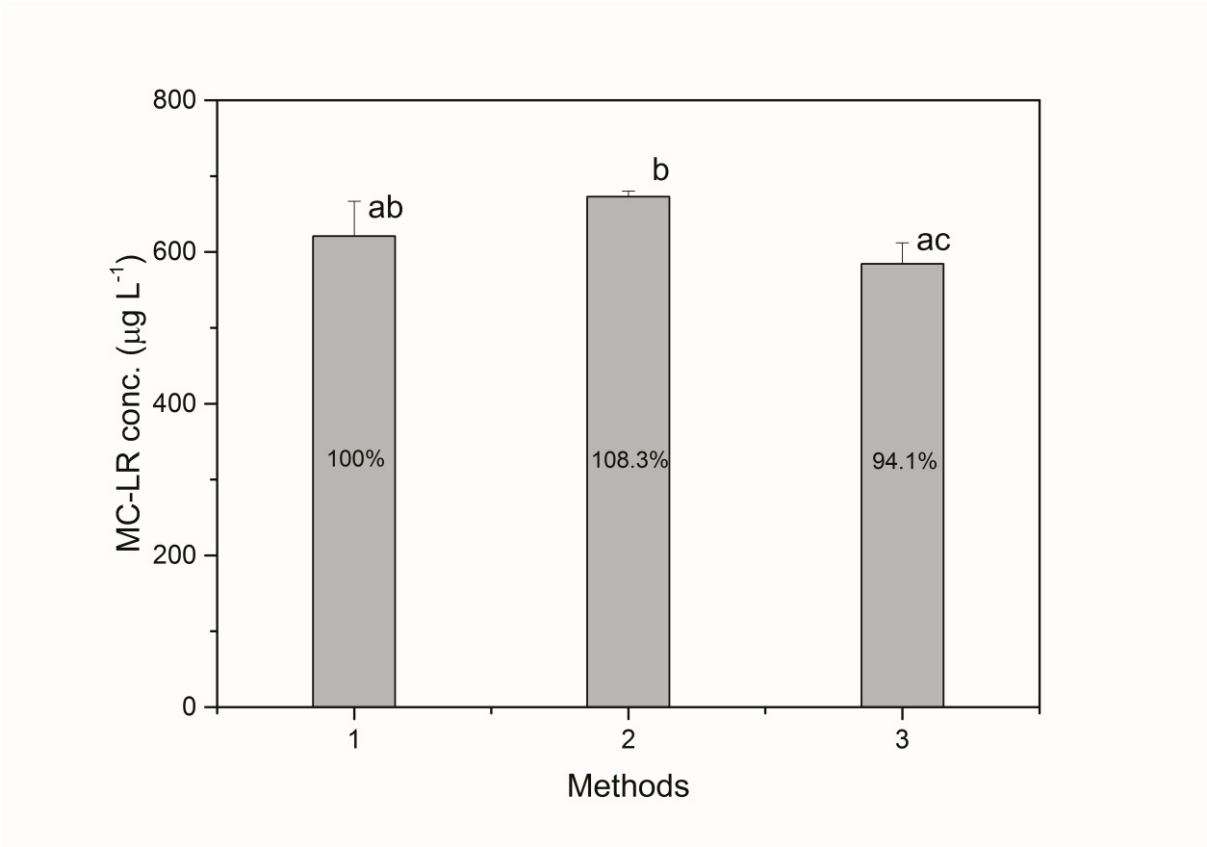

Fig. 2. The extracted MC-LR concentration by treatment 1, 2 and 3 (1, 2 and 3). Different letters represent significant differences between treatment concentrations (Tukey's multiple-comparison test, $p < 0.05$)

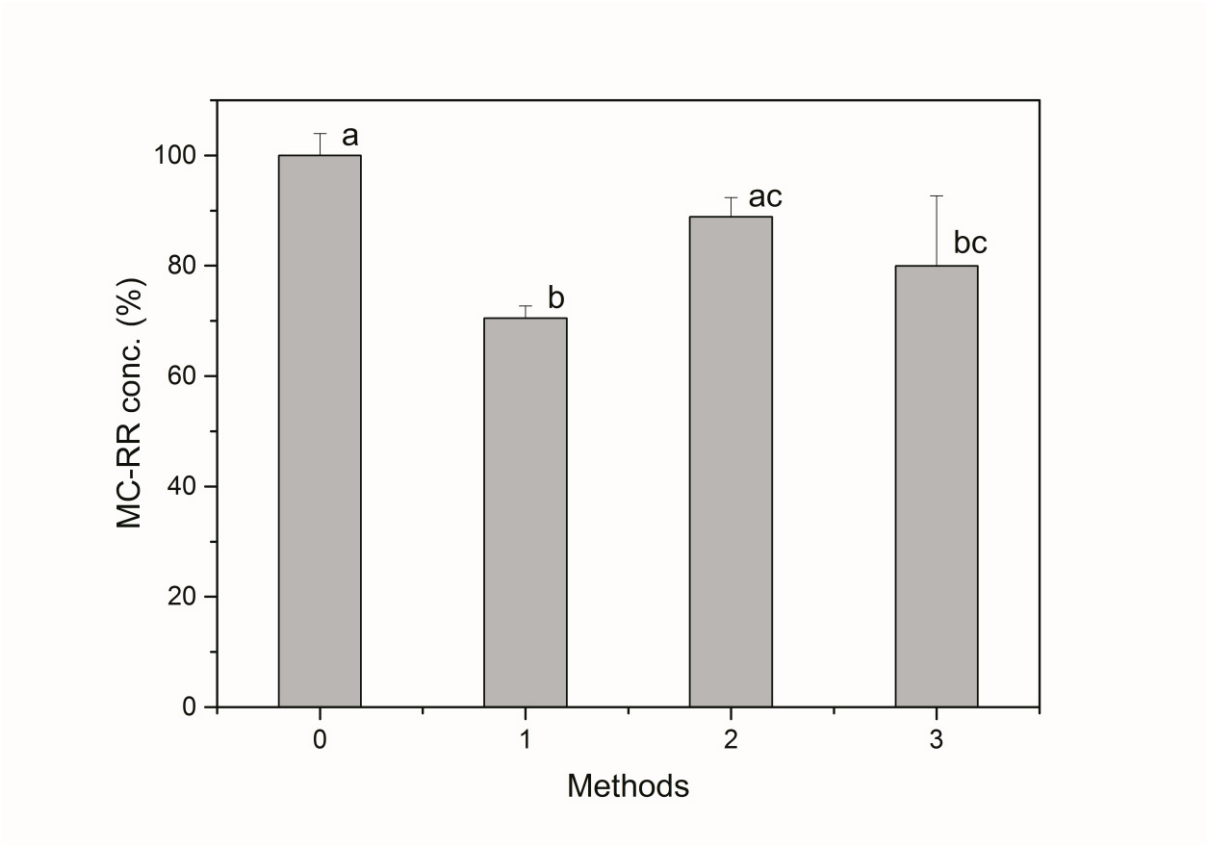

Fig. 3. The recovery of MC-RR concentration by not treated (0) and treatment 1, 2 and 3 (1, 2 and 3). Different letters represent significant differences between treatment concentrations (Tukey's multiple-comparison test, $p < 0.05$)

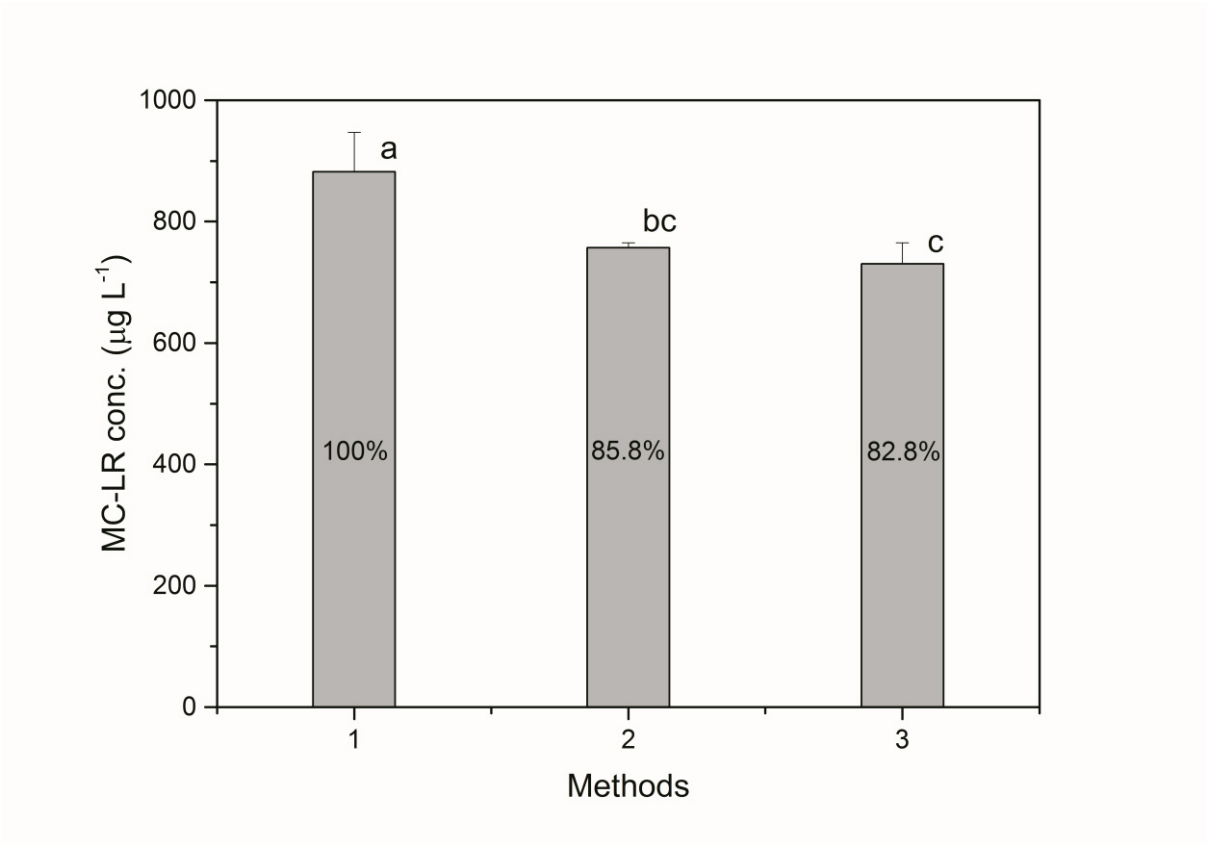

Fig. 4. The MC-LR concentration without the loss during process by treatment 1, 2 and 3 (1, 2 and 3). These results were calculated by eq. 1. Different letters represent significant differences between treatment concentrations (Tukey's multiple-comparison test, $p < 0.05$)

References

Botes, D.P., Kruger, H., Viljoen, C.C. (1982) Isolation and characterization of four toxins from the blue-green alga, Microcystis aeruginosa. Toxicon 20, 945-954.

Gjølme, N., Utkilen, H. (1996) The extraction and stability of microcystin-RR in different solvents. Phycologia 35, 80-82.

Harada, K.I., Suzuki, M., Dahlem, A.M., Beasley, V.R., Carmichael, W.W., Rinehart, K.L. (1988) Improved method for purification of toxic peptides produced by cyanobacteria. Toxicon 26, 433-439.

Krishnamurthy, T., Carmichael, W.W., Sarver, E.W. (1986) Toxic peptides from freshwater cyanobacteria (blue-green algae) 1. Isolation, puri¢cation and characterisation of peptides from *Microcystis aeruginosa* and *Anabaena flos-aquae*. Toxicon 24, 865-873.

Metcalf, J.S., Codd, G.A. (2000) Microwave oven and boiling waterbath extraction of hepatotoxins from cyanobacterial cells, FEMS Microbiology Letters 184, 241-246.

R Core Team (2013). R: A language and environment for statistical computing. R Foundation for Statistical Computing, Vienna, Austria. URL http://www.R-project.org/.

Yokoyama, A., Park, H.D. (2003) Depuration kinetics and persistence of the cyanobacterial toxin microcystin–LR in the freshwater bivalve *Unio douglasiae*. Environ. Toxicol. 18 (1), 61–67.

Yu, T., Xie, P., Dai, M., Liang, G. (2009) Determinations of MC-LR and [Dha^7] MC-LR concentrations and physicochemical properties by liquid chromatography-tandem mass spectrometry. Bulletin of Environmental Contamination and Toxicology 83, 757-760.